BIOHYDROGEN PRODUCTION BY IMMOBILIZED PURPLE NON-SULFUR BACTERIA

A THESIS SUBMITTED TO
THE GRADUATE SCHOOL OF NATURAL AND APPLIED SCIENCES
OF
MIDDLE EAST TECHNICAL UNIVERSITY

BY

EMRAH SAĞIR

IN PARTIAL FULFILLMENT OF THE REQUIREMENTS
FOR
THE DEGREE OF DOCTOR OF PHILOSOPHY
IN
BIOCHEMISTRY

JANUARY 2018

Approval of the Thesis;

BIOHYDROGEN PRODUCTION BY IMMOBILIZED PURPLE NON-SULFUR BACTERIA

submitted by **EMRAH SAĞIR** in partial fulfillment of the requirements for the degree of **Doctor of Philosophy in Biochemistry Department, Middle East Technical University** by,

Prof. Dr. Gülbin Dural Ünver
Dean, Graduate School of **Natural and Applied Sciences** _____

Prof. Dr. Bülent İçgen
Head of the Department, **Biochemistry** _____

Prof. Dr. Meral Yücel
Supervisor, **Biological Sciences Dept., METU** _____

Asst. Prof. Dr. Harun Koku
Co-Supervisor, **Chemical Engineering Dept**, **METU** _____

Examining Committee Members:

Prof. Dr. İnci Eroğlu
Chemical Engineering Dept., METU _____

Prof. Dr. Meral Yücel
Biological Sciences Dept., METU _____

Prof. Dr. Ayşe Gül Gözen
Biological Sciences Dept., METU _____

Prof. Dr. Füsun Eyidoğan
Elementary Education Dept., Başkent University _____

Asst. Prof. Dr. Çağla Sönmez
Agriculture and Natural Sciences,
Konya Food and Agriculture University _____

Date: 12/01/2018

I hereby declare that all information in this document has been obtained and presented in accordance with academic rules and ethical conduct. I also declare that, as required by these rules and conduct, I have fully cited and referenced all material and results that are not original to this work.

Name, Last name: Emrah Sağır

Signature :

ABSTRACT

BIOHYDROGEN PRODUCTION BY IMMOBILIZED PURPLE NON-SULFUR BACTERIA

Sağır, Emrah

Ph.D., Department of Biochemistry

Supervisor: Prof. Dr. Meral Yücel

Co-Supervisor: Asst. Prof. Dr. Harun Koku

January 2018, 175 pages

Biological hydrogen production by purple non-sulfur bacteria is an attractive route to build a large scale hydrogen production system in outdoor natural conditions from various renewable sources. In this study, biological hydrogen production was carried out by agar immobilized purple non-sulfur bacteria in indoor and outdoor conditions. A novel photobioreactor (1.4 L volume) was built and operated continuously for 20 to 64 days in sequential batch mode for long-term hydrogen production using agar-immobilized *Rhodobacter capsulatus* YO3. The immobilized panel photobioreactor was also operated under natural outdoor conditions to show the feasibility of hydrogen production on a pre-pilot scale. The experiments were carried out in Middle East Technical University, Ankara, Turkey between May and June, 2016. The effects of initial sucrose concentration on hydrogen production, productivity and yield were examined in a long-term operation. Long-term hydrogen production was realized either on sucrose or sugar beet molasses by agar (4% w/v) immobilized *Rhodobacter capsulatus* YO3. The

highest hydrogen yield and hydrogen productivity obtained were 19 mol H_2/mol sucrose and 0.73 mmol H_2 $L^{-1}h^{-1}$ in indoors on 5 mM initial sucrose. The effects of higher initial sucrose concentration on hydrogen production were also investigated. The highest hydrogen yield and productivity were 6.1 ± 0.2 mol H_2/mol sucrose and 0.87 ± 0.06 mmol H_2 $L^{-1}h^{-1}$, respectively on 10 mM sucrose. The highest hydrogen yield (9.1mol H_2/mol sucrose) and productivity (0.64 mmol H_2 $L^{-1}h^{-1}$) were obtained by using sugar beet molasses in indoor conditions. The highest productivity of 0.79±0.04 mmol H_2 L^{-1} h^{-1} and yield of 5.2±0.4 mol H_2/mol sucrose were obtained in outdoors. The present study demonstrated that the immobilized system is feasible for long-term hydrogen production even under varying temperature and illumination. The immobilized system also prevented sudden pH drops by sucrose utilization during the process.

Hydrogen production from glucose was carried out as the last part of the study, which was carried out in University of Montreal, Canada. For this purpose, microaerobic dark fermentation was employed to demonstrate and enhance hydrogen production from glucose. Therefore, immobilized cultures of *R. capsulatus* JP91 and *R. palustris* CGA009 have been used in single and sequential dark and photofermentative processes. Response surface methodology with the Box-Behnken design was employed to optimize the key parameters such as glucose, inoculum and oxygen concentrations. The highest hydrogen yield and productivity obtained were 7.8 mol H_2/mol glucose and 0.15 mmol H_2 $L^{-1}h^{-1}$, respectively by *R. capsulatus* JP91. These results indicated that biohydrogen production by immobilized purple non-sulfur bacteria is promising particularly for large-scale outdoor natural conditions.

Keywords: Biohydrogen, cell immobilization, photobioreactor, *Rhodobacter capsulatus*, photofermentation, *Rhodopseudomonas palustris*, Response Surface Methodology, microaerobic dark fermentation.

ÖZ

İMMOBİLİZE MOR KÜKÜRTSÜZ BAKTERİLER İLE BİYOHİDROJEN ÜRETİMİ

Sağır, Emrah

Doktora, Biyokimya Bölümü

Tez Yöneticisi : Prof. Dr. Meral Yücel

Ortak Tez Yöneticisi : Yrd. Doç. Dr. Harun Koku

Ocak 2018, 175 sayfa

Mor kükürtsüz bakteriler ile biyolojik hidrojen üretimi büyük ölçekte, dış ortamda doğal şartlarda, çeşitli yenilenebilir kaynaklardan hidrojen üretim sistemi oluşturmak için çarpıcı bir yoldur. Bu çalışmada, biyolojik hidrojen üretimi, agara immobilize (hareketsiz) mor kükürtsüz bakteriler tarafından iç ve dış mekanlarda gerçekleştirilmiştir. Yeni bir fotobiyoreaktör (1.4 L hacim) tasarlanıp ardışık seri mod ile 20 ila 64 gün süreyle sürekli olarak uzun süreli hidrojen üretimi için agar-immobilize *Rhodobacter capsulatus* YO3 kullanılarak çalıştırıldı. İmmobilize panel fotobiyoreaktör, pilot-ölçek öncesinde hidrojen üretiminin fizibilitesini göstermek için doğal dış ortamda da kullanıldı. Deneyler, 2016 yılı Mayıs ve Haziran ayları arasında Orta Doğu Teknik Üniversitesi, Ankara, Türkiye'de gerçekleştirilmiştir.

Başlangıç sükroz konsantrasyonunu yükseltmenin hidrojen üretimi, verimi ve üretkeliği üzerine etkileri, uzun vadeli bir hidrojen üretimi için incelenmiştir.

Uzun süreli hidrojen üretimi, sükroz veya şeker pancarı pekmezi üzerinde agar (% 4 w/v) immobilize *Rhodobacter capsulatus* YO3 ile gerçekleştirildi. En yüksek hidrojen verimi ve hidrojen üretkenliği, 5 mM sükroz üzerinde kapalı ortamda 19 mol H_2/mol sukroz ve 0.73 mmol H_2 $L^{-1}h^{-1}$ olarak elde edildi. Başlangıç sükroz konsantrasyonunun hidrojen üretimi üzerindeki etkileri de araştırılmıştır. En yüksek hidrojen verimi ve üretkenlik sırasıyla 10 mM sükroz üzerinde 6.1 ± 0.2 mol H_2/mol sukroz ve 0.87 ± 0.06 mmol H_2 L^{-1} h^{-1} idi. Ayrıca, en yüksek hidrojen verimi (9.1 mol H_2/mol sukroz) ve üretkenlik (0.64 mmol H_2 $L^{-1}h^{-1}$) şeker pancarı melası kullanılarak kapalı ortam koşullarında elde edilmiştir. En yüksek hidrojen üretkenliği 0.79±0.04 mmol H_2 L^{-1} h^{-1} ve verimi 5.2±0.4 mol H_2/mol sucrose olarak dış ortamda elde edildi. Bu çalışmada, immobilize sistemin, değişen sıcaklık ve güneş enerjisi altında bile uzun süreli bir hidrojen üretimi için uygulanabilir olduğu gösterildi. Immobilize sistem aynı zamanda işlem sırasında sükroz kullanımıyla ani pH düşüşlerini de önledi.

Bu çalışmanın son kısmı olarak hidrojen üretimi glukoz kullanılarak, Montreal Üniversitesi Kanada'da gerçekleştirildi. Bu amaçla, mikroaerobik karanlık fermantasyon glikozdan hidrojen üretimini göstermek arttırmak için kullanıldı. Bu nedenle, *R. capsulatus* JP91 ve *R. palustris* CGA009'un immobilize (hareketsiz) kültürleri tekli ve ardışık karanlık ve fotofermentatif işlemlerde kullanılmıştır. Box-Behnken tasarımı ile tepki yüzeyi metodolojisi, glikoz, inokulum ve oksijen konsantrasyonları gibi anahtar parametreleri optimize etmek için kullanıldı. En yüksek hidrojen verimi ve üretkenliği sırasıyla 7.8 mol H_2/mol glikoz ve 0.15 mmol H_2 $L^{-1}h^{-1}$ olarak *R. capsulatus* JP91 ile elde edildi. Bu sonuçlar, hareketsiz mor kükürtsüz bakterilerin biyolojik hidrojen üretiminin, özellikle büyük ölçekli açık doğal koşullar için umut vaat ettiğini gösterdi.

Anahtar Kelimeler: Biyohidrojen, hücre immobilizasyonu, fotobiyoreaktör, *Rhodobacter capsulatus*, fotofermentasyon, *Rhodopseudomonas palustris*, Tepki Yüzey Metodu, mikroaerobik karanlık fermentasyon.

To my family,

ACKNOWLEDGEMENTS

I would like to thank sincerely to my supervisor Prof. Dr. Meral Yücel and my co-supervisor Asst. Prof. Dr. Harun Koku for their guidance, support, valuable comments and suggestions throughout my thesis study.

I would like to thank Prof. Dr. İnci Eroğlu and Prof. Dr. Ayşe Gül Gözen for their valuable ideas, aids and support. I would also thank to thesis examining members Prof. Dr. Füsun Eyidoğan and Asst. Prof. Dr. Çağla Sönmez for their contributions.

I would like to thank Prof. Dr. Patrick C. Hallenbeck for his guidance, help and all support during my research in his laboratory in University of Montreal, School of Medicine, Department of Microbiology, Infectious diseases and Immunology, in Canada.

I would like to thank Dr. Siamak Alipour for his contributions, comments and ideas about the research.

I would like to thank Dr. Kamal El-Kahlout for his contributions and support. I would like to thank Emine Kayahan for her help, support and friendship in Hydrogen Research Laboratory. I am thankful to Taha Ceylani in Biology Department for his friendship and support. I would like to thank Alev Ateş and Görkem Baysal for their friendships and help.

I am grateful to my family for their valuable support. I would like to give my special thanks and appreciation to my wife, Tuğçe Sağır, for her endless patience and support throughout all my work and life.

I would like to thank Scientific and Technological Research Council of Turkey (TÜBİTAK BİDEB) for their support with 2214a International Doctoral Research Fellowship Program (Project number: 1059B141500983). I also want to thank METU Teaching Staff Training Program (ÖYP) for the support (07/02/2011-003).

TABLE OF CONTENTS

ABSTRACT v

ÖZ vii

ACKNOWLEDGEMENTS x

TABLE OF CONTENTS xi

LIST OF TABLES xv

LIST OF FIGURES xx

LIST OF SYMBOLS AND ABBREVIATIONS xxv

CHAPTERS

1. INTRODUCTION 1

2. A SURVEY OF LITERATURE 5

2.1 Hydrogen Production Methods and Techniques 7

2.2 Biological Hydrogen Production 8

2.2.1 Biophotolysis 9

2.2.2 Dark fermentation 10

2.2.3 Photofermentation 13

2.2.4 Microaerobic dark fermentation 17

2.2.5 Integrated systems 20

2.3 Purple non-sulfur bacteria 21

2.4 Cell immobilization 23

2.5 Hydrogen production by immobilized systems 25

2.6 Photobioreactors 29

2.7 Aim of the study 32

3. MATERIALS AND METHODS 33

3.1 Bacterial Strains 33

3.2 Growth and hydrogen production media 33

3.3 Immobilization procedure 34

3.4 Experimental Setup 36

3.5 Operation of the reactors 37

3.6 Temperature Control 38

3.7 Analytical methods 38

3.7.1 pH measurement 38

3.7.2 Organic acid and sugar analyses 38

3.7.3 Gas composition analysis 39

3.8 Data analyses and calculations 39

3.9 Microaerobic dark fermentative hydrogen production by suspended culture 40

3.10 Microaerobic dark fermentative hydrogen production by immobilized culture 41

4. RESULTS AND DISCUSSION 43

4.1 Indoor and outdoor hydrogen production by immobilized *R. capsulatus* YO3 on sucrose 43

4.1.1 Indoor hydrogen production by immobilized *R. capsulatus* YO3 on sucrose 43

4.1.2 Outdoor hydrogen production by immobilized *R. capsulatus* YO3 on sucrose 56

4.1.3 Comparison of indoor and outdoor hydrogen production by immobilized *R. capsulatus* YO3 on sucrose 61

4.2 Indoor and outdoor hydrogen production by immobilized *R. capsulatus* YO3 on sugar beet molasses 63

4.2.1 Indoor hydrogen production by immobilized *R. capsulatus* YO3 on sugar beet molasses..... 63

4.2.2 Outdoor hydrogen production by immobilized *R. capsulatus* YO3 on molasses 73

4.2.3 Comparison of indoor and outdoor hydrogen production by immobilized *R. capsulatus* YO3 on molasses..... 79

4.2.4 Comparison of immobilized and suspended culture of *R. capsulatus* YO3 80

4.3 Microaerobic dark fermentative hydrogen production by *R. palustris* CGA009 and *R.capsulatus* JP91 on glucose 81

4.3.1 Microaerobic dark fermentative hydrogen production by suspended culture of *Rp. palustris* CGA009 using RSM 82

4.3.2 Microaerobic dark fermentative hydrogen production by immobilized *Rp. palustris* CGA009 using RSM…….88

4.3.3 Long-term hydrogen production via cyclic microaerobic dark fermentation by immobilized *Rp. palustris* CGA009 92

4.3.4 Hydrogen production by immobilized *Rp. palustris* CGA009 via sequential microaerobic dark and photofermentation..... 97

4.3.5 Hydrogen production by immobilized *Rp. palustris* CGA009 via sequential microaerobic dark and photo fermentation using RSM..... 103

4.3.6 Hydrogen production by immobilized *R. capsulatus* JP91 via sequential microaerobic dark and photofermentation using RSM 109

5. CONCLUSIONS.....115

REFERENCES.....118

APPENDICES

A. COMPOSITION OF THE GROWTH AND HYDROGEN PRODUCTION MEDIA AND SOLUTIONS.....129

B. ORGANIC ACID ANALYSIS.....137

C. SAMPLE SUGAR ANALYSIS.....143

D. SAMPLE GAS CHROMATOGRAM.....145

E. COMPOSITION OF SUGAR BEET MOLASSES..... 147

F. INDOOR EXPERIMENTAL DATA..... 151

G. OUTDOOR EXPERIMENTAL DATA..... 159

H. DATA IN MICROAEROBIC DARK FERMENTATION..... 161

I. SAMPLE CALCULATION..... 171

CURRICULUM VITAE 173

LIST OF TABLES

TABLES

Table 4.1 Summary of long-term hydrogen production on 5 mM initial sucrose concentration 46

Table 4.2 Organic acids produced during the photofermentation on 5 mM initial sucrose concentration 47

Table 4.3 Summary of the long-term hydrogen production on 5 mM initial sucrose concentration. 50

Table 4.4 Summary of the results on 10 mM initial sucrose concentration..... 53

Table 4.5 Organic acids produced during the photofermentation on 10 mM initial sucrose concentration 53

Table 4.6 Summary hydrogen production on 20 mM initial sucrose concentration. 55

Table 4.7 Final concentrations of organic acids produced during the photofermentation on 20 mM initial sucrose concentration 56

Table 4.8 Summary of the results of outdoor hydrogen production by immobilized *R. capsulatus* YO3 on 10 mM sucrose. 59

Table 4.9 Final concentrations of organic acids produced during the outdoor photofermentation on 10 mM initial sucrose concentration. 59

Table 4.10 Summary of the results of indoor hydrogen production on molasses containing 5 mM sucrose. 67

Table 4.11 Final organic acids produced during the indoor photofermentation on molasses containing 5 mM sucrose. 67

Table 4.12 Summary of the results of indoor hydrogen production on molasses containing 10 mM sucrose. 70

Table 4.13 Final organic acids produced during the indoor photofermentation on molasses containing 10 mM sucrose. 70

Table 4.14 Summary of the results of indoor hydrogen production on molasses containing 20 mM sucrose. 73

Table 4.15 Final organic acids produced during the indoor photofermentation on molasses containing 20 mM sucrose. 74

Table 4.16 Summary of the results of outdoor hydrogen production on molasses with 10 mM sucrose. 79

Table 4.17 Final organic acids produced during the outdoor photofermentation on molasses containing 10 mM sucrose. 80

Table 4.18 Summary of the results with suspended and immobilized culture of *R. capsulatus* YO3 on different sucrose concentrations in indoor conditions. 82

Table 4.19 Box-Behnken experimental design table for hydrogen yield by *Rp. palustris* CGA009 85

Table 4.20 Box-Behnken experimental design table for hydrogen yield by immobilized *Rp. palustris* CGA009 90

Table 4.21 ANOVA analysis for hydrogen yield by immobilized *Rp. palustris* CGA009 93

Table 4.22 Hydrogen yields of cyclic microaerobic dark fermentation by immobilized *Rp. palustris* CGA009 95

Table 4.23 Hydrogen yields of cyclic microaerobic dark fermentation by immobilized *Rp. palustris* CGA009 on different oxygen concentrations (1%, 4.5%, 8%). 96

Table 4.24 Hydrogen yields of cyclic microaerobic dark fermentation by immobilized *Rp. palustris* CGA009 on different initial glucose concentrations (2 mM, 6 mM, 10 mM). 97

Table 4.25 Glucose consumption of cyclic microaerobic dark fermentation by immobilized *Rp. palustris* CGA009 on different initial glucose concentrations (2 mM, 6 mM, 10 mM). 98

Table 4.26 Effects of different inoculum volume on hydrogen production and yield in sequential microaerobic dark fermentation and photofermentation 99

Table 4.27 Effects of oxygen concentration on hydrogen production and yield in sequential microaerobic dark fermentation and photofermentation 101

Table 4.28 Effects of different initial glucose concentration hydrogen production and yield in sequential microaerobic dark fermentation and photofermentation. 101

Table 4.29 Actual design and results of the experiments by *Rp. palustris* CGA009 105

Table 4.30 ANOVA analysis of the quadratic model by *Rp. palustris* CGA009 107

Table 4.31 Actual design and results of the experiments by *R. capsulatus* JP91. 111

Table 4.32 ANOVA analysis of the quadratic model by *R. capsulatus* JP91..... 112

Table A1 Composition of the growth medium (Acetate/Glutamate, 20 mM /10 mM)..... 133

Table A2 Composition of sucrose/acetate growth medium (Sucrose/Acetate/Glutamate, 10 mM/20 mM/2 mM). 134

Table A3 Composition of sucrose growth medium (Sucrose/Glutamate, 10 mM/2 mM)..... 135

Table A4 Hydrogen production media with different sucrose concentrations. [a]: 5 mM, [b]: 10 mM, [c]: 20 mM. 136

Table A5. Composition of trace elements solution (1X) components. 137

Table A6. Composition of RCV-lactate medium. 137

Table A7. Composition of RCV-glucose medium. 138

Table A8. Composition of the supersalts of RCV medium. 138

Table A9. Composition of the trace elements of RCV medium. 139

Table E1. Composition of raw sugar beet molasses. 147

Table E2. Composition of raw sugar beet molasses. The analysis was carried out by Ankara Sugar Factory. 149

Table F.1 pH change and hydrogen production of long-term process on 5 mM sucrose medium by *R. capsulatus* YO3 151

Table F.2 pH change and hydrogen production on 10 mM sucrose medium by *R. capsulatus* YO3..... 153

Table F.3 pH change and hydrogen production on 20 mM sucrose medium by *R. capsulatus* YO3..... 154

Table F.4 pH change and hydrogen production on molasses with 5 mM sucrose by *R. capsulatus* YO3 155

Table F.5 pH change and hydrogen production on molasses with 10 mM sucrose by *R. capsulatus* YO3 156

Table F.6 pH change and hydrogen production on molasses with 20 mM sucrose by *R. capsulatus* YO3 157

Table G.1 pH change and hydrogen production on 10 mM sucrose by *R. capsulatus* YO3 159

Table G.2 pH change and hydrogen production on molasses with 10 mM sucrose by *R. capsulatus* YO3 160

Table H.1 Hydrogen production by cyclic microaerobic dark fermentation by immobilized *Rp. palustris* CGA009 on 2 mM glucose, 4% oxygen and different inoculum volume (Cycle 1) 161

Table H.2 Hydrogen production by cyclic microaerobic dark fermentation by immobilized *Rp. palustris* CGA009 on 2 mM glucose, 4% oxygen and different inoculum volume (Cycle 2) 161

Table H.3 Hydrogen production by cyclic microaerobic dark fermentation by immobilized *Rp. palustris* CGA009 on 2 mM glucose, 4% oxygen and different inoculum volume (Cycle 3). 162

Table H.4 Hydrogen production by cyclic microaerobic dark fermentation by immobilized *Rp. palustris* CGA009 on 2 mM glucose, 4% oxygen and different inoculum volume (Cycle 4). 162

Table H.5 Hydrogen production by cyclic microaerobic dark fermentation by immobilized *Rp. palustris* CGA009 on 2 mM glucose, 4% oxygen and different inoculum volume (Cycle 5). 163

Table H.6 Hydrogen production by cyclic microaerobic dark fermentation by immobilized *Rp. palustris* CGA009 on 2 mM glucose, 100 (v/v%) inoculum and different oxygen concentrations (Cycle 1). 163

Table H.7 Hydrogen production by cyclic microaerobic dark fermentation by immobilized *Rp. palustris* CGA009 on 2 mM glucose, 100 (v/v%) inoculum and different oxygen concentrations (Cycle 2). 164

Table H.8 Hydrogen production by cyclic microaerobic dark fermentation by immobilized *Rp. palustris* CGA009 on 2 mM glucose, 100 (v/v%) inoculum and different oxygen concentrations (Cycle 3). 164

Table H.9 Hydrogen production by cyclic microaerobic dark fermentation by immobilized *Rp. palustris* CGA009 on 2 mM glucose, 100 (v/v%) inoculum and different oxygen concentrations (Cycle 4) 165

Table H.10 Hydrogen production by cyclic microaerobic dark fermentation by immobilized *Rp. palustris* CGA009 on 2 mM glucose, 100 (v/v%) inoculum and different oxygen concentrations (Cycle 5). 165

Table H.11 Hydrogen production via cyclic microaerobic dark fermentation by immobilized *Rp. palustris* CGA009 on 100 (%v/v) inoculum, 4% oxygen and different initial glucose concentrations (Cycle 1). 166

Table H.12 Hydrogen production via cyclic microaerobic dark fermentation by immobilized *Rp. palustris* CGA009 on 100 (%v/v) inoculum, 4% oxygen and different initial glucose concentrations (Cycle 2). 166

Table H.13 Hydrogen production via cyclic microaerobic dark fermentation by immobilized *Rp. palustris* CGA009 on 100 (%v/v) inoculum, 4% oxygen and different initial glucose concentrations (Cycle 3). 167

Table H.14 Hydrogen production via cyclic microaerobic dark fermentation by immobilized *Rp. palustris* CGA009 on 100 (%v/v) inoculum, 4% oxygen and different initial glucose concentrations (Cycle 4) 167

Table H.15 Hydrogen production via cyclic microaerobic dark fermentation by immobilized *Rp. palustris* CGA009 on 100 (%v/v) inoculum, 4% oxygen and different initial glucose concentrations (Cycle 5). 168

Table H.16 Cumulative hydrogen production throughout the sequential microaerobic dark fermentation and photofermentation on different inoculum concentration. 168

Table H.17 Cumulative hydrogen production throughout the sequential microaerobic dark fermentation and photofermentation on different oxygen concentration. 169

Table H.18 Cumulative hydrogen production throughout the sequential microaerobic dark fermentation and photofermentation on different initial glucose concentration. 170

LIST OF FIGURES

FIGURES

Figure 2.1 Distribution of World total primary energy supply from 1973 to 2014. 5

Figure 2.2 Fuel shares of CO_2 emissions from fuel combustion in 1973 and 2014.6

Figure 2.3 Hydrogen production in dark fermentation..... 11

Figure 2.4 Metabolic pathways in hydrogen production. 12

Figure 2.5 Hydrogen production mechanisms of purple non-sulfur bacteria (PNSB) including main processes under photoheterotrophic conditions. 14

Figure 2.6 Hydrogen production metabolism of PNSB on sugars (glucose, fructose, sucrose) 16

Figure 2.7 Microaerobic dark fermentative hydrogen production by purple non-sulfur bacteria. 18

Figure 2.8 Sequential microaerobic dark- and photo fermentation of *R. capsulatus* JP91 19

Figure 2.9 Flat panel photobioreactors (1-4) operated at outdoors 31

Figure 2.10 Stacked U-tube photobioreactor at outdoor conditions..... 31

Figure 3.1 A rectangular empty frame (23 cm x 19 cm x 1 cm) made from nylon fabric network and glass sheets. 35

Figure 3.2 A frame of agar immobilized *R. capsulatus* YO3..... 35

Figure 3.3 Indoor experimental setup..... 36

Figure 3.4 Outdoor experimental setup 37

Figure 4.1 Sequential hydrogen production by immobilized *R. capsulatus* YO3 on 5 mM sucrose in indoor conditions. 44

Figure 4.2 Cumulative hydrogen production of immobilized R. capsulatus YO3 on 5 mM sucrose in indoor conditions. 45

Figure 4.3 pH change vs time by immobilized *R. capsulatus* YO3 on 5 mM sucrose in indoor conditions. 46

Figure 4.4 Long-term sequential hydrogen production of immobilized *R. capsulatus* YO3 on 5 mM sucrose for 64 days in indoor conditions. 47

Figure 4.5 Cumulative hydrogen production of immobilized *R. capsulatus* YO3 throughout the long-term hydrogen production on 5 mM sucrose for 64 days. ... 48

Figure 4.6 The change in pH during the long-term hydrogen production of immobilized *R. capsulatus* YO3 on 5 mM sucrose for 64 days..... 49

Figure 4.7 Sequential hydrogen production by immobilized *R. capsulatus* YO3 on 10 mM sucrose in indoor conditions. 51

Figure 4.8 Cumulative hydrogen production by immobilized *R. capsulatus* YO3 on 10 mM sucrose in indoor conditions. 52

Figure 4.9 pH change vs time by immobilized *R. capsulatus* YO3 on 10 mM sucrose in indoor conditions. 52

Figure 4.10 Sequential hydrogen production by immobilized *R. capsulatus* YO3 on 20 mM sucrose in indoor conditions. 54

Figure 4.11 pH change vs time by immobilized *R. capsulatus* YO3 on 20 mM sucrose in indoor conditions 55

Figure 4.12 Sequential hydrogen production by immobilized *R. Capsulatus* YO3 on 10 mM initial sucrose in outdoor conditions. 57

Figure 4.13 Cumulative hydrogen production of *R. Capsulatus* YO3 on 10 mM initial sucrose in outdoor conditions. 57

Figure 4.14 pH change vs time by immobilized *R. capsulatus* YO3 on 10 mM initial sucrose in outdoor conditions 58

Figure 4.15 Variation of the reactor internal temperature, T (In), ambient air temperature, T (Out), and incident solar radiation during outdoor hydrogen production on 10 mM initial sucrose concentration..... 60

Fig. 4.16 Cumulative hydrogen production of immobilized *R. capsulatus* YO3 on different initial sucrose concentrations by indoor (●:5 mM; ▲: 10 mM; ■: 20 mM) and outdoor (Δ:10 mM) photofermentation throughout the process..... 62

Figure 4.17 Comparison of mean substrate conversion efficiency, productivity and sucrose consumption on different initial sucrose concentrations (5 mM, 10 mM, 20 mM) in indoor and outdoor conditions. 63

Figure 4.18 Sequential hydrogen production by immobilized *R. capsulatus* YO3 on molasses with 5 mM initial sucrose in indoor conditions.. 65

Figure 4.19 Cumulative hydrogen production of immobilized *R. capsulatus* YO3 on molasses with 5 mM initial sucrose in indoor conditions. 65

Figure 4.20 pH change vs time on molasses with 5 mM initial sucrose by immobilized *R. capsulatus* YO3 in indoor conditions.. 66

Figure 4.21 Sequential hydrogen production on molasses with 10 mM initial sucrose in indoor conditions. 68

Figure 4.22 Cumulative hydrogen production on molasses with 10 mM initial sucrose in indoor conditions. 68

Figure 4.23 pH change vs time on molasses with 10 mM initial sucrose in indoor conditions. 69

Figure 4.24 Cumulative hydrogen production of immobilized *R. capsulatus* YO3 on molasses with 20 mM initial sucrose in indoor conditions. 71

Figure 4.25 Cumulative hydrogen production on molasses with 20 mM initial sucrose in indoor conditions. 72

Figure 4.26 pH change vs time on molasses with 20 mM initial sucrose in indoor conditions. 73

Figure 4.27 Sequential hydrogen production on molasses with 10 mM initial sucrose in outdoor conditions 75

Figure 4.28 Cumulative hydrogen production on molasses with 10 mM initial sucrose in outdoor conditions. 76

Figure 4.29 pH change vs time on molasses with 10 mM initial sucrose in outdoor conditions. 77

Figure 4.30 Temperature (In and out) and solar radiation vs time on molasses with 10 mM initial sucrose in outdoor conditions. 78

Figure 4.31 Cumulative hydrogen production in indoor (■) and outdoor (▲) conditions on 10 mM molasses. 81

Figure 4.32 RSM contour plots for the hydrogen yields of *Rp. palustris* CGA009. 87

Figure 4.33 RSM contour plots for the hydrogen yields of immobilized *Rp. palustris* CGA009 91

Figure 4.34 RSM contour plots for the hydrogen production of immobilized *Rp. palustris* CGA009. 92

Figure 4.35 Hydrogen production by cyclic microaerobic dark fermentation by immobilized *Rp. palustris* CGA009 at different inoculum volume (25%, 50% and 100%) 94

Figure 4.36 Hydrogen production by cyclic microaerobic dark fermentation by immobilized *Rp. palustris* CGA009 on different oxygen concentrations (1%, 4.5%, 8%). 95

Figure 4.37 Hydrogen production via cyclic microaerobic dark fermentation by immobilized *Rp. palustris* CGA009 on different initial glucose concentrations (2 mM, 6 mM, 10 mM). 97

Figure 4.38 Cumulative hydrogen production throughout the sequential microaerobic dark fermentation and photofermentation on different inoculum concentration (25-50-100 v/v %).. 100

Figure 4.39 Cumulative hydrogen production throughout the sequential microaerobic dark fermentation and photofermentation on different oxygen concentration (1%, 4.5% and 8 %)..... 102

Figure 4.40 Cumulative hydrogen production throughout the sequential microaerobic dark fermentation and photofermentation on different initial glucose concentration (2-6-10 mM). 103

Figure 4.41 pH change of the sequential microaerobic dark fermentation and photofermentation on different initial glucose concentration (2-6-10 mM). 103

Figure 4.42 RSM plots for hydrogen yields (A, B, C) of immobilized *Rp. palustris* CGA009.. 108

Figure 4.43 RSM plots for hydrogen production (A, B, C) of immobilized *Rp. palustris* CGA009. 109

Figure 4.44 Perturbation analysis for hydrogen yield as functions of changes in inoculum conc; (A), glucose conc; (B) and oxygen conc; (C)..... 110

Figure 4.45 RSM plots for hydrogen yields (A, B, C) of immobilized *R. capsulatus* JP91..... 113

Figure 4.46 RSM plots for hydrogen production (A, B, C) of immobilized *R. capsulatus* JP91..... 114

Figure 4.47 Perturbation analysis for hydrogen yield as functions of changes in inoculum conc; (A), glucose conc; (B) and oxygen conc; (C)..... 115

Figure B1. Sample HPLC organic acid chromatogram 141

Figure B2. HPLC calibration for acetic acid. 142

Figure B3. HPLC calibration for formic acid 142

Figure C1. Sample HPLC sucrose chromatogram 143

Figure C2 Sample standard sucrose calibration curve 144

Figure D1. Sample gas chromatogram 145

LIST OF SYMBOLS AND ABBREVIATIONS

Acetyl-CoA	Acetyl Coenzyme A
ADP	Adenosine di-Phosphate
ATP	Adenosine tri-Phosphate
C	Carbon
C_0	Initial concentration
C_f	Final concentration
COD	Chemical Oxygen Demand
Fd	Ferredoxin
GC	Gas Chromatography
gdcw	Gram dry cell weight of bacteria
H_2	Hydrogen
h	Hour
HPLC	High Pressure Liquid Chromatography
Hup-	Uptake Hydrogenase Deficient
L	Liter
L_c	Liter-culture
mM	Millimolar
mmol	Millimole
N	Nitrogen
NAD	Nicotineamid Adenine Dinucleotide
PBR	Photobioreactor
PHB	Poly-β-hydroxy butyrate
p_i	Inorganic Phosphate
PNS	Purple Non-Sulphur
PNSB	Purple Non-Sulphur Bacteria
PFL	Pyruvate formate lyase
PFOR	Pyruvate:ferredoxin oxidoreductase

TCA	Tricarboxylic acid
R. capsulatus	*Rhodobacter capsulatus*
R. palustris	*Rhodopseudomonas palustris*
R. sphaeroides	*Rhodobacter sphaeroides*

CHAPTER 1

INTRODUCTION

The depletion of fossil resources and accelerated increase in the accumulation of the greenhouse gases gradually contribute to global warming and climate change in the earth. This problem currently holds a high concern by the researchers who deal particularly with the environment, energy, biodiversity, and climate.

Global energy demand increases gradually in our life day by day. The main problem in energy production arises from increasing human population and limited energy reserves in the world. Therefore, an energy crisis is inevitable as the available energy facilities are limited and will be depleted soon by the growing human activities, an energy crisis is inevitable if alternative energy sources cannot be found. Total consumption of energy in the world doubled between 1973 (4244 Mtoe) and 2014 (9426 Mtoe). About half of the total produced energy comes from the United States (~2000 Mtoe). The remaining part of the energy production belong to Canada, Australia, Norway and Mexico in order of a decreasing amount (International Energy Agency, 2016). Currently, most of the energy is obtained from the utilization of oil (31%), coal (28%), natural gas (21%), biofuels and waste (10%) nuclear (5%), hydro (3%) and others (2%) (Wind, Solar, Heat) (International Energy Agency, 2016). Energy consumption is distributed into many sections including industry, transport, residential, services and others. Transport system mostly depend on oil while residential and services rely on electricity and gas. Moreover, economic structure of the countries also play an important role for the need of type and amount of the energy supply. However, all of the current energy supply heavily depends on fossil fuels which have limited reserves. Therefore, efforts to develop alternative energy supplies receive high attention all over the

fossil fuels which have limited reserves. Therefore, efforts to develop alternative energy supplies receive high attention all over the world and to search for alternative energy sources are already in the policies of most of the governments as one of the major issues (IEA, 2016).

The fossil fuel based energy production systems apparently lead to inevitable problems in the environment. The greenhouse gases cause global warming and climate change, which eventually change human life.

Hydrogen is a clean and renewable energy source as an alternative to the traditional energy production methods and a promising energy carrier for the future energy demand of the world. Hydrogen has two times more energy per volume than all of hydrocarbons in combustion (Das and Veziroğlu, 2001). At present, a number of methods are available for hydrogen production at various scales. The most widely used methods are electrolysis, pyrolysis, gasification, steam reforming of natural gas, and gasificaton of biomass. Industrial hydrogen production is mainly realized from steam reforming of natural gas, coal gasification, and electrolysis of water (Brentner et al., 2010; Dincer and Acar, 2015). Each production route has its own advantages and disadvantages in their applications. Biological hydrogen production can be carried out via biophotolysis, dark fermentation, and photofermentation processes.

Photofermentation is a biological process where purple non-sulfur bacteria (PNSB) utilize organic compounds and produce hydrogen. PNSB belong to a diverse group of photoheterotrophic organisms. Biohydrogen production by photofermentation offers many distinct advantages including the ability to utilize a large number of substrates, the ability of utilization from a wide range of wavelengths of light and the ability of achieving higher hydrogen yields (Das and Veziroğlu, 2001). There has been a great number of studies in photofermentative hydrogen production so far. Organic acids such as acetic acid, lactic acid and malic acid were widely used as substrates in photofermentation (Hallenbeck and Liu, 2015; Eroglu et al., 1999).

Hydrogen production from sucrose and molasses was also carried out by single-stage photofermentation. The highest hydrogen yield obtained from sucrose and molasses were 14 and 10.5 mol H_2/mol sucrose, respectively (Keskin and Hallenbeck, 2012). Similarly, hydrogen production was realized by using various PNSB on pure sucrose and molasses (Sagir et al., 2017a). They achieved a maximum hydrogen yield of 10.5 and 19 mol H_2/mol sucrose on sucrose and sugar beet molasses, respectively. Single-stage photofermentation was realized by *Rhodobacter capsulatus* YO3 in a compact tubular photobioreactor in outdoor conditions on molasses. The maximum H_2 productivity was 0.88 mol H_2/mol sucrose (Kayahan et al., 2016).

Cell immobilization is a method for confinement of cells on a matrix. This technique offers a great number of advantages over suspension cell culture systems. Among the various techniques, cell entrapment is widely used for immobilization of cells for various purposes. The support materials for cell immobilization can be polymers such as agar, alginate, porous glass, latex etc (Tsygankov and Kosourov, 2014). Agar has been widely used as support as it is a natural and cheap material (Asada et al., 2008; Elkahlout et al., 2016).

Biohydrogen production has been carried out by agar-immobilized *Rhodobacter capsulatus* on acetate in lab-scale (250 mL) photobioreactors. The highest hydrogen productivity was 2.04 mmol/L.h by immobilized *Rhodobacter capsulatus* YO3 (Elkahlout et al., 2016).

The aim of this work was to build a large scale, stable and sustainable hydrogen production system under natural conditions by using biomass. In this work, sucrose and sugar beet molasses was used as the substrate and feedstock by immobilized bacteria. Long-term hydrogen production was realized either in indoor and outdoor conditions. In addition, microaerobic dark fermentative hydrogen production was also demonstrated at lab-scale by using PNSB.

CHAPTER 2

A SURVEY OF LITERATURE

Hydrogen is a clean, renewable, and alternative fuel for the future energy requirement of the world. The energy demand increases rapidly as the world population increases day by day. Currently, most of the energy requirement is met by fossil fuel dependent resources. However, fossil-fuels have limited reserves, and therefore alternative sources are highly needed to meet the energy demand. The distribution of world primary energy supply is shown in Figure 2.1.

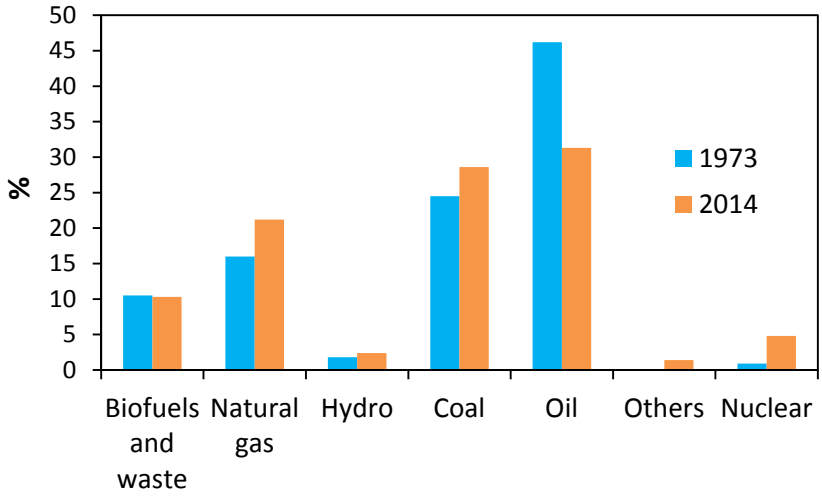

Figure 2.1 Distribution of World total primary energy supply from 1973 (6101 Mtoe) to 2014 (13699 Mtoe) (IEA, 2016). Others include solar, wind, heat, geothermal etc. Mtoe, million tons of oil equivalent.

Global warming, a phenomenon resulting from the accumulation of greenhouse gas emissions, is a critical factor affecting the nature and our life severely (IPCC, 2014). Low-carbon energy systems are highly required to alleviate potential risks of global warming. Figure 2.2 illustrates CO_2 emissions from fuel combustion in 1973 and 2014. Throughout this period, the emissions coming from natural gas and others are lower than the emissions resulting from oil and coal usage. The annual emission needs to be decreased by 85% by 2050. Therefore, low-carbon renewable power systems should be increased to mitigate overall energy demand and reduce the emissions (IEA, 2015). Energy from renewables including wind, solar and hydrogen could be promising in developing a sustainable system. Hydrogen is considered as a promising energy carrier for the future energy requirement of the world.

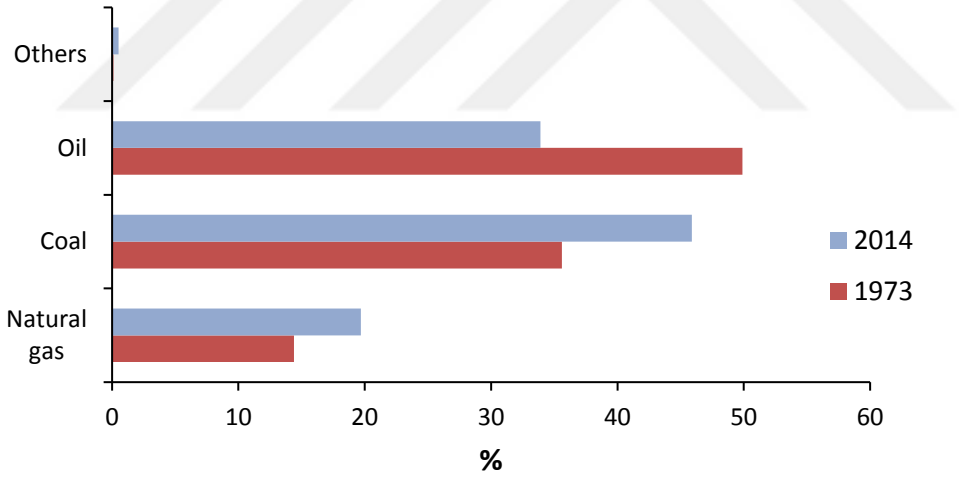

Figure 2.2 Fuel shares of CO_2 emissions from fuel combustion in 1973 (15458 Mtoe) and 2014 (32381 Mtoe) (IEA, 2016). Others include industrial waste and non-renewable municipal waste.

The following sections are comprised of major non-biological (2.1) and biological hydrogen production technologies (2.2).

2.1 Hydrogen Production Methods and Techniques

Hydrogen production is implemented by using a number of technologies including thermochemical, electrical and biological production methods. Steam reforming, partial oxidation and auto-thermal reforming are primary techniques and methods to produce hydrogen from hydrocarbons. Steam reforming is the best one among the others by requiring a lower temperature and providing high hydrogen to carbon monoxide. Therefore, steam reforming is used widely in industrial scale production (Levin and Chahine, 2009).

Hydrocarbons can also be converted into hydrogen by combustion with oxygen in a process of partial oxidation. This process does not require a catalyst and realize at higher temperatures. Auto-thermal technique provides a neutral thermal process by using partial oxidation as the source of heat and steam reforming to increase total hydrogen yield. Although steam reforming is preferred mostly, the highest emission occurs also with this process among these techniques. Both of these techniques require complex and expensive gas separation systems (Holladay et al., 2009).

Coal gasification is another common and commercially used method to obtain hydrogen. In this technology, coal is reacted with oxygen and steam under high pressure (450 psi) and temperature over 700-800 ^{0}C. As a fossil fuel, coal also has limited reserves in the world. Therefore, coal gasification is not promising for long-term since it requires high energy and results in CO_2 emission (Kothari et al., 2008).

The limited reserves of fossil sources made researchers to find alternative strategies to mitigate the energy shortage in the world. Studies on hydrogen production from renewable sources increased especially in the last decades of the 21th century (Singh and Wahid, 2015).

One of the most known methods to produce H_2 is electrolysis of water. In this method, water is separated into hydrogen and oxygen by the process of electrolysis. However, this process requires high amounts of renewable sources

and electricity. All of these requirements make the process of limited usage. Biomass is also a potential organic source for production of hydrogen. Biomass gasification is one of the common methods to obtain hydrogen, methane, and mixture of other gases. Biomass gasification is still not commercial and cost effective production plants are necessary for better hydrogen production system (Holladay et al., 2009). Biomass can also be used for H_2 production by the aid of biological processes. There are numerous biological hydrogen production methods for utilization of biomass.

All of the methods and production techniques mentioned above, have advantages and disadvantages at present. One of the challenges in this area is to build an environmentally friendly, cost effective and sustainable hydrogen production system for the long-term applications. Biological hydrogen is considered as a developing energy source to alleviate greenhouse gas emission and dependency for fossil fuels (Show et al., 2012).

2.2 Biological Hydrogen Production

Biological hydrogen production can be realized using a variety of microorganisms including green algae, cyanobacteria, PNSB and facultative anaerobic bacteria. Biophotolysis, dark and photofermentation are the major routes of biohydrogen production among the biohydrogen production methods. Biohydrogen is considered as an alternative energy production as it has a high potential of meeting energy demand of the world as a green source. Although there are some improvements with bench scale and pilot scale, industrial applications of biohydrogen production are not common (Singh and Rathore, 2015).

2.2.1 Biophotolysis

Green algae or cyanobacteria can perform photolysis by splitting of water into oxygen and hydrogen (Reaction 2.1). These organisms only require solar energy, CO_2 and basic nutrients for hydrogen production by the action of the hydrogenase enzyme. Hydrogen is produced by photolysis either directly or indirectly.

$$2H_2O \rightarrow 2H_2 + O_2 \quad (2.1)$$

Light energy absorbed by the reaction centers of green algae provides transfer of electrons from water to ferredoxin. Then, the reduced ferredoxin gives the electrons to the hydrogenase which catalyzes the production of H_2 (Eroglu and Melis, 2011). In direct photolysis, the activity of Fe-hydrogenase of some green algae was inhibited by the presence of oxygen produced during water splitting. This can be considered as an obstacle for an efficient hydrogen production. Cyanobacteria are able to consume CO_2 and water to carry out photosynthesis and then produce hydrogen in the presence of sun light and water (Reactions 2.2 and 2.3). The inhibition of hydrogenase to oxygen is circumvented by the separation of oxygen and hydrogen evolution (Hallenbeck and Benemann, 2002).

$$6H_2O + 6CO_2 + hv \rightarrow C_6H_{12}O_6 + 6O_2 \quad (2.2)$$

$$C_6H_{12}O_6 + 6H_2O + hv \rightarrow 6CO_2 + 12H_2 \quad (2.3)$$

2.2.2 Dark fermentation

Hydrogen can be produced anaerobically and in the absence of light by dark fermentation. Dark fermentative hydrogen production is the result of heterotrophic growth of bacteria under dark, anaerobic and certain temperature conditions.

All of the sugars and other organic substrates are broken down through glycolysis by resulting in pyruvate. Further oxidation of pyruvate forms acetyl-CoA and this step requires reduction of ferredoxin (Reactions 2.4 and 2.5).

$$Pyruvate + CoA + 2Fd\ (oxidized) \rightarrow Acetyl - CoA + 2Fd\ (reduced) + CO_2 \quad (2.4)$$

$$2H^+ + Fd\ (reduced) \rightarrow H_2 + Fd\ (oxidized) \quad (2.5)$$

Facultative anaerobic bacteria are more suitable than strict anaerobes due to tolerance of facultative anaerobes to oxygen, which causes inhibition of hydrogenase and reduces hydrogen production efficiency (Das and Veziroglu, 2008). Figure 2.3 illustrates major steps in dark fermentation (Hallenbeck, 2014).

Dark fermentative bacteria are usually involved in degradation of organic substrates and sugars by oxidizing them into smaller molecules to maintain their growth. Thermophilic conversion of major sugars results in formation of organic acids, CO_2 and H_2. Reactions (2.6), (2.7) and (2.8) represent conversion of glucose, xylose and sucrose by dark fermentation (Urbaniec and Grabarczyk, 2009).

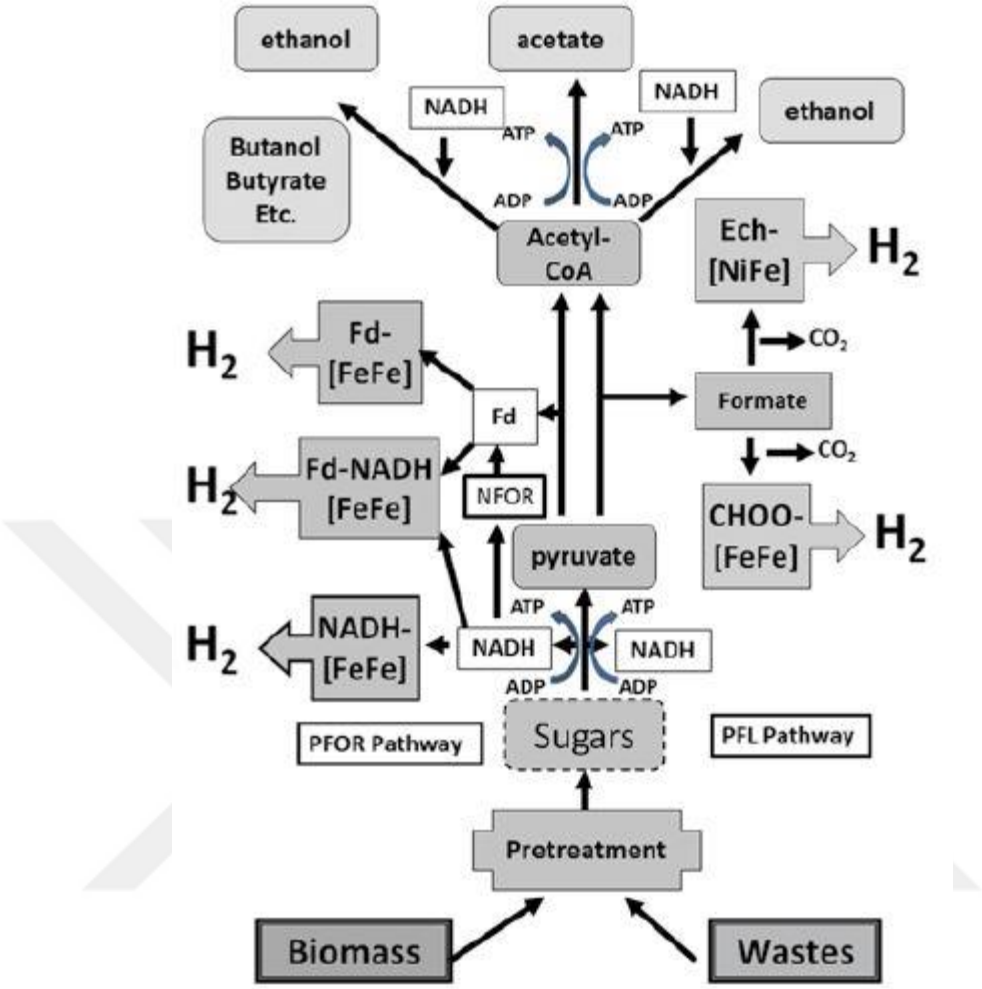

Figure 2.3 Hydrogen production in dark fermentation (Hallenbeck, 2014)

$$C_6H_{12}O_6 + 2H_2O \rightarrow 4H_2 + 2CH_3COOH + 2CO_2 \quad (2.6)$$

$$3C_5H_{10}O_5 + 5H_2O \rightarrow 10H_2 + 5CH_3COOH + 5CO_2 \quad (2.7)$$

$$C_{12}H_{22}O_{11} + 5H_2O \rightarrow 8H_2 + 4CH_3COOH + 4CO_2 \quad (2.8)$$

Clostridium species and Enterobacter are well known and used bacteria that have ability to grow under fermentative dark and anoxic conditions (Kothari et al., 2012). Hydrogen yields with glucose were obtained in the range of 0.68-3.8 mol/mol hexose by using various strains of bacteria such as *Enterobacter aerogenes* (0.68), *Clostridium beijerincki* (2.8 mol/mol hexose) *Escherichia coli* (3.12 mol/mol hexose), *Clostridium butyricum* (3.26 mol/mol hexose), *C.*

saccharolyticus (3.6 mol/mol hexose), *Enterobacter cloacae* (3.8 mol/mol hexose). Compared to glucose, hydrogen yields with fructose was low and between (0.39-2.6 mol/mol hexose). Hydrogen yields with sucrose ranged between 0.35-2.07 mol/mol hexose (Patel et al., 2012). Figure 2.4 illustrates hydrogen production pathways of glucose (Hallenbeck and Liu, 2015). After break-down of glucose via glycolysis, the fate of pyruvate change depending on the type of microorganism and expression of pyruvate degrading enzymes. Of the two major pathways, Pyruvate Formate Lyase (PFL) belongs to facultative anaerobes such as *E. coli*, and Pyruvate Formate Oxido-Reductase (PFOR), which is typical for strict anaerobes such as *Clostridium species*.

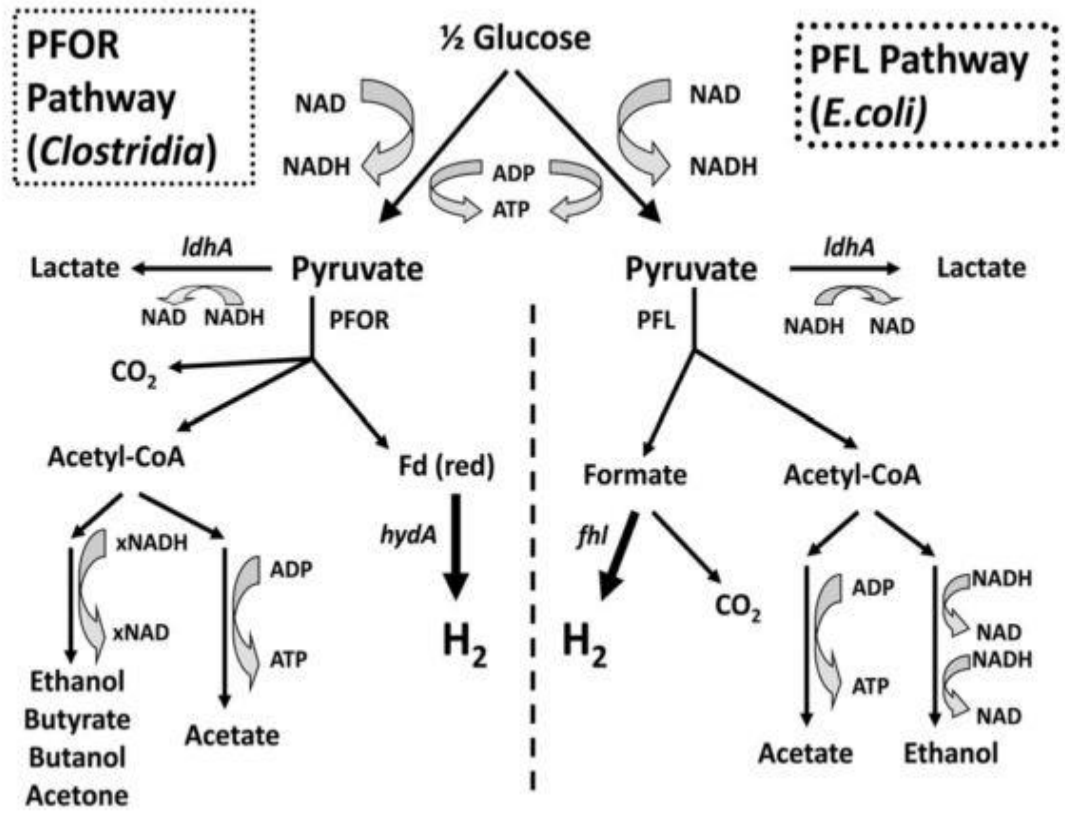

Figure 2.4 Metabolic pathways in hydrogen production (Hallenbeck and Liu, 2015).

Many of industrial and agricultural wastes are also utilized to produce biogas especially CO_2, H_2, and CH_4 by using dark fermentative process. There has been various studies using bio-wastes in dark fermentative processes such as on bagasse by using *C. butyricum* (Pattra et al., 2008), on wheat straw by *C. saccharolyticus* (Ivanova et al., 2009), on molasses by *E. coli* (Chittibabu et al., 2006), on corn starch by *E. aerogenes* (Fabiano and Perego, 2002), on palm oil trunk by *Clostridium beijerincki* (Noparat et al., 2011), and on Mischantus by *C. saccharolyticus* and *T. neapolitana* (de Vrije et al., 2009).

Although dark fermentation offers high production rates, substrate conversion yields are low and this limits efficient hydrogen production. To achieve a sustained hydrogen production, metabolic engineering studies are needed to overcome these problems. The ability of utilization of lignocellulosic wastes by a wide range of microorganisms can be a target in dark fermentative process. In addition, modification of the key pathways or introduction of new hydrogen production pathways could lead improvement of hydrogen production rate and yields (Abo- Hashesh et al., 2011).

2.2.3 Photofermentation

Biological hydrogen production can take place anaerobically by the exploitation of photosynthetic bacteria using the energy of sunlight (Figure 2.5). Nitrogenase, which is the main enzyme in the process, catalyzes molecular hydrogen production under nitrogen-limiting conditions using reduced compounds and light (Das and Veziroglu, 2008). Reactions (2.9) and (2.10) indicate the action of nitrogenase in presence or absence of nitrogen, respectively. Reaction (2.11) indicates hydrogen production by photofermentation on acetic acid under illumination.

$$N_2 + 8e^- + 8H^+ + 16ATP \rightarrow 2NH_3 + H_2 + 16ADP + 16P_i \quad (2.9)$$

$$8e^- + 8H^+ + 16ATP \rightarrow 4H_2 + 16ADP + 16P_i \quad (2.10)$$

$$CH_3COOH + 2H_2O + hv \rightarrow 4H_2 + 2CO_2 \quad (2.11)$$

Photofermentation offers a promising hydrogen production capacity using sunlight to drive photosynthesis. Particularly purple non-sulfur bacteria such as *Rhodobacter sphaeroides, Rhodospirillum rubrum, Rhodobacter capsulatus and Rhodopseudomonas palustris* are examples of widely used species for H_2 production. Photosynthetic bacteria can utilize organic substrates to produce

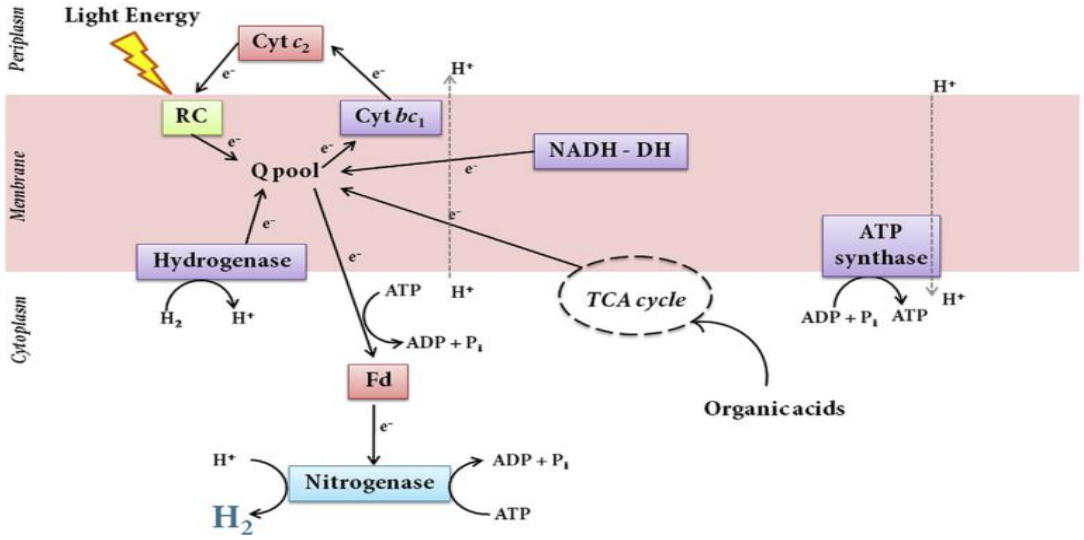

Figure 2.5 Hydrogen production mechanisms of purple non-sulfur bacteria (PNSB) including main processes under photoheterotrophic conditions (Adessi & De Philippis, 2014).

molecular hydrogen under nitrogen limitation and solar light. Of the various substrates, acetate was used mostly in photofermentation by different PNSB. Acetate concentration of 30-40 mM was found to be optimum with *Rhodobacter capsulatus* for a better hydrogen yield and productivity (Ozgur et al., 2010). Androga et al. (2011) investigated the long term stability of H_2 production by using *Rhodobacter capsulatus* on acetate for 60 days. The highest hydrogen

productivity was 0.51 mmol/L/h operation with a 4 L outdoor photobioreactor on acetate by *Rhodobacter capsulatus* YO3 (Androga et al., 2011).

Different organic wastes were used as substrates in photofermentation. In a study photobiological hydrogen production was realized using olive mill wastewater by *Rhodobacter sphaeroides* O.U.001 (Eroglu et al., 2004). Another study with *Rhodobacter sphaeroides* O.U.001 also showed that hydrogen production was achieved from sugar refinery wastewater (Yetis et al., 2000).

In a study, continuous hydrogen production from dark fermentation effluents of molasses was operated in a 4 L outdoor photobioreactor with *Rhodobacter capsulatus* YO3 (hup-) for 75 days. A hydrogen productivity of 0.67 mmol/L/h and a hydrogen yield of 78% of theoretical value have been achieved (Avcioglu, 2011).

Photofermentation was also carried out for sugars such as glucose, fructose, sucrose, xylose on a single stage process. Ghosh and Hallenbeck carried out hydrogen production from various sugars and reported highest yields with fructose, sorbitol and D-glucose (Ghosh and Hallenbeck, 2009). Single stage photofermentation was also performed with a continuous mode by *Rhodobacter capsulatus* JP91 (hup-). The highest yield of 9.0 mol H_2/mol glucose and productivities ranging from 0.57-0.81 mmol/h were obtained (Abo-Hashesh et al., 2013). In addition, biohydrogen production was carried out by various PNSB on sucrose and molasses in a single-stage photofermentation (Sagir et al., 2017a). Figure 2.6 illustrates hydrogen production pathway of PNSB from sugars.

The major drawbacks of photofermentation are presence of uptake hydrogenase, toxic effect of oxygen, ammonium or high levels of nitrogen source to nitrogenase, requirement of light and scaling up problems (Das and Veziroglu, 2008). On the other hand, different strategies will be required to overcome these problems and improve hydrogen rates and yields in photofermentative process. These studies can be modification of microorganisms or pathways such as

blocking of PHB synthesis, inhibiting acetate and formate production, changing hydrogenase and nitrogenase activities (Hallenbeck, 2014).

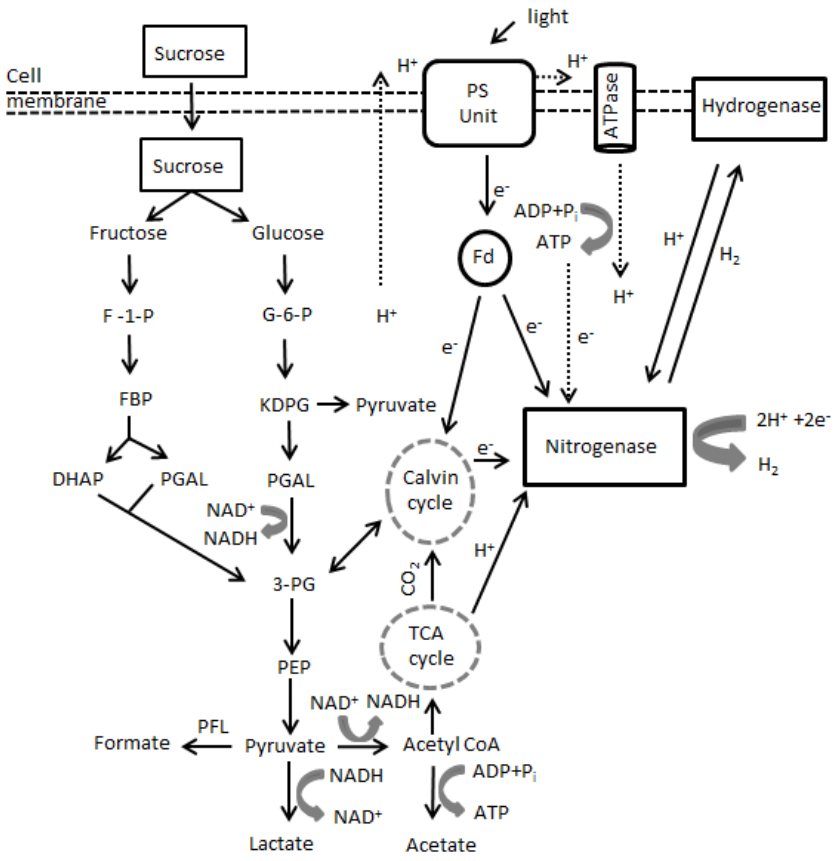

Figure 2.6 Hydrogen production metabolism of PNSB on sugars (glucose, fructose, sucrose) (Sagir et al., 2017b).

Sucrose is transported from the extracellular matrix into the cell through transmembrane carbohydrate system. Sucrose is utilized after its hydrolysis to glucose and fructose. Glucose and fructose are broken down by Purple non-sulfur bacteria via glycolysis for ATP and NADH production employing Embden-Meyerhoff-Parnas (EMP) and/or Entner Doudouroff (ED) pathways. As the result of sucrose degradation and light excitation, the produced electrons are transferred by NADH and ferredoxin to Calvin-Benson-Bassham cycle, TCA cycle and enzymes (Koku et al., 2002).

Nitrogenase catalyzes the hydrogen production by utilizing ATP and electrons coming from the TCA cycle. Hydrogenase works bi-directionally as it catalyzes both hydrogen production and consumption. Organic acids (e.g. Lactic acid, acetic acid and formic acid) were produced as byproducts of sucrose metabolism in photofermentation. Acetyl-CoA and formic acid production are carried out by PFL (Pyruvate:formate lyase) pathway (Hallenbeck et al., 2012).

2.2.4 Microaerobic dark fermentation

One of the drawbacks of employing photofermentation is low light conversion efficiency. Therefore, new photobioreactor designs and constructions are required to enhance light utilization. Photofermentation is realized under anoxygenic conditions. It is well known that nitrogenase is inhibited by oxygen. Oxidative phosphorylation offers the advantages of producing maximum energy in utilization of the substrates including sugars and organic acids. Hence, the required reducing energy could be provided instead of photophosphorylation. This metabolic pathway (TCA) takes place in the presence of oxygen. Biohydrogen production can be achieved by purple non-sulfur bacteria under microaerobic dark conditions (Rey & Harwood, 2010). Figure 2.7 illustrates the mechanism of hydrogen production through microaerobic dark fermentation. Microaerobic conditions represent an oxygen concentration lower than 21%. Microaerobic dark fermentation has been employed for hydrogen production from various substrates including acetate, lactate, malate and glucose (Abo-Hashesh & Hallenbeck, 2012).

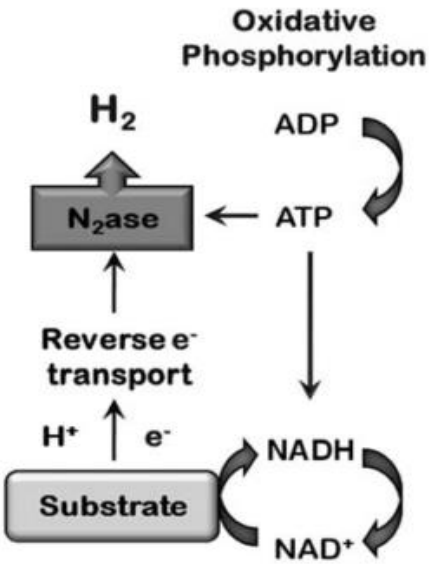

Figure 2.7 Microaerobic dark fermentative hydrogen production by purple non-sulfur bacteria (Abo-Hashesh and Hallenbeck, 2012).

Recently, hydrogen production from lactate was carried out using microaerobic conditions with a relatively high yield (1.4±0.1mol H_2/mol lactate) (Lazaro et al., 2017). They proved that hydrogen production is possible from lactate under dark fermentative microaerobic conditions. Moreover, hydrogen production by sequential microaerobic dark and photo fermentation was also demonstrated by using agar immobilized purple non-sulfur bacteria (Sagir et al., 2017c). Figure 2.8 illustrates sequential microaerobic dark and photofermentation by PNSB.

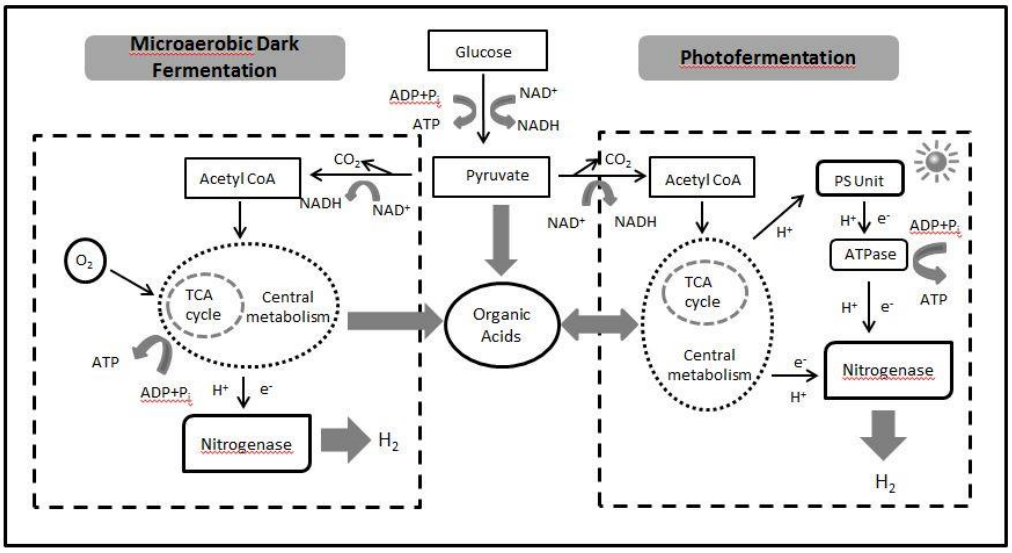

Figure 2.8 Sequential microaerobic dark- and photo fermentation of *R. capsulatus* JP91 (Sagir et al., 2017c).

Glucose is utilized via glycolysis for energy (ATP) and reducing equivalent (NADH) requirements. Organic acids are produced as byproducts of the glucose utilization throughout the microaerobic dark fermentation stage. Then, the organic acids are consumed in the photofermentation stage under continuous light illumination at 30 ^{0}C. In the dark fermentative stage, TCA cycle produces maximum ATP and NADH in response to oxygen availability via the oxidative phosphorylation. The protons coming from the glucose degradation and central metabolism are transferred to the nitrogenase, which reduces the protons and generates molecular hydrogen. As the light excites the PS unit, the protons moves to the ATPase, which produces the energy (ATP) for nitrogenase activity. In this stage, the required energy is compensated by photophosphorylation instead of oxidative phosphorylation (Sagir et al., 2017c).

2.2.5 Integrated systems

Hydrogen production can be conducted effectively by consumption of organic substrates (glucose, cellulose, sucrose etc.) in dark fermentation as the first stage, and then effluents (acetate, lactate and malate) of the first stage could be given as feed to the second stage where photofermentation takes place. In the integrated system, fermentation products are usually utilized in the second stage of the process by other microorganisms. Reduced organic compounds are transferred as substrates in the second stage by various photosynthetic bacteria (Kotay and Das, 2008). Sequential reactors and a suitable transfer method are necessary to run the whole system. However, this contributes to cost and time to complete the process. Centrifugation is followed by autoclaving in most of the cases for a sterile feed for the second stage (Redwood et al., 2009). The following reactions are for the two-stage biohydrogen production from a hexose.

Stage 1 (Dark fermentation): $C_6H_{12}O_6 + 2H_2O \rightarrow 4H_2 + 2CH_3COOH + 2CO_2$

Stage 2 (Photofermentation): $2CH_3COOH + 4H_2O \rightarrow 8H_2 + 4CO_2$

Presently, there are also combined co-culture systems for hydrogen production. To reduce time and cost, co-cultures were formed and tested for an efficient hydrogen production. In a study, hydrogen production was conducted by co-culture of *Clostridium butyricum* and *Rhodopseudomonas faecalis* RLD-53. Ding et al. obtained a hydrogen yield of 4.1 mol H_2/mol glucose and productivity of 33.85 mL/L/h by using 6 g/L glucose in 100 mL bottle reactors (Ding et al., 2009).

Co-immobilization of *Lactobacillus delbrueckii* NBRC13953 and *Rhodobacter sphaeroides*-RV resulted in a yield of 7.1 mol H_2/mol glucose, by using a 200 mL Roux bottle as the reactor (Asada et al., 2006).

Barley straw hydrolysate, which is a lignocellulosic waste, was used in dark fermentation by *C. sacchaharolyticus* followed by photofermentation with *R. capsulatus* YO3 in process to make a sequential hydrogen production. The highest

productivity (0.58 mmol $L^{-1}h^{-1}$) was achieved in 55 mL glass bottle bioreactors (Ozgur and Peksel, 2013).

In a two stage process, yields up to 14.2 mol H_2/mol sucrose have been reported with dark fermentation by *Clostridium pasteurianum* followed by photofermentation with *Rhodopseudomonas palustris* (Chen et al., 2008). Hydrogen yield of 13.7 mol H_2/mol sucrose with dark fermentation by *Caldicellulosiruptor saccharolyticus* followed by photofermentation with *Rhodobacter capsulatus* YO3 was achieved in a two-stage hydrogen production system (Ozgur et al., 2010).

Despite the fact that two stage system resulted in higher hydrogen yields (Tao et al., 2007; Chen et al., 2010; Sun et al., 2010), there are still major drawbacks related to its operation, including extensive pretreatment needs before supplying the effluent to photobioreactor and operational costs (Singh and Wahid, 2015).

2.3 Purple non-sulfur bacteria

Purple non-sulfur bacteria (PNSB) are quite versatile and categorized in the diverse groups of either *Alpha-* or *Betaproteobacteria*. *Rhodobacter capsulatus, Rhodobacter sphaeroides*, and *Rhodopseudomonas palustris* are well known mostly studied species in hydrogen production (Koku et al., 2002; Ozgur et al., 2010). They are able to consume a variety of substrates, including fatty acids, amino acids, alcohols and sugars (Madigan et al., 2000). The cells of PNSB can be ovoid, rod shaped, spherical or spiral. They can be motile or non-motile (Imhoff, 2006). PNSB can show various growth modes (photoautotrophs, photoheterotrophs or chemoheterotrophs) depending on the availability of carbon source, light and oxygen in the environment. The cells of PNSB have an optimum pH range of 6 to 9, and temperature between 25 ^{0}C and 35 ^{0}C (Sasikala et al., 1991). Hydrogen production is realized under anoxygenic, light and photoheterotrophic conditions (Basak & Das, 2006). Nitrogenase is the enzyme responsible for hydrogen production in PNSB. Hydrogen production is achieved

by the action of nitrogenase in the presence of nitrogen limited conditions (Eq. 2.12).

$$8H^+ + 8e^- + 16\ ATP \rightarrow 4\ H_2 + 16\ ADP + 16\ P_i \quad (2.10)$$

$$H_2 \leftrightarrow 2H^+ + 2e^- \quad (2.11)$$

Three different types of nitrogenase: Mo-nitrogenase, V-nitrogenase and Fe-nitrogenase are available in various strains of PNSB (McKinlay & Harwood, 2010). Hydrogenase is a membrane bound enzyme, which catalyzes reversible conversion of hydrogen into proton (Eq. 2.13). In some studies, uptake hydrogenase has been deleted to increase hydrogen production (Ozturk, 2006). Purple non-sulfur bacteria are able to utilize a wide range of substrates including acetic acid, butyric acid, lactic acid, propionic acid, malic acid, glucose, fructose, and sucrose (Eq. 2.12, 2.13, 2.14). Vitamins (Biotin, thiamin, and niacin), trace elements and iron-citrate are required as the supplementary components for PNSB (Appendix A).

$$\text{Acetate: } C_2H_4O_2 + 2H_2O \rightarrow 4H_2 + 2CO_2 \quad (2.12)$$

$$\text{Lactate: } C_3H_6O_3 + 3H_2O \rightarrow 6H_2 + 3CO_2 \quad (2.13)$$

$$\text{Malate: } C_4H_6O_5 + 3H_2O \rightarrow 6H_2 + 4CO_2 \quad (2.14)$$

The conversion of sucrose into hydrogen (24 mol) in two-stage hydrogen fermentation is given in Eq. 2.15 and 2.16 (Urbaniec and Grabarczyk, 2014).

$$C_{12}H_{22}O_{11} + 5H_2O \rightarrow C_2H_4O_2 + 8H_2 + 4CO_2 \quad (2.15)$$

$$4C_2H_4O_2 + 8H_2O \rightarrow 16H_2 + 8CO_2 \quad (2.16)$$

Purple non-sulfur bacteria, as mentioned above, are considered to be highly promising for biological hydrogen production processes by utilizing a variety of substrates.

2.4 Cell immobilization

Cell immobilization is a process of confinement of live cells localized in a region distinguished from the surrounding environment. Immobilization of cells can be divided into two broad categories: natural cell immobilization and artificial cell immobilization. Biofilm is the major example to the natural immobilization developed by microorganisms. However, the operation of natural biofilm formation is not easy and requires more time than artificial immobilization. The immobilization systems can be built by using various approaches including cell adhesion, cell encapsulation, and cell entrapment (Tsygankov and Kosourov, 2014).

Immobilization methods can be realized either as artificial cell or natural cell entrapments. An ideal immobilization is summarized to meet the following requirements. Immobilization matrix should be non-toxic to cellular activities. The matrix should also have mechanical strength characteristics against shear forces and long-time. The properties of the matrix should enhance diffusion of substances in both ways; nutrient infusion and product effusion. Simplicity, ease of operating on and low cost are also important factors. The support material should be transported to allow the penetration of the light in the reactor (Tsygankov and Kosourov, 2014).

Adsorption, encapsulation, and cell entrapment are the major methods of immobilization of the cells. The type of binding in adsorption can be specific or non-specific. Most of the bacteria have a negative charge on their surfaces. If a positively charged material is given to the bacteria, they will occupy most of the area through the surface of the material.

Bacteria have been encapsulated using various methods and materials. Gel encapsulation, latex coating, and alginate films are some major examples to

bacterial encapsulation. In gel encapsulation, different materials (alginate, silica, alumina, PVA) have been used to improve cell viability, high transparency, reduced brittle structure, desired flexibility, and porosity. However, all of these features are not found together in the same material, thereby limits the applications. Latex coating also has advantages of mechanical stability in immobilization of the bacteria. Alginate films were also used in green algal and bacterial cell immobilization. Although alginate films have low mechanical stability, different materials and polymers such as chitosan, PVA, polyurethane etc. have been crosslinked with alginate to improve the strength and stability (Kosourov and Seibert, 2009).

Gel entrapment is carried out by using a variety of natural or synthetic organic and inorganic materials including carbohydrates, proteins and polymers. Protein matrices are transparent in the visible spectrum but expensive to use in immobilization studies (Kourkoutas et al., 2004). Polysaccharides have been used extensively to immobilize cells, including agar, alginate, agarose, chitosan, cellulose, starch, pectin, and carrageenan. The major disadvantages of polysaccharides are low physical and chemical durability and stability. Therefore, its application requires other materials for further support. Polyvinyl alcohol is another material for entrapment of the cells due to its stability, transparency and low price (Tsygankov and Kosourov, 2014). UV- light polymerization, cooling, pH change, bivalent ions are some applications required for the formation of immobilized matrices.

Natural immobilization can also be used to make immobilized microorganisms for both small and large-scale industrial applications. Biofilm is natural immobilization of bacteria when they attach to a surface. Biofilm is a survival strategy of bacteria against stress conditions in the environment. Reactors including biofilms can also be used for the biological production of fuels at various conditions. Biofilm formation is a natural but slow process though it results in higher stability compared to artificial immobilization methods (Smirnova et al., 2010).

2.5 Hydrogen production by immobilized systems

Biomass can be obtained by agricultural or industrial processes; energy crops such as sugar cane, sugar beet, and corn are common plants used in energy production. Sugar-containing wastes are particularly eligible for fermentative biohydrogen production as they provide a readily utilizable carbon source for most microorganisms (Claassen et al., 2010). Immobilization of bacteria is another type of method to improve hydrogen production. Early studies of immobilization of purple non-sulfur bacteria have been carried out in the 1980s. These studies demonstrated that bacteria could be packed at high concentration. Therefore higher volumetric rates of hydrogen have been possible with immobilization (Tsygankov, 2001).

Studies in immobilization have blossomed in the 1980s and then decreased to a low level in the last decades. However, there are currently a number of groups that study immobilized systems for biofuel production. So far, a great number of immobilized purple bacteria have been reported with a variety of supporting matrices including agar (Planchard et al., 1984; von Felton et al., 1985; Liu et al., 2009), PVA (Tian et al., 2009; Bai et al., 2010), alginate (Merugu et al., 2012), latex (Gosse et al., 2007), porous glasses (Tsygankov et al., 1994; Zagrodnik et al., 2015), glass beads (Tian et al., 2010), active carbon fibers (Xie et al., 2012a).

The advantages of using immobilized cells in bioprocess systems are use of higher cell concentrations per volume of the reactor, the ability for operation in the growth phase for a long-time, requiring less space than suspension cultures, providing a more stable catalytic activity and resistance to contamination, side products and inhibitors (Basak et al., 2014; Singh and Wahid 2015).

There have been many reports in hydrogen production with cell immobilization. One of the purposes of immobilization is to prevent the bacteria from the inhibitory effect of the metabolites. Various materials such as cationic polyelectrolytes, polyethyleneimine, and trimethyl ammonium glycol chitosan iodide were used to entrap *Rhodobacter sphaeroides* RV for prevention of the

inhibitory effect of ammonium. Hydrogen production was enhanced by the bacteria immobilized with chitosan in the presence of NH_4^+. It was also reported that chitosan increased the resistance to diffusion of NH_4^+ in the matrice but not that of negatively charged lactate which was used as the carbon source (Zhu et al., 1999a). Similarly, the inhibitory effect of ammonium was alleviated by agar gel-immobilized *Rhodobacter sphaeroides* in a study of hydrogen production on wastewater of tofu factory (Zhu et al., 1999b).

In a study, reverse micelles were used as the microreactors to entrap the whole cells of *Rhodopseudomonas sphaeroides* or *Rhodobacter sphaeroides* 2.4.1. Hydrogen production was improved and increased to 25-35 folds. This microreactor system also protected the nitrogenase from the adverse effects of oxygen (Pandey and Pandey 2008).

The cells of *Rhodopseudomonas palustris* DSM 131 were immobilized by using different materials such as agar, carrageenan, agarose and sodium alginate. Hydrogen production by alginate-immobilized bacteria from mandelate, benzoylformate cinnamate and benzoate were twice as much of that obtained from the suspension culture (Fißler et al., 1995).

Asada et al. studied hydrogen production from five different (*Rhodobacter sphaeroides* RV, *Rhodobacter sphaeroides* NR-3, *Rhodobacter sphaeroides* S, *R. palustris*) immobilized strains of bacteria on acetate under photoheterotrophic conditions. The highest hydrogen yield of 3.03 mol H_2/mol acetate was obtained by *Rhodobacter sphaeroides* RV on 21 mM acetate. It was also concluded that acetate concentration higher than 21 mM inhibited hydrogen production. Besides, the lowest hydrogen production was obtained with *R. palustris* (Asada et al., 2008).

Two stage dark and photofermentation was conducted with a photosynthetic *R. faecalis* RLD-53 and a dark fermentative *E. harbinense* B-49 bacterium from glucose. The effluents of the dark fermentative process (mainly ethanol and acetate) were given to the agar immobilized *R. faecalis* RLD-53. The optimal

glucose concentration for dark fermantaion was 9 g/L. The hydrogen yield was lower than 2 mol H_2/mol glucose. The maximum hydrogen yield was achieved with a 9 g/L glucose and 30 mM buffer concentration. Also, an acetate/ethanol ratio of 1.2-1.5 was favorable for hydrogen production in photofermentation (Liu et al., 2009).

Hydrogen production by wild type and M55 mutant of *Synechocystis* sp. PCC 6803 encapsulated in silica sol-gel was evaluated in a study. The encapsulation process was done successfully by using some additives like glycerol and polyethylene glycol to increase the porosity. Hydrogen production was also comparable to cells suspended in the liquid culture (Dickson et al., 2009).

Recently, continuous hydrogen production with an immobilized consortium of purple non-sulfur bacteria was reported. Different materials included acrylic rods, high-density polyethylene cylinders and luffa were tested for the immobilization of the bacteria. The highest biomass was observed with luffa fibers. The highest hydrogen obtained in the study was 20 mL H_2/g VS/h (Guevara-Lopez and Buitron, 2015).

In a study, *Rhodopseudomonas palustris* CQK 01 was immobilized with PVA, alginate and carrageenan in a bioreactor in a continuous operation. The highest hydrogen production of 2.61 mmol H_2/L/h was obtained with a light conversion efficiency of 82.3% (Wang et al., 2013).

Immobilization has also been provided with natural ways. For instance, a biofilm reactor enhanced by optical fibers and additional rough surface was operated using *Rhodopseudomonas palustris* CQK 01. It was observed that these modifications enhanced the biofilm formation and thereby improved H_2 production. They also concluded that the optimal conditions for hydrogen production were glucose concentration of 60 mM, temperature 30 ^{0}C and pH 7.0. Also, the highest hydrogen production rate of 1.75 mmol/L/h was obtained in the study (Guo et al., 2011).

Different organic wastes have also been used in immobilized systems to produce hydrogen. The entrapped *Clostridium* sp. LS2 in polyethylene glycol gel beads was used on palm oil mill effluent to enhance hydrogen production rate. The researchers also optimized the PEG concentration (10% w/v), initial biomass (2.2 gcdw) and temperature 37 ^{0}C. The hydrogen production rate of 7.3 L/$_L$-POME/day and a yield of 0.31 L H_2/g COD have been achieved (Singh and Wahid, 2014).

Biohydrogen production from a PVA-boric acid gel granule containing immobilized photosynthetic *Rhodopseudomonas palustris* CQK 01 has been conducted in a PMMA vessel. The PVA-boric acid gel granule facilitated light penetration and mass transport due to their porous character. The effects of different parameters like illumination, temperature, pH and substrate solution were also investigated. The highest hydrogen of 3.6 mmol/gcdw was obtained at pH 7.0 and 30 ^{0}C (Tian et al., 2009).

A continuous hydrogen production with a groove-type biofilm reactor with *Rhodopseudomonas palustris* CQK 01 was realized under LED light illumination. The results were also compared to another flat panel photobioreactor operated in the study. The highest hydrogen rate, yield and light conversion efficiency were 3.8 mmol/m^2/h, 0.75 mol H_2/mol glucose and 3.8%, respectively. These values were 75% higher than that obtained in flat panel photobioreactor (Zhang et al., 2010).

A novel bio-carrier was developed with organic polymer that mixed with nano-size inorganic compounds for a better immobilization of *Rhodopseudomonas faecalis* RLD-53. The results indicated that the particle size, amount of the carrier and light intensity had influenced the hydrogen production of the immobilized *Rhodopseudomonas faecalis* RLD-53 significantly in a continuous process. The maximum hydrogen yield and rate were 3.24 mol H_2/mol acetate and 36.06 mL/L/h, respectively with optimum conditions of particle size (2x2 mm), amount (3% w/v) and light intensity (6000 lux) (Xie et al., 2011).

Various support materials have been used in immobilization studies. Porous glass with thickness of 6.8 mm and diameter of 100 mm were used to immobilize *Rhodobacter sphaeroides* O.U. 001 for hydrogen production. The process was conducted on a flat plate 200 cm^3 reactor in a semi-continuous manner. The maximum hydrogen yield was 4.2 mol H_2/mol malic acid. The results also showed that porous glasses are appropriate for cell immobilization for a stable hydrogen production (Zagrodnik et al., 2013). The same research group also performed a continuous hydrogen production by modified porous glass with *Rhodobacter sphaeroides* O.U. 001 on malic acid in 235 mL glass photobioreactor. The average hydrogen production rate was 12.7 mL/L.medium/h. The hydrogen production activity decreased due to the accumulation of formate and biomass in the medium (Zagrodnik et al., 2015).

Surface modified activated carbon fibers were developed to enhance biohydrogen production by *Rhodopseudomonas faecalis* RLD-53. The modification was done by HNO_3 oxidation, enhanced immobilization capacity of the cells. Thus, this changes allowed the bioreactor to operare at a low HRT and with a high organic loading rate. Besides, a hydrogen production yield of 3.3 mol H_2/mol acetate was achieved in this immobilized system (Xie et al., 2012a). In a similar study of the same group, different size and lengths of carbon fibers were examined to enhance the biological hydrogen production by *Rhodopseudomonas faecalis* RLD-53. The maximum hydrogen yield of 3.08 mol H_2/mol acetate and hydrogen production rate of 32.85 mL/L/h were obtained by using carbon fiber having a surface area of 1500 m^2/g, a length of 1 mm and an amount of 0.8 g/L (Xie et al., 2012b).

2.6 Photobioreactors

Photobioreactors (PBRs) are designed and used for biological hydrogen production. Operational parameters are key factors for the efficiency of the PBRs. Physical and chemical parameters highly influence a reactor's performance. Light

distribution, area to volume ratio, characteristics of construction material, temperature and mixing controls are some critical factors affecting the performance of a reactor (Dasgupta, 2010). An ideal photobioreactor is expected to meet at least some of the critical characteristics* below.

*Having a high surface area for the utilization of light

*Ability of providing sufficient mixing inside the photobioreactor.

*To have a temperature control system with heating and cooling.

*Having a durable, inert, transparent, cheap construction material.

There are many different reactor configurations for various purposes. METU Hydrogen Research Laboratory in Chemical Engineering department designed and built different bioreactors since 1999 for hydrogen production operating either in indoor and outdoor conditions. In photofermentation, panel (Androga et al., 2011; Avcioglu et al., 2012) and tubular (Boran et al., 2012; Kayahan et al., 2016) photobioreactors have been extensively used for hydrogen production as they have a high surface area for light utilization. Figure 2.9 and 2.10 illustrate panel and tubular photobioreactors constructed in our laboratory previously.

Figure 2.9 Flat panel photobioreactors (1-4) operated at outdoors (Androga, 2009).

Figure 2.10 Stacked U-tube photobioreactor at outdoor conditions (Kayahan et al., 2016).

2.7 Aim of the study

The aim of this thesis is to build a hydrogen producing system with a biological route for long-term hydrogen production using agar-immobilized purple non-sulfur bacteria (PNSB) in panel photobioreactors on sucrose. For this purpose, *Rhodobacter capsulatus* YO3 (hup-), a purple non-sulfur bacterium, was immobilized on agar matrix and used for hydrogen production. Firstly, the effects of initial sucrose concentration on hydrogen production capacity of the *Rhodobacter capsulatus* YO3 were investigated in indoor conditions. Thus, the optimum sucrose concentration was determined indoors. Then, the immobilized photobioreactor was operated in outdoor under natural sunlight during May and June, 2016 in Ankara, Middle East Technical University. In the second part of the study, sugar beet molasses was used as the feedstock for a sustainable long-term hydrogen production in both indoor and outdoor conditions. Outdoor long-term H_2 production was carried out after optimal initial molasses concentration has been determined. The ultimate aim was to increase hydrogen production, yield and productivity from sucrose and sucrose-based wastes. Notably, this is the first time of reporting an immobilized photobioreactor in outdoor conditions for photofermentative hydrogen production.

In the third part of the study, hydrogen production from glucose was performed by using PNSB. For this reason, microaerobic dark fermentation was examined by agar immobilized *R. capsulatus* JP91 and *Rp. palustris* CGA009 on glucose. Response surface methodology with Box-Behnken design was employed to optimize some of the critical parameters such as inoculum concentration, substrate concentration and oxygen concentration. Overall, agar immobilized PNSB was demonstrated to produce long term hydrogen production in microaerobic dark fermentative process.

CHAPTER 3

MATERIALS AND METHODS

3.1 Bacterial Strains

Rhodobacter capsulatus YO3 (Hup-), a mutant strain lacking the uptake hydrogenase, was obtained by genetic modification by Dr. Yavuz Öztürk (GMBE, TÜBİTAK-MAM, Gebze) from *Rhodobacter capsulatus* MT 1131 (Öztürk *et al*., 2006) was used in the scale-up experiments. *R. capsulatus* JP91, a markerless hup derivative of the wild-type strain, B10 and *Rp. palustris* CGA009 was kindly provided by Prof. Dr. Patrick C. Hallenbeck and used for small scale microaerobic dark fermentative studies in University of Montreal, Canada.

3.2 Growth and hydrogen production media

The bacterial strains were taken from stock culture (-80 ^{0}C) and activated by using streaking plate method. Then, the bacteria were grown on acetate/glutamate (20/10 mM) containing modified BP growth medium (Biebl and Pfennig, 1981). After autoclaving of the BP medium, vitamin solution, trace elements and iron-citrate were added to the prepared medium. The recipe of the growth medium is given in Appendix A.

In this work, hydrogen production medium contained sucrose as carbon source. Therefore, before the hydrogen production experiments, *R. capsulatus* YO3 was acclimatized to grow on sucrose. The bacteria, previously grown on acetate/glutamate (20/10 mM) containing modified BP growth medium (Biebl and Pfennig, 1981) were transferred to an acetate/sucrose/glutamate (20/10/10 mM) medium and subsequently to a sucrose/glutamate (10/10 mM) medium. Then, the cultures were incubated at 30 ºC under continuous illumination with a tungsten lamp of 2000 lux. The growth of the bacteria was monitored by a spectrophotometer (Shimadzu UV-1201) at 660 nm wavelength. The optical

density was measured using a fresh medium as the blank solution. The cell concentration has been determined by conversion of absorbance values to dry cell weights.

In scale-up studies, sucrose and sugar beet molasses were used as carbon sources for hydrogen production. Glutamate (4 mM) was used as nitrogen source for the bacteria in the sucrose experiments. The hydrogen production media was prepared with different sucrose concentrations (5 mM, 10 mM and 20 mM) and 4 mM glutamate as carbon and nitrogen sources, respectively. The initial pH of the hydrogen production medium was set to 7.5 by using potassium phosphate (30 mM) buffer. For small scale experiments, glucose was used as the sole carbon source. Monosodium glutamate (4 mM) was used as the nitrogen source in all of the experiments.

3.3 Immobilization procedure

Sucrose acclimated activated culture was grown at a temperature of 30 ^{0}C and under a continuous illumination of 200 W/m^2 in small photo-bioreactors (50 mL). The grown bacteria (OD_{660} = 1.5) were collected by centrifugation at 10000 g for 20 min. The bacterial pellets were collected and re-suspended into the basal medium. Then, the agar solution was prepared with distilled water and autoclaved at 121°C for 20 minutes. Agar was used to entrap the bacteria for hydrogen production. The bacteria were entrapped with 4% concentration of agar to immobilize the bacteria for hydrogen production. The molten agar was kept at 45 °C within a water-bath. Then, bacterial cell suspension was added to the agar solution. The concentration of immobilized bacterial cells was adjusted to 5.0 mg DCW/mL agar-gel.

The agar-bacteria gel was supported with a network of nylon fabric and sealed within a plate-frame enclosure. The rectangular frame (23 cm x 19 cm x 1 cm) was placed horizontally on a glass panel and then 200 ml of bacteria-agar complex was poured until the inner part of the frame until completely filled with the complex. A second glass panel was used to cover the agar-bacteria mixture

inside the frame to prevent leakage while the frame was cooled at 4 °C in the fridge. The reactor was then closed, filled with the hydrogen production medium and flushed with argon for 15 minutes. At the start of each round, the reactor and agar-bacteria mixture were washed with basal medium (free of nutrient). After the addition of the hydrogen production medium, the culture was flushed again with argon. Figure 3.1 and 3.2 illustrate rectangular empty and immobilized agar-bacteria frame respectively.

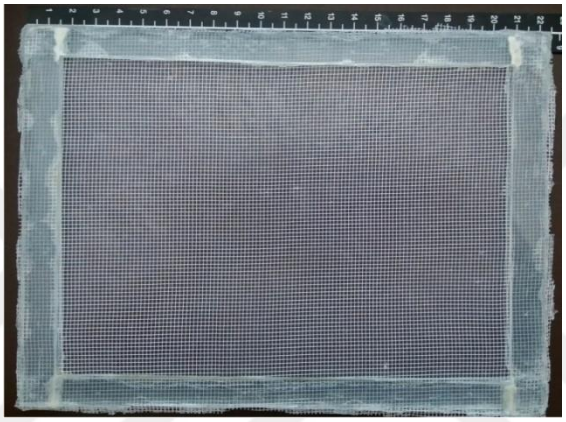

Figure 3.1 A rectangular empty frame (23 cm x 19 cm x 1 cm) made from nylon fabric network and glass sheets.

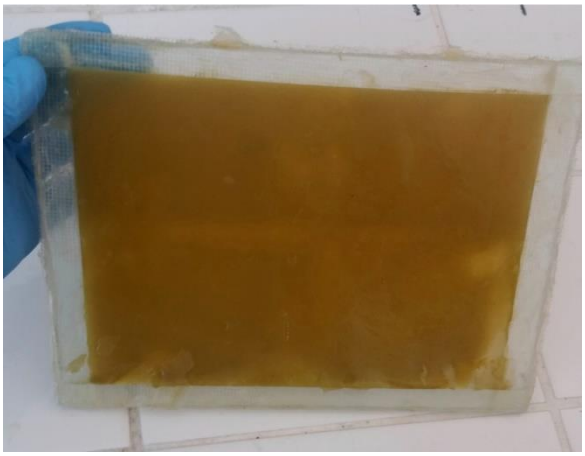

Figure 3.2 A frame of agar immobilized *R. capsulatus* YO3

3.4 Experimental Setup

Following the preparation of the agar and centrifuged bacteria, the agar-immobilized bacteria were placed on the frame (Figure 3.1, 3.2). Then, the photobioreactor was closed, washed with basal medium, filled with the hydrogen production media and flushed with argon gas for 10 minutes (Figure 3.3, 3.4). The hydrogen production media (1.1 L) was put into the reactor. The initial pH was set to 7.5 by using potassium phosphate buffer (30 mM). The photobioreactor was operated in sequential-batch mode for a total of 20 days consisting of at least 5 rounds, where each sequential batch is accepted as a round. Before each round argon gas was re-flushed to the reactor. The period of each round was 3 days. After each round, the used culture was removed and then bacteria-agar complex was washed with basal medium. The photobioreactor was then re-filled with the production medium.

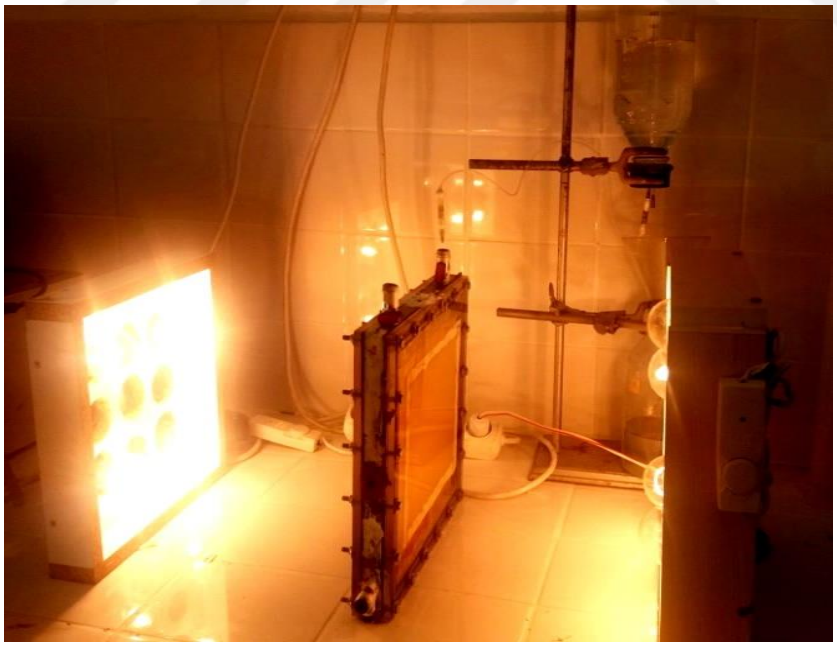

Figure 3.3 Indoor experimental setup

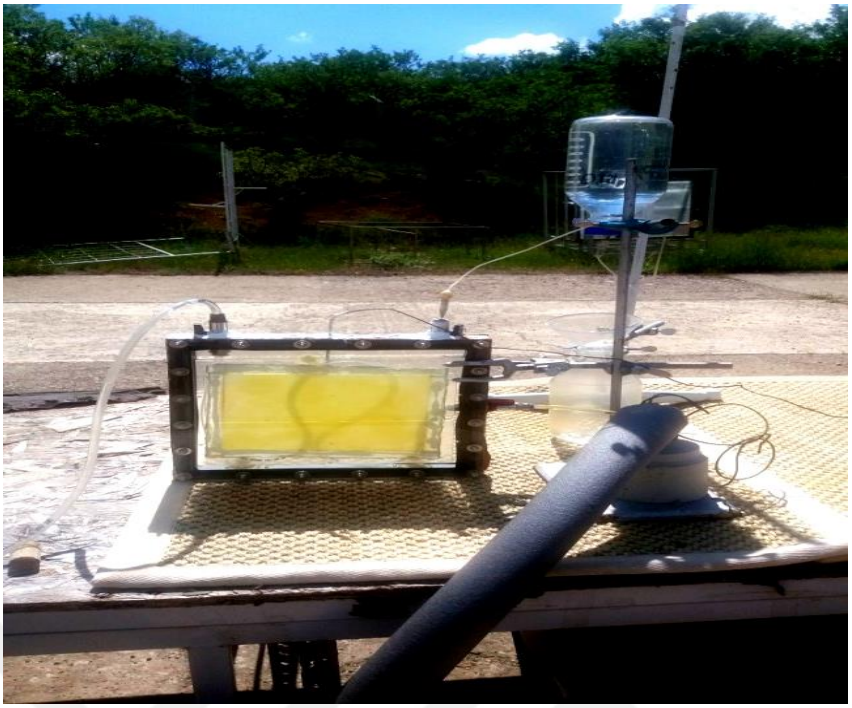

Figure 3.4 Outdoor experimental setup

3.5 Operation of the reactors

A panel reactor built from plexiglass sheets and a PVC frame was used for hydrogen production using immobilized bacteria (Figure 3.3, 3.4). The reactor had a square shape with an outer dimension of 29 cm x 29 cm x 4 cm, resulting in a total volume of 3.64 L, a ground area of 0.0116 m^2, and an area of immobilized bacteria of 0.04 m^2. The empty volume of the reactor was 1.4 L. For each batch, 1.1 L culture was added to the reactor. Natural rubber strips were used to seal the plexiglass sheets and PVC frame. Two plexiglass sheets were connected to a PVC frame together with stainless steel screws and nuts with plastic inserts. The evolved gas was collected in a cylindrical glass bottle with plastic tubing. Two globe-valves were placed at the top for gas outlet and nutrient feed, and two at one side for sampling and effluent outlet. The reactor was illuminated continuously from two sides with tungsten lamps under 4000 lux at 30 ^{0}C incubation. The experiments were performed during May and June, 2016 in Ankara, Turkey.

3.6 Temperature Control

Indoor experiments were carried out at 30 ^{0}C under continuous illumination of 200 W/m^2. External cooling fans were used to keep the internal temperature of the reactors constant. For outdoor experiments, an internal cooling system was constructed and used to keep the reactor's internal temperature around 30 ^{0}C by circulating cold (4 ^{0}C) water by using a water bath. The instant temperature and light intensity were monitored using a weather station (Davis Vantage Pro2 Weather Station).

3.7 Analytical methods

3.7.1 pH measurement

The change in pH was monitored throughout the process. Liquid samples (4 mL) were taken daily from the photobioreactors for pH measurement. The pH change was measured daily by a pH meter (Mettler Toledo 3311, Greifensee, Switzerland).

3.7.2 Organic acid and sugar analyses

Organic acid analysis was performed by HPLC (Shimadzu 20A series, Kyoto, Japan) equipped with Alltech I0A-1000 (300 mm x 7.8 mm) ion-exchange column having a UV detector (Shimadzu FCV-10AT, Kyoto, Japan). Absorbance value was set at 210 nm. H_2SO_4 (0.085 M) was used as mobile phase with a flow rate of 0.4 mL/min. Oven temperature was adjusted to 60 ºC. Organic acids such as acetic acid, formic acid and lactic acid were analyzed. Appendix B is given for a sample organic acid chromatogram.

Sugar analysis was performed by using an HPLC (Shimadzu 20A series) having Alltech I0A-1000 (300 mm x 7.8 mm) ion-exchange column. Two detectors (UV and RID) were connected in parallel series. The sugar content was determined from the results of the RID detector. The column was Alltech IOA-1000 (300 mm x 7.8 mm). 0.0085 M H_2SO4 was used as the mobile phase. The oven temperature was kept at 60

ºC. A pump (Shimadzu LC- 20AT) with a degasser (Shimadzu DGU-20A5) was used to keep the flow rate at 0.4 mL/min. RID detector (Shimadzu RID-20A) was used to determine sucrose, glucose and fructose content. Daily samples was taken from the reactors and (10 μL) were analyzed by a refractive index detector with the help of an auto sampler (Shimadzu SIL-10AC). A sample of sugar analysis chromatogram is given in Appendix C.

3.7.3 Gas composition analysis

The evolved gas was analyzed by using a gas chromatograph (GC, Agilent Technologies 6890N, California) equipped with a thermal conductivity detector and a Supelco Carboxen 1010 column. Argon gas was the carrier gas with a flow rate of 26 mL/min. Oven, injector and detector temperatures were set at 140 ºC, 160 ºC, and 170 ºC, respectively. A sample gas chromatogram is given in Appendix D. The evolved gas was composed of 80% H_2 and 20% CO_2 as averages in all the runs.

3.8 Data analyses and calculations

For the evaluation of the hydrogen production experiments, some important calculations were done such as hydrogen productivity, hydrogen yield and substrate conversion efficiency.

Hydrogen productivity is the rate of hydrogen production through the duration of H_2 production process. It was calculated and the results were compared to determine the productivities of hydrogen by PNSB bacteria on sucrose or molasses media (Eq. 3.1).

.

Hydrogen Productivity = Cumulative millimoles of hydrogen produced / volume of culture (L) x t (hour) Eq.(3.1)

Hyrogen yield was measured as the ratio of the actual mole of produced H_2 to the mole of H_2 that could be produced by the complete utilization of the

consumed sucrose. The evolved hydrogen was calculated using ideal gas equation shown in Eq. (3.2).

$$P_{H_2} \cdot V_{H_2} = n_{H_2} \cdot R \cdot T_{H_2}\ , \qquad \text{Eq.(3.2)}$$

where P_{H_2} is the pressure of hydrogen (atm) and assumed as equivalent to atmospheric pressure of Ankara, Turkey; V_{H_2} is the volume of hydrogen (L); T_{H_2} is the temperature of hydrogen (K); n_{H_2} is mol of hydrogen and R is the ideal gas constant (L·atm/mol).

Substrate conversion efficiency is the ratio of experimental produced mole of hydrogen to theoretical hydrogen production and calculated by the following formula in equation 3.3;

Substrate conversion efficiency (%) = (Experimental moles of H_2)/(Moles of theoretically produced H_2 over consumed substrate) x 100 Eq.(3.3)

The results represent mean values of at least two independent experiments ± SD (standard deviation). Appendix I is given for sample calculations of hydrogen yield, substrate conversion efficiency and hydrogen productivity.

The light conversion efficiency is the ratio of the total energy of hydrogen which was obtained to the total energy given by light radiation to the photobioreactors. Light conversion efficiency (%) = (33.6 x d_{H2} x V_{H2}) / (I x A x t) x 100, Eq.(3.4) where A is the irradiated area (m^2); I is the light intensity (W/m^2); t is the photofermentation time (h); d is density of hydrogen (0.089 g/L) and V is the produced hydrogen (L).

3.9 Microaerobic dark fermentative hydrogen production by suspended culture

In this part of the study, microaerobic dark fermentative hydrogen production by *Rp. palustris* CGA009 has been carried out. Design of experiment

with Response Surface Methodology (RSM) was used to optimize important parameters including inoculum, oxygen and glucose concentrations.

The purple non-sulfur bacterium *Rp. palustris* CGA009 was grown on RCV lactate medium and incubated at 30 ^{0}C in an Biotronette Mark III environmental chamber (Lab-line Instruments) with 150 W incandescent bulbs. The culture was used for hydrogen production experiments after the culture has grown and reached an OD of 1.5-2.0 at 660 nm.

The experiments were carried out with 160 mL glass bottles. These bioreactors was filled with 40 mL RCV glucose medium with a head space of 120 mL. Then, different volume of bacteria inoculum (25-50-75 v/v %) was added to the medium. The initial pH of 7.0 was set up with 30 mM potassium phosphate buffer. The reactors were argon flushed for 10 min in order to have the anaerobic environment. The experiment was performed for 9 days. Daily samples (2 mL) from the reactors were taken for the analysis of glucose concentration, pH, and OD_{660}.

3.10 Microaerobic dark fermentative hydrogen production by immobilized culture

The purple non-sulfur bacteria, *Rp. palustris* CGA009 and *R. capsulatus* JP91, were immobilized on agar matrix and used in separate experiments. The cultures were firstly grown on RCV lactate medium and incubated at 30 ^{0}C in an Biotronette Mark III environmental chamber (Lab-line Instruments) with 150 W incandescent bulbs. The suspension cultures were centrifuged at 10,000 rpm for 20 min when the OD of the grown culture was 1.5-2.0 at 660 nm. Bacterial pellets were re-suspended and adjusted to various concentrations. Different concentration of bacterial inoculum (25-50-75 v/v %) was mixed with 10 mL molten agar (4%) in a falcon tube. Then, the mixture was transferred to the 160 mL glass bottles. Agar-bacteria complex solidified completely after 10 min. Then bioreactors were filled with 30 mL RCV glucose medium. The initial pH of medium was adjusted to 7.0 using potassium phosphate buffer. The reactors were argon flushed for 10

min in order to maintain the anaerobic environment. Then, oxygen was taken from an oxygen tank and injected from the top of the reactors. Afterwards, the bioreactors were placed to an incubator at 30 ^{0}C for microaerobic dark fermentative process (New Brunswick Scientific Co. Inc) with an agitation of 120 rpm. In the sequential process, the bioreactors were transferred to the environmental chamber with a continuous illumination of 120 W/m^{2}. Hydrogen gas production was analyzed with a gas chromatograph (Shimadzu GC-8A) equipped with a thermal conductivity detector and a 1 m column packed with crystalline metal aluminosilicates (molecular sieve 5A) with argon as carrier gas. The oven temperature was maintained at 60 ^{0}C and the flow rate was 25 mL/min. Glucose concentration was determined by 3,5-Dinitrosalicylic Acid (DNS) Method (Miller, 1959).

CHAPTER 4

RESULTS AND DISCUSSION

4.1 Indoor and outdoor hydrogen production by immobilized *R. capsulatus* YO3 on sucrose

Utilization of sucrose in a single-stage photofermentation process is considered as a promising approach for biohydrogen production. For this reason, photofermentative hydrogen production was employed using purple non-sulfur bacteria in a panel photobioreactor. Hydrogen production was carried out by immobilized *R. capsulatus* YO3 on sucrose both in indoor and outdoor conditions. The results and discussion is given for indoor and outdoor conditions in section 4.1.1 and 4.1.2, respectively.

4.1.1 Indoor hydrogen production by immobilized *R. capsulatus* YO3 on sucrose

Initial sucrose concentration is a critical factor that has impact on cost associated with feed preparation. For instance, a feedstock with a high concentration of substrate would require less dilution if the system can tolerate high levels of substrate. Evaluation of the results obtained from different initial sucrose concentration can help to understand the effect of sucrose concentration and carbon to nitrogen ratio, on hydrogen production, productivity, and yield.

Indoor hydrogen production was started with determination of the effects of initial sucrose concentration on hydrogen production. To this end, various sucrose concentrations (5 mM, 10 mM, and 20 mM) were prepared with modified BP

medium (Biebl and Pfening, 1980). Glutamate (4 mM) was added to the medium as the nitrogen source for the bacteria. The carbon to nitrogen (C/N) ratios were 20, 35 and 65 for 5 mM, 10 mM, and 20 mM sucrose, respectively. Figure 4.1 illustrates hydrogen production obtained by immobilized *R. capsulatus* YO3 on 5 mM initial sucrose.

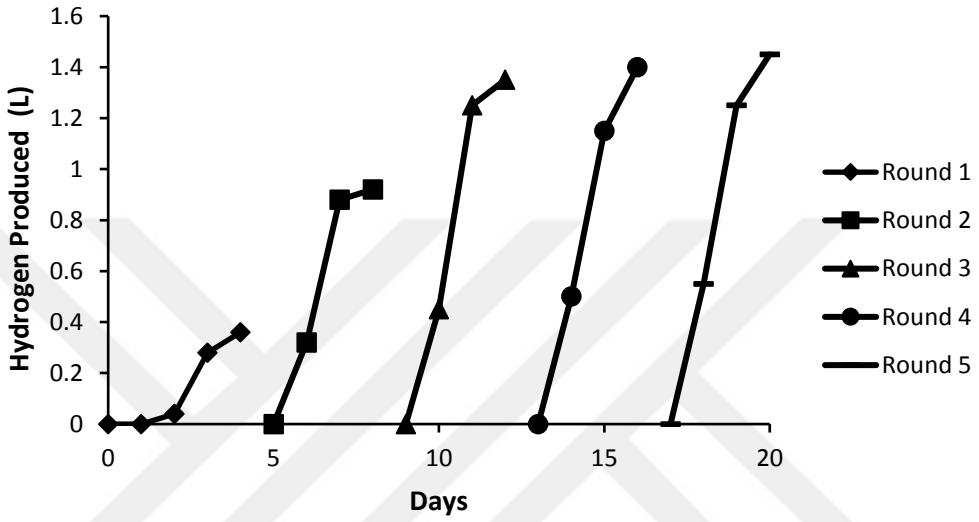

Figure 4.1 Sequential hydrogen production by immobilized *R. capsulatus* YO3 on 5 mM sucrose in indoor conditions.

The cumulative hydrogen production was 5.47 L at the end of the 5 rounds (Figure 4.2). It should be noted that the produced hydrogen at each round increased as the number of rounds increased in the sequential mode. Hydrogen production, hydrogen productivity, hydrogen yield, and sucrose consumption are illustrated in Table 4.1.

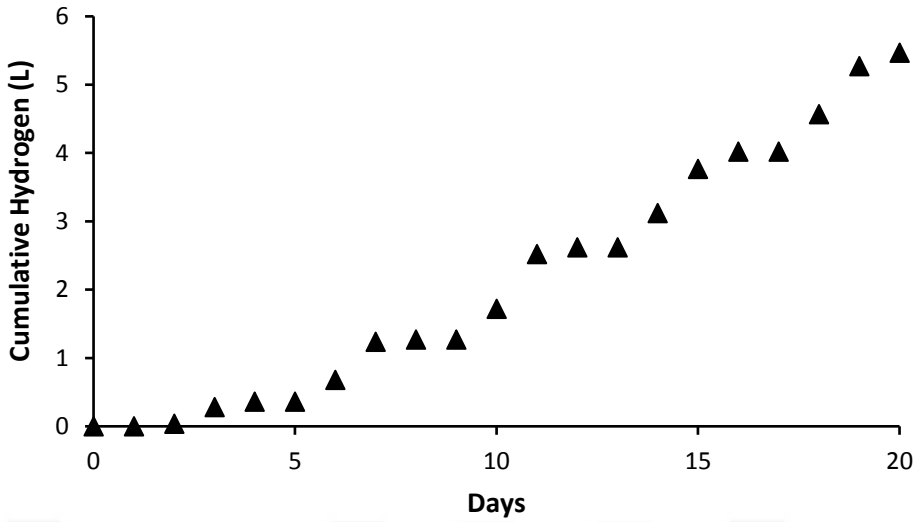

Figure 4.2 Cumulative hydrogen production of immobilized R. capsulatus YO3 on 5 mM sucrose in indoor conditions.

pH decreased from an initial pH of 7.5 to 6.3-6.4 throughout the process. The change in pH was shown in Figure 4.3. The reason of drop in pH is probably due to the accumulation of organic acids produced as the result of sucrose consumption. The majority of the produced organic acids were acetic acid, formic acid and lactic acid. The final concentrations of the organic acids are shown in Table 4.2.

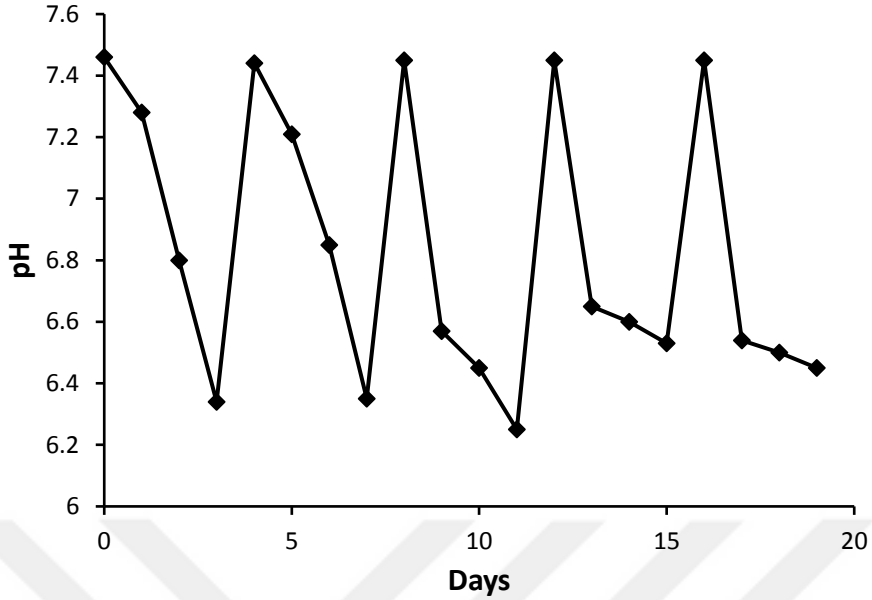

Figure 4.3 pH change vs time by immobilized *R. capsulatus* YO3 on 5 mM sucrose in indoor conditions.

It was noteworthy that hydogen productivity, yields and conversion efficiency increased as the number of rounds increased from the first to the others. The highest hydrogen yield obtained on 5 mM was 19 mol H_2/mol sucrose in the 4th round. Also, mean sucrose consumption was 50% for all the rounds (Table 4.1).

Table 4.1 Summary of long-term hydrogen production on 5 mM initial sucrose concentration

Rounds	Productivity (mmol H_2 L^{-1} h^{-1})	Molar Yield (mol H_2/mol sucrose)	Sub. Conv. Efficiency (%)	Total H_2 (L)	Sucrose Consumption (%)
Round 1	0.19	7.8	32.0	0.36	36
Round 2	0.43	14.1	58.7	0.82	43
Round 3	0.54	14.8	61.0	1.05	50
Round 4	0.71	19.0	79.0	1.40	55
Round 5	0.73	15.8	65.5	1.45	68
Mean	0.52	14.3	59.2	1.01	50.4

Table 4.2 Organic acids produced during the photofermentation on 5 mM initial sucrose concentration

Rounds	**Acetic acid (mM)**	**Formic acid (mM)**	**Lactic acid (mM)**
Round 1	4.7	0.65	0.23
Round 2	4.5	1.30	0.36
Round 3	4.3	1.32	0.44
Round 4	4.6	1.30	0.50
Round 5	4.5	1.45	0.56

Long-term hydrogen production was realized on 5 mM sucrose for 64 days comprising 16 sequential rounds. Hydrogen production was carried out in a sequential mode and shown in Figure 4.4. Hydrogen productivity ranged from 0.19 to 0.73 mmol H_2 L^{-1} h^{-1} during the sequential rounds. The H_2 yield ranged between 7.8 and 19.0 mol H_2/mol sucrose.

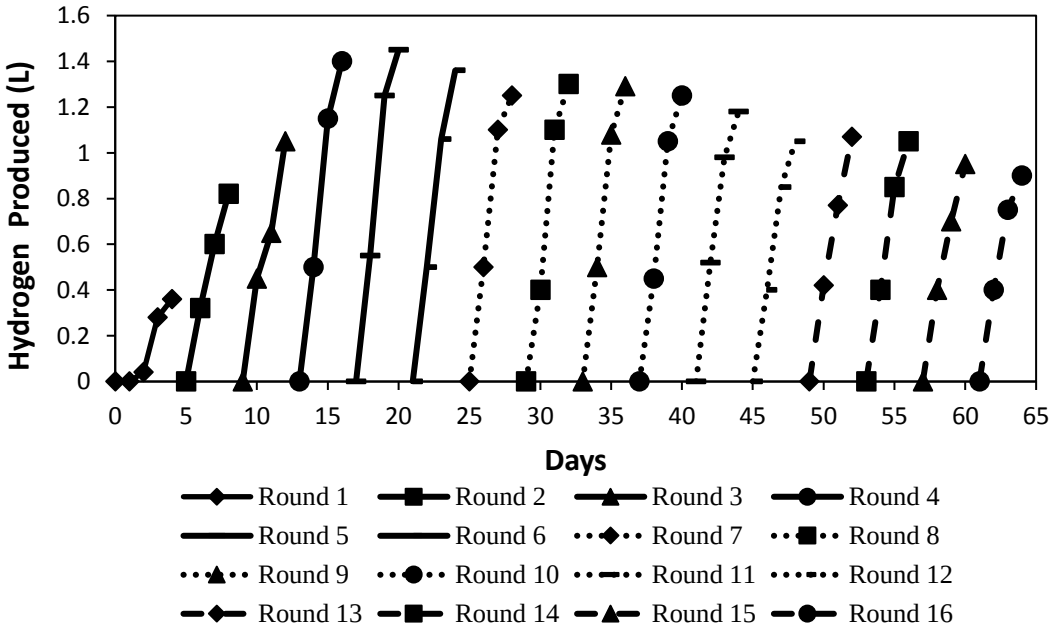

Figure 4.4 Long-term sequential hydrogen production of immobilized *R. capsulatus* YO3 on 5 mM sucrose for 64 days in indoor conditions.

The maximum hydrogen production (1.45 L) and the max H_2 productivity (0.73 mmol H_2 L^{-1} h^{-1}) were obtained in the 5th round. However, the lowest H_2 productivity was obtained at the 1st round, which might be due to the initial adaptation of the bacteria to its environment (Table 4.7). The mean H_2 production was 1.1 L per round and the mean H_2 productivity was 0.57 mmol H_2 $L^{-1}h^{-1}$. The cumulative hydrogen was around 18 L at the end of 64 days operation (Figure 4.5).

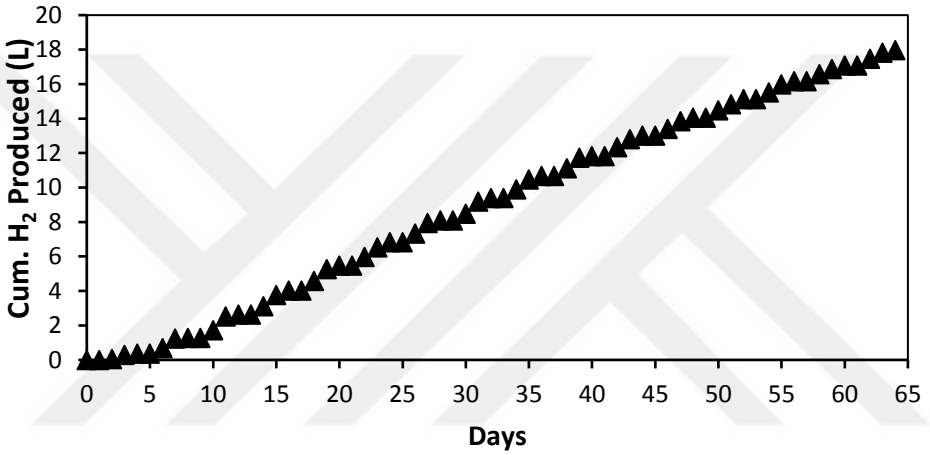

Figure 4.5 Cumulative hydrogen production of immobilized *R. capsulatus* YO3 throughout the long-term hydrogen production on 5 mM sucrose for 64 days.

Total hydrogen produced at each round increased from the first round (0.36 L) to 1.45 L at the 5th round, then started to decrease and reached 0.9 L at the end of the 16th round (Table 4.7). The hydrogen yields were comparable with the maximum yield (14 mol H_2/mol sucrose) obtained from suspended culture of *R. capsulatus* JP91 on 1 g/L sucrose in a single-stage photofermentation on sucrose (Keskin and Hallenbeck, 2012). The mean substrate conversion efficiency and sucrose consumption were 56% and 60%, respectively. The highest (19 mol H_2/mol sucrose) H_2 yield was achieved in the fourth round. It was observed that hydrogen productivity did not decrease significantly even at the latest round (16th

round). The cracks in agar-bacteria complex possibly led to the decrease in hydrogen production. pH decreased from 7.5 to ~6.2 following the first three rounds (Fig. 4.6). After the 3th round, it was observed that final pH of the subsequent rounds was about 6.5. This indicates suitability of the immobilized system for long-term hydrogen production as it allows the operation under optimal conditions.

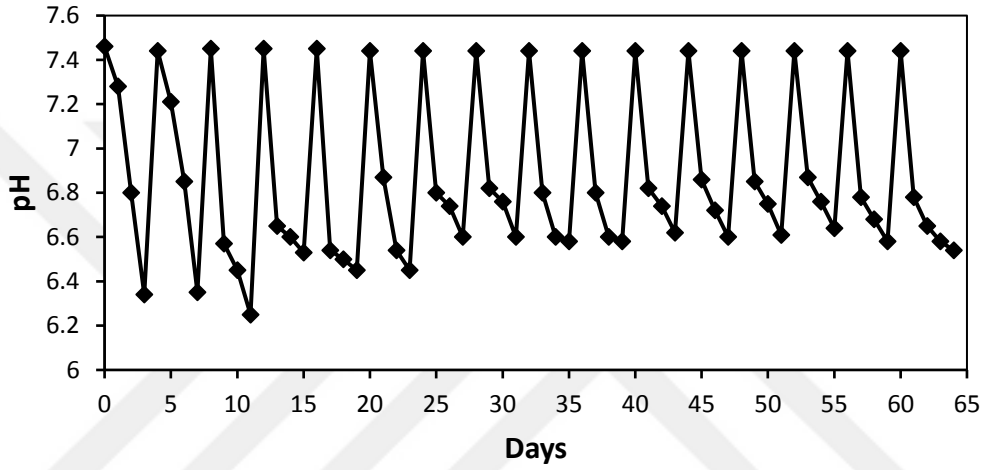

Figure 4.6 The change in pH during the long-term hydrogen production of immobilized *R. capsulatus* YO3 on 5 mM sucrose for 64 days.

Table 4.7 summarizes long-term hydrogen production, productivity, yield, conversion efficiency and sucrose consumption. The highest hydrogen productivity of 0.73 mmol H_2 L^{-1} h^{-1} was obtained in the 5th round with a substrate conversion efficiency of 65%. A maximum hydrogen yield of 19 mol H_2/mol sucrose was achieved with a substrate conversion efficiency of 79% in the 4th round. Although the loss of physical structure and other disadvantages such as limitations in diffusion of the substrate and light conversion efficiency, the use of agar is promising because of its non-toxic and biodegradable nature, low-cost and adjustable mesh size (Song et al., 2011). In the future work, some modifications in the agar frame can be done to eliminate the crack formation.

Table 4.3 Summary of the long-term hydrogen production on 5 mM initial sucrose concentration.

Rounds	Productivity (mmol H_2 L^{-1} h^{-1})	Molar Yield (mol H_2/mol sucrose)	Sub. Conv. Efficiency (%)	Total H_2 (L)	Sucrose Consumption (%)
Round 1	0.19	7.8	32.0	0.36	36
Round 2	0.43	14.1	58.7	0.82	43
Round 3	0.54	14.8	61.0	1.05	50
Round 4	0.71	19.0	79.0	1.40	55
Round 5	0.73	15.8	65.5	1.45	68
Round 6	0.70	15.7	65.4	1.36	64
Round 7	0.65	13.1	54.5	1.25	70
Round 8	0.67	16.0	66.5	1.30	60
Round 9	0.66	13.7	57.0	1.29	70
Round 10	0.65	14.2	59.1	1.25	65
Round 11	0.60	14.5	60.4	1.18	55
Round 12	0.54	12.1	50.4	1.05	65
Round 13	0.56	12.2	50.5	1.07	62
Round 14	0.54	13.0	54.1	1.05	60
Round 15	0.48	10.6	44.0	0.95	65
Round 16	0.47	10.2	42.5	0.90	65
Mean	0.57	13.5	56.3	1.10	60

When the initial sucrose concentration was 10 mM, higher hydrogen production (~1.8 L) was obtained than in 5 mM (Figure 4.7). Figure 4.7 and 4.8 are given for the sequential and cumulative hydrogen production. The cumulative hydrogen was around 7.1 at the end the of 5 rounds. Besides, hydogen productivities were also high with 10 mM initial sucrose. The maximum hydrogen productivity, 0.91±0.02 mmol H_2 L^{-1} h^{-1}, obtained in the 3rd round on 10 mM sucrose (Table 4.3). On the other hand, hydrogen yields were lower compared to 5 mM sucrose. The highest yield were 11.4±0.2 mol H_2/mol sucrose on 10 mM initial sucrose.

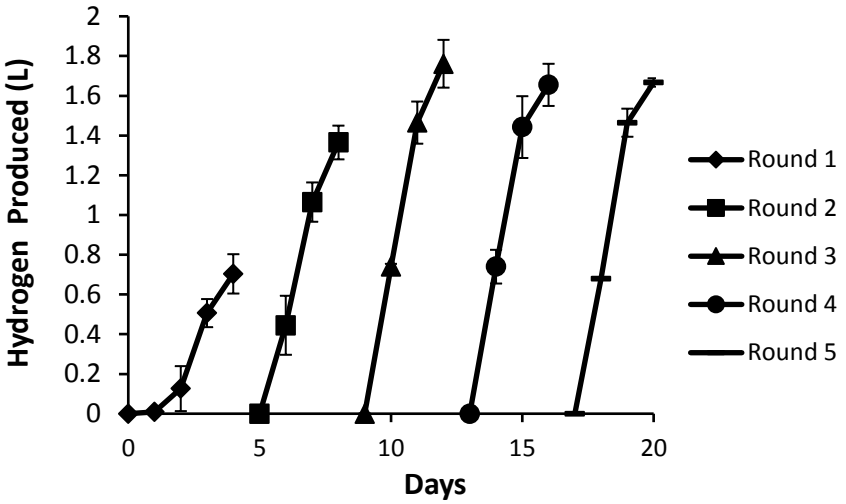

Figure 4.7 Sequential hydrogen production by immobilized *R. capsulatus* YO3 on 10 mM sucrose in indoor conditions. The values represent mean±STD.

The first round seemed as an adaptation round for the immobilized bacteria. Hydrogen production was lower in the first round than the subsequent rounds. Guevara-Lopez and Buitron reported lower H_2 production with purple non-sulfur bacteria in the first batch, as a dual effect of non-adapted bacteria and a non-optimal cell concentration on various support materials (Guevara-Lopez and Buitron, 2015). The produced hydrogen in the 5th round doubled the first round. Lag time for hydrogen production was 24 h for the first round. However, lag time was around 12 h in the subsequent rounds. This might also be explained by the adaptation of immobilized bacteria for sucrose consumption and hydrogen production.

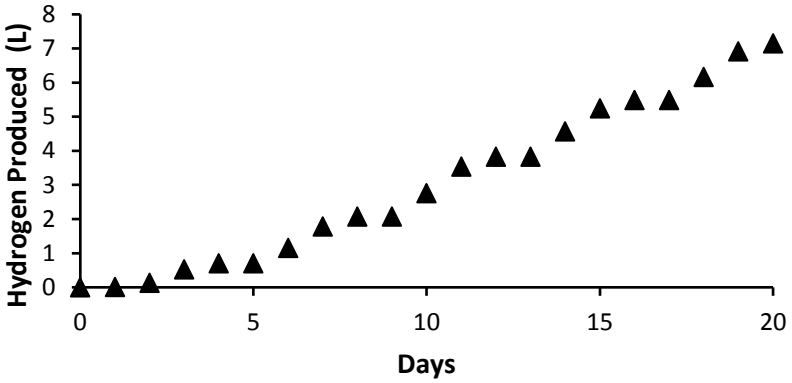

Figure 4.8 Cumulative hydrogen production by immobilized *R. capsulatus* YO3 on 10 mM sucrose in indoor conditions.

pH started to drop as the process continue to produce hydrogen. Throughout all rounds of photofermentation, final pH was above 6.0 (Figure 4.9). The system allowed the process to be carried out under optimal pH for PNSB (Sasikala et al., 1991). Acetic acid was dominant among all produced organic acids (Table 4.4). Lactic acid concentration was the lowest of all and ranged between 0.21-0.54 mM.

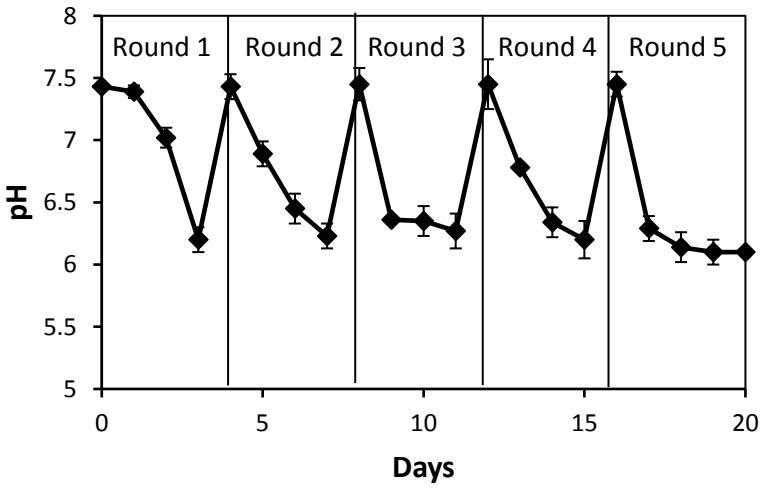

Figure 4.9 pH change vs time by immobilized *R. capsulatus* YO3 on 10 mM sucrose in indoor conditions. The values represent mean±STD.

Table 4.4 Summary of the results on 10 mM initial sucrose concentration. The values represent mean±STD.

Rounds	**Productivity (mmol H_2 L^{-1} h^{-1})**	**Molar Yield (mol H_2/mol sucrose)**	**Sub. Conv. Efficiency (%)**	**Total H_2 (L)**	**Light conversion efficiency (%)**	**Sucrose Consumption (%)**
Round 1	0.35±0.08	7.1±0.9	29.0±4.1	0.67±0.18	0.34	35±2.4
Round 2	0.67±0.07	8.9±1.5	36.0±5.2	1.31±0.16	0.66	54±2.3
Round 3	0.91±0.02	11.4±0.2	48.0±1.2	1.76±0.03	0.9	57±1.5
Round 4	0.83±0.03	10.2±0.3	43.0±1.6	1.60±0.04	0.82	58±1.8
Round 5	0.85±0.04	10.2±0.5	43.0±1.6	1.65±0.1	0.84	60±2.5
Mean	0.72±0.05	9.6±0.06	40.0±2.7	1.40±0.1	0.72	53±2.1

Table 4.5 Organic acids produced during the photofermentation on 10 mM initial sucrose concentration. The values represent mean±STD.

Rounds	**Acetate (mM)**	**Formate (mM)**	**Lactate (mM)**
Round 1	5.6	0.53	0.21
Round 2	6.1	1.7	0.41
Round 3	6.2	2.1	0.45
Round 4	5.8	2.3	0.52
Round 5	5.3	2.4	0.54

Hydrogen production was the lowest on 20 mM sucrose among the all initial sucrose concentration. This can be explained by the effects of substrate inhibition. Therefore, hydrogen productivity and yields were also low as expected (Table

4.5). Figure 4.10 is given for the sequential hydrogen production on 20 mM sucrose. It can be emphasized that hydrogen yield significantly depends on initial sucrose concentration. H_2 yield decreased from 13.5 to 3.3 mol H_2/mol sucrose when the initial sucrose concentration was increased from 5 mM to 20 mM. However, considering the overall cost, diluting the prepared feed to lower sucrose concentrations (5 mM) will require additional water and thereby increase the cost of the system. The highest light conversion efficiency (0.9%) was obtained on 10 mM sucrose.

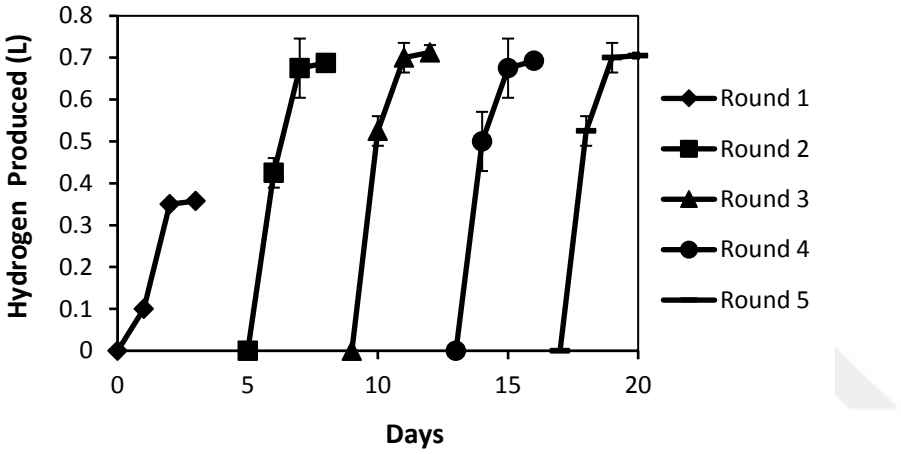

Figure 4.10 Sequential hydrogen production by immobilized *R. capsulatus* YO3 on 20 mM sucrose in indoor conditions. The values represent mean±STD.

The final pH of each round was around 5.9-6.0 (Figure 4.11). The reason of the steep drop can be attributed to the higher concentrations of produced organic acids. The decline in pH could be attributed to the highly accumulation of carbon dioxide, which has been produced during the photofermentation, caused formation of carbonic acid in the medium (Montiel-Corona et al., 2015; Kayahan et al., 2016).

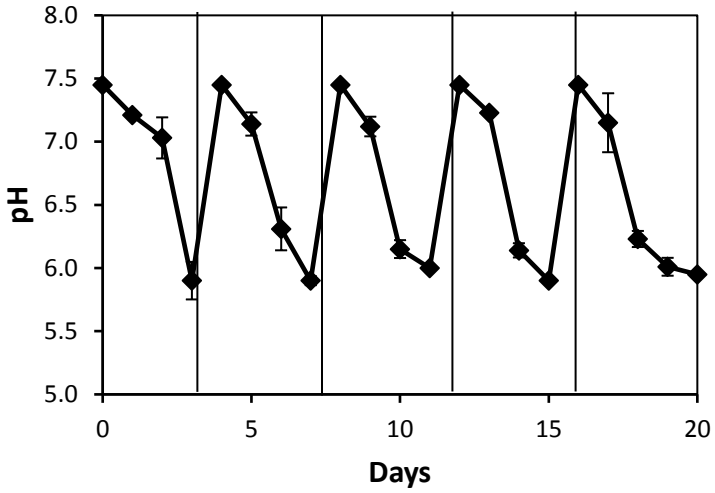

Figure 4.11 pH change vs time by immobilized *R. capsulatus* YO3 on 20 mM sucrose in indoor conditions. The values represent mean±STD.

Hydrogen yield, productivity, total hydrogen, sucrose consumption and substrate conversion efficiency are illustrated in Table 4.6.

Table 4.6 Summary hydrogen production on 20 mM initial sucrose concentration.

Rounds	**Productivity (mmol H_2 L^{-1} h^{-1})**	**Molar Yield (mol H_2/mol sucrose)**	**Sub. Conv. efficiency (%)**	**Total H_2 (L)**	**Sucrose Consumption (%)**
Round 1	0.18±0.04	2.5±0.1	10.4±0.3	0.35±0.08	25±3.2
Round 2	0.35±0.02	4.3±0.3	18.0±0.3	0.69±0.06	29±3.5
Round 3	0.37±0.02	3.8±0.2	15.8±1.8	0.71±0.05	35±3.2
Round 4	0.35±0.01	2.9±0.1	12.1±1.2	0.70±0.01	46±3.5
Round 5	0.35±0.01	3.0±0.2	12.5±0.4	0.70±0.01	44±4.2
Mean	0.32±0.02	3.3±0.2	13.7±0.8	0.63±0.04	36±3.5

The amount of the produced acetic acid and formic acid was higher as the initial sucrose concentration was 20 mM (Table 4.7). These organic acids probably responsible for the decrease in pH during the hydrogen production.

Table 4.7 Final concentrations of organic acids produced during the photofermentation on 20 mM initial sucrose concentration

Rounds	**Acetic acid (mM)**	**Formic acid (mM)**	**Lactic acid (mM)**
Round 1	7.7	1.2	0.52
Round 2	8.3	2.3	0.52
Round 3	9.1	2.3	0.43
Round 4	10.3	3.5	0.44
Round 5	10.8	4.2	0.42

4.1.2 Outdoor hydrogen production by immobilized *R. capsulatus* YO3 on sucrose

The results of the indoor studies revealed that 10 mM initial sucrose yielded higher hydrogen production and productivity values compared to the other concentrations. For this reason, outdoor hydrogen production was realized by using immobilized *R. capsulatus* YO3 on 10 mM sucrose. Figure 4.12 shows produced hydrogen throughout the sequential process while Figure 4.13 represents the cumulative hydrogen production throughout the 20 days of operation.

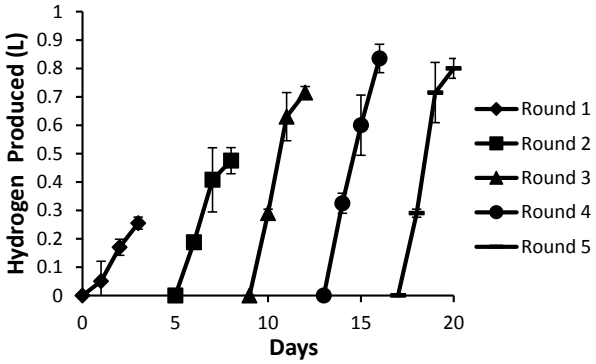

Figure 4.12 Sequential hydrogen production by immobilized *R. Capsulatus* YO3 on 10 mM initial sucrose in outdoor conditions. The values represent mean±STD.

Two times more hydrogen was produced in the 4th round than the first one. This can be attributed to the adaptation of the bacteria to its environment. The cumulative hydrogen was around 3L during the whole process (Fig. 4.12). This is lower than the values in indoor conditions. Because day/night cycle affects hydrogen production as the sunlight is critical for the photofermentation.

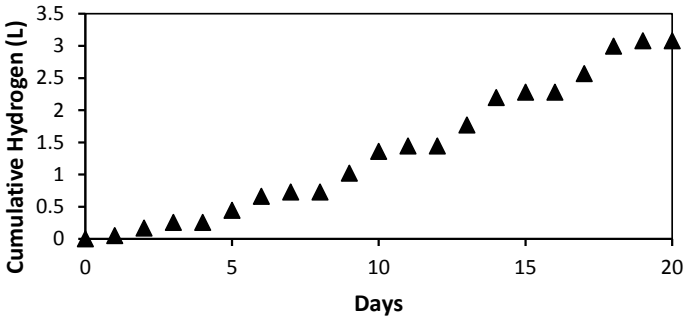

Figure 4.13 Cumulative hydrogen production of *R. Capsulatus* YO3 on 10 mM initial sucrose in outdoor conditions.

The pH during the outdoor photofermentation decreased from the initial set of 7.5 (Fig. 4.14). Although a decrease was observed at each round, the final values of the pH were above 6.0. The accumulation of organic acids including acetic acid, formic acid, and lactic acid caused a decrease in pH throughout the process. The decline in pH was less than that obtained in a study with a suspended culture of *R. capsulatus* JP91, where a final pH of 4.5–5.0 was observed in the single-stage photofermentative process on sucrose (Keskin and Hallenbeck, 2012).

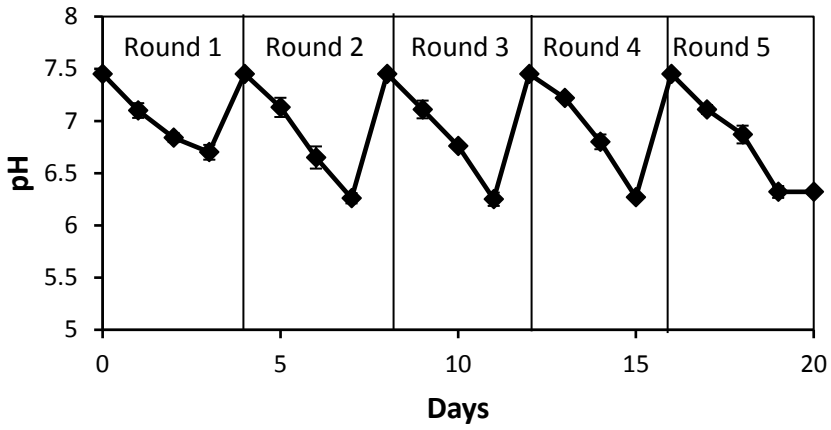

Figure 4.14 pH change vs time by immobilized *R. capsulatus* YO3 on 10 mM initial sucrose in outdoor conditions. The values represent mean±STD.

The highest hydrogen productivity and yield were achieved at the 4th round as 0.87±0.06 mmol H_2 L^{-1} h^{-1} and 6.1±0.2 mol H_2/mol sucrose, respectively (Table 4.8). The sucrose consumption ranged from 36% to 50% between the rounds. The mean sucrose consumption was 45% throughout the experiment.

The produced organic acids were acetic acid, formic acid and lactic acid (Table 4.9). The produced organic acids are responsible for the reason of decline in the pH. The drop in pH could also be caused by the accumulation of carbon dioxide, which has been produced during the process, causes acidification by forming carbonic acid. This result correlates with the findings of a related study, which reported that accumulation of carbon dioxide in the head space of the reactor developed acidification and led to a decrease in pH in the medium (Montiel-Corona et al., 2015).

Table 4.8 Summary of the results of outdoor hydrogen production by immobilized *R. capsulatus* YO3 on 10 mM sucrose.

Rounds	**Productivity (mmol H_2 L^{-1} h^{-1})**	**Molar Yield (mol H_2/mol sucrose)**	**Sub. Conv. Efficiency (%)**	**Total H_2 (L)**	**Sucrose Consumption (%)**
Round 1	0.24±0.04	2.6±0.5	14.0±2.2	0.25±0.08	36±1.2
Round 2	0.47±0.05	4.0±0.6	23.3±2.4	0.50±0.13	42±1.4
Round 3	0.71±0.02	5.0±0.3	25.3±1.2	0.70±0.12	51±3.5
Round 4	0.87±0.06	6.1±0.2	34.0±0.8	0.85±0.07	47±2.2
Round 5	0.83±0.01	5.9±0.3	34.0±1.2	0.80±0.14	50±4.2
Mean	0.62±0.03	4.7±0.4	26.1±1.3	0.62±0.2	45±2.5

Table 4.9 Final concentrations of organic acids produced during the outdoor photofermentation on 10 mM initial sucrose concentration.

Rounds	**Acetate (mM)**	**Formate (mM)**	**Lactate (mM)**
Round 1	4.3	1.2	0.44
Round 2	5.4	2.2	0.52
Round 3	5.6	2.4	0.43
Round 4	6.4	2.8	0.45
Round 5	6.3	2.7	0.52

The ambient air and inner temperature of the reactor were monitored throughout the process (Figure 4.15). The differences between internal and air temperature were 1-3 ^{0}C. This means that cooling system worked well to keep the temperature at optimal values. The air temperature ranged between 6 and 28 ^{0}C during the operation. The variations and fluctuations in temperature and solar radiation affected the H_2 production substantially. Nitrogenase, which is the main enzyme involved in hydrogen production, has an optimum temperature at 30 ^{0}C (Androga et al., 2014). The solar radiation ranged from 0 to 1200 W/m^2 during the

process. However, more stable and higher values (800–1000 W/m^2) were recorded between days 9 – 16, where higher H_2 yield and productivities were achieved.

The differences in temperature resulted in a decrease in H_2 yield and productivity apparently since bacteria used the majority of the energy in favor of adaptation to survive instead of generating hydrogen during the adverse conditions (Ozgur et al., 2010). The optimal temperature was recorded between the days of 9 and 16. The highest hydrogen production values were also obtained between days 9-17.

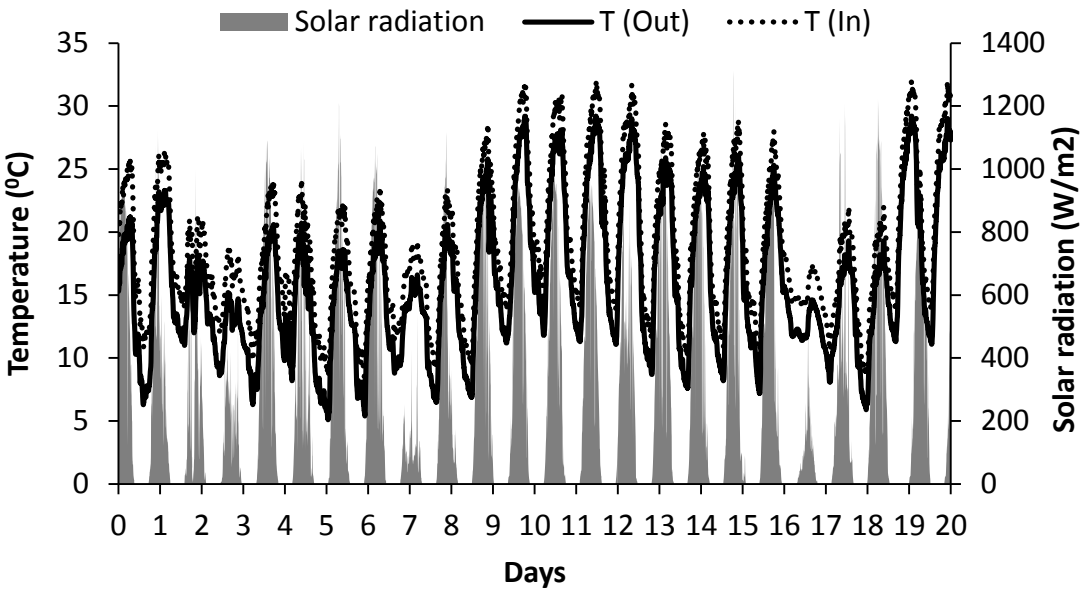

Figure 4.15 Variation of the reactor internal temperature, T (In), ambient air temperature, T (Out), and incident solar radiation during outdoor hydrogen production on 10 mM initial sucrose concentration.

4.1.3 Comparison of indoor and outdoor hydrogen production by immobilized *R. capsulatus* YO3 on sucrose

In indoor conditions, since continuous illumination was provided to the bioreactors, illumination time was about two times more than the bioreactors in outdoor. Therefore, hydrogen production and yields were lower with outdoor bioreactors than indoors. The effects of initial sucrose concentration played an important role to select the optimum substrate concentration for the operation of the reactors. Indoor studies indicated that sucrose concentration higher than 10 mM led to lower hydrogen production, yield, and productivity. Figure 4.16 is given for a comparison of cumulative hydrogen production in indoor and outdoor conditions. The cumulative hydrogen production (3.1 L) in outdoor was lower than the indoor (7.0 L) at the end of the 5th round (Figure 4.16). This could be explained by the variations in temperature and light intensity due to the day/night cycle. The maximum H_2 yield, 6.1±0.2 mol H_2/mol sucrose, in outdoor was about half of that obtained in indoors (11.4±0.2 mol H_2/mol sucrose). This correlates with the fact that during the night periods the bacteria remain dormant in terms of hydrogen production, since light dependent nitrogenase is inactive. Noteworthily, it must be underlined that the mean hydrogen productivity was only slightly lower in outdoor (0.62±0.03 mmol H_2 L^{-1} h^{-1}) than in indoor (0.72±0.05 mmol H_2 L^{-1} h^{-1}) conditions.

In indoor and outdoors, the lowest hydrogen productivity and sucrose consumption was observed in the first round. The first round seemed to be a lag period, indicating the need for an appropriate time for the initial population of bacteria to grow and adapt to the environment. A more stable and efficient hydrogen producing system was consistently observed in the subsequent rounds. Similar findings were also reported in a study with purple non-sulfur bacteria immobilized on different support materials, where they obtained lower H_2 production in the first round as a combined effect of non-adapted bacteria and a sub-optimal cell concentration on support materials (Guevara-Lopez and Buitron, 2015).

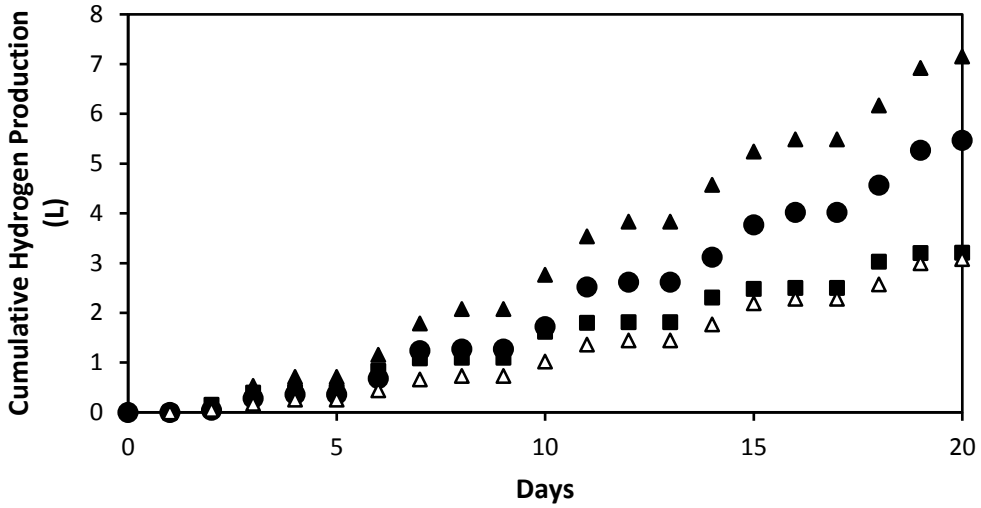

Fig. 4.16 Cumulative hydrogen production of immobilized *R. capsulatus* YO3 on different initial sucrose concentrations by indoor (●:5 mM; ▲: 10 mM; ■: 20 mM) and outdoor (Δ:10 mM) photofermentation throughout the process.

It can be concluded that when the initial sucrose concentration increase from 5 mM to 20 mM, hydrogen productivity, substrate conversion efficiency and sucrose consumption decrease (Figure 4.17). The indoor results confirm that 10 mM sucrose is optimal for operation of a reactor for a long-term process.

The carbon to nitrogen ratio (C/N) of the feed is a critical factor influencing the H_2 production and cell growth in photobioreactors. A low C/N ratio improves cell growth and decreases H_2 production, whereas a high C/N ratio reduces growth and rises H_2 production (Androga et al., 2011). In the present work, the carbon to nitrogen ratio (sucrose/glutamate) was 20, 35 and 65 at various sucrose concentrations (5 mM, 10 mM, and 20 mM). The results of this study also verify the findings of previous works, where they stated that the optimum C/N ratio was 30 for purple non-sulfur bacteria (Androga et al., 2011; Eroglu et al., 1999). Indoor studies also revealed that 10 mM sucrose and 4 mM glutamate were the optimal concentrations in terms of total hydrogen and H_2 productivity.

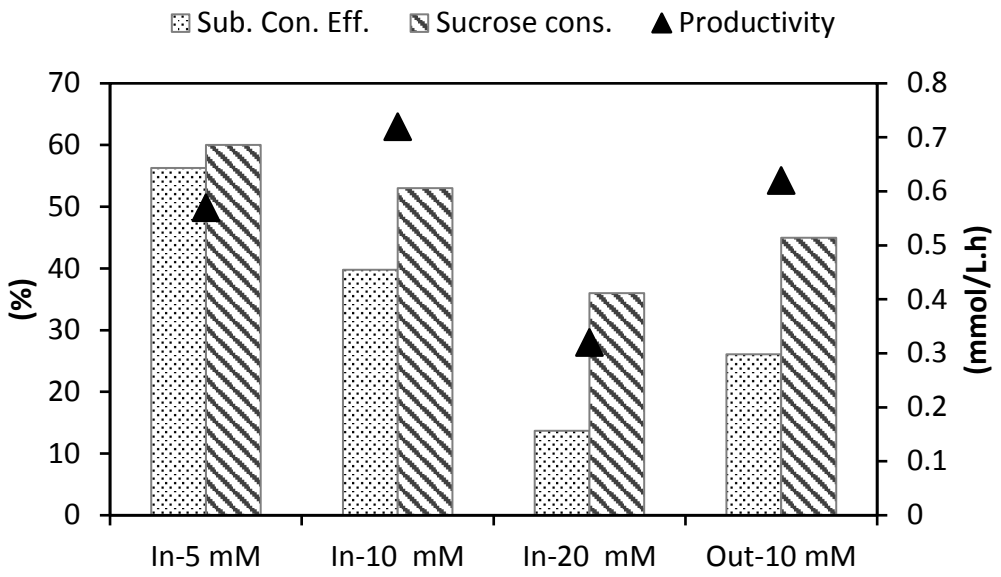

Figure 4.17 Comparison of mean substrate conversion efficiency, productivity and sucrose consumption on different initial sucrose concentrations (5 mM, 10 mM, 20 mM) in indoor and outdoor conditions.

4.2 Indoor and outdoor hydrogen production by immobilized *R. capsulatus* YO3 on sugar beet molasses

Sucrose can be found in many different industrial, agricultural and municipial wastes. Sugar beet molasses are also a potential source of sucrose. Therefore, sugar beet molasses was diluted to certain concentrations of sucrose (5 mM, 10 mM, and 20 mM) and used as carbon source for the bacteria. The required amount of molasses was calculated and added to hydrogen production medium. The experiments were carried out in indoor and outdoor natural conditions. Indoor and outdoor studies are given in section 4.2.1 and 4.2.2, respectively.

4.2.1 Indoor hydrogen production by immobilized *R. capsulatus* YO3 on sugar beet molasses

First of all, the effects of initial concentration of molasses (specifically sucrose) were examined. Raw molasses was diluted to specific concentrations of sucrose and then used as feed for the immobilized bacteria. Appendix E is given for the composition of the raw sugar beet molasses. Sequential hydrogen production on molasses with 5 mM initial sucrose in indoor conditions is shown in Figure 4.18. Single-stage photofermentation was carried out for the consecutive 5 rounds.

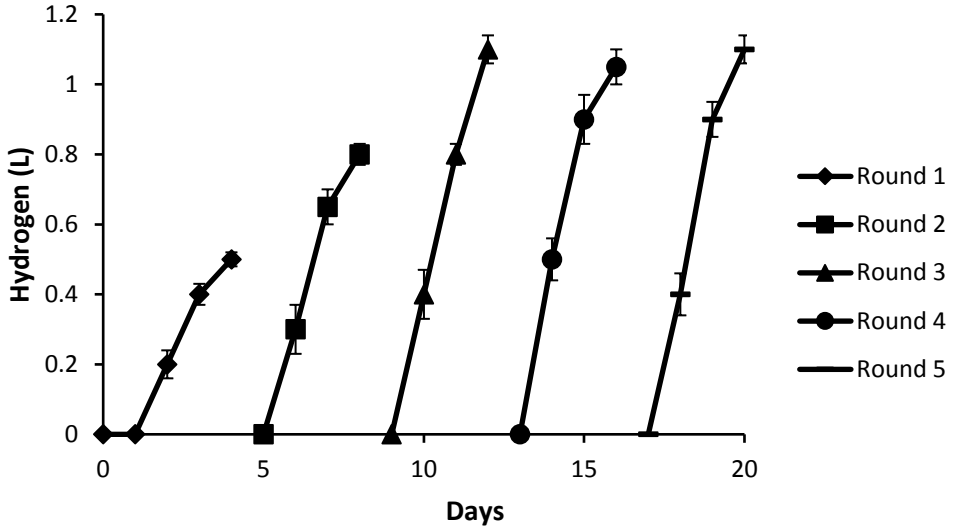

Figure 4.18 Sequential hydrogen production by immobilized *R. capsulatus* YO3 on molasses with 5 mM initial sucrose in indoor conditions. The values represent mean±STD.

The cumulative hydrogen was about 4.6 L at the end of 20 days. It was observed that hydrogen production increased from first (0.5 L) round to the last one (1.1 L) (Figure 4.19).

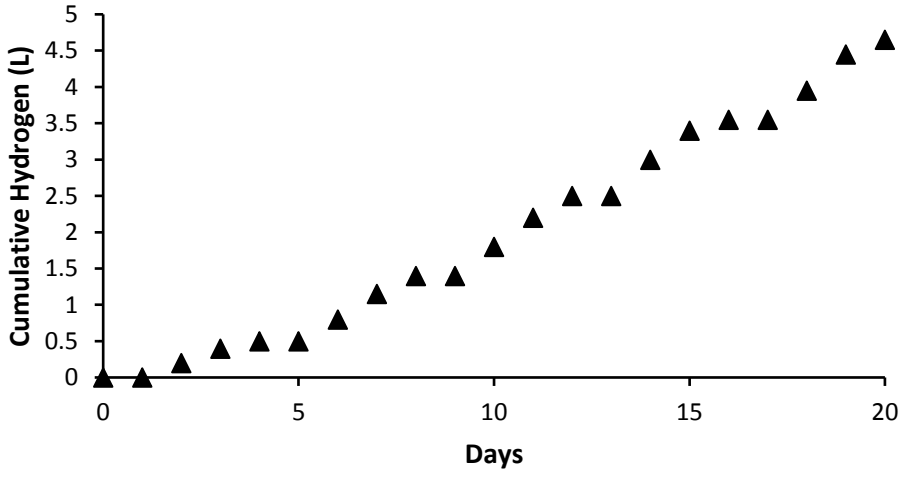

Figure 4.19 Cumulative hydrogen production of immobilized *R. capsulatus* YO3 on molasses with 5 mM initial sucrose in indoor conditions.

In the first round, pH decreased to around 7.0 (Figure 4.20). However, decrease in pH was higher between Round 2 and Round 5 compared to the first round. This is due to higher consumption of sucrose by the immobilized system between these rounds. The first round can be accepted as the adaptation round of the long-term process. The final pH of Round 2 and Round 5 was around 6.0-6.2. It also proves that photofermentation was carried out intensely between these rounds. In addition, Kayahan et al. (2017) studied hydrogen production by using a novel compact tubular photobioreactor in a single-stage photofermentation in outdoor conditions. They also observed that pH was around 6.0 during the continuous feeding of molasses (Kayahan et al., 2017).

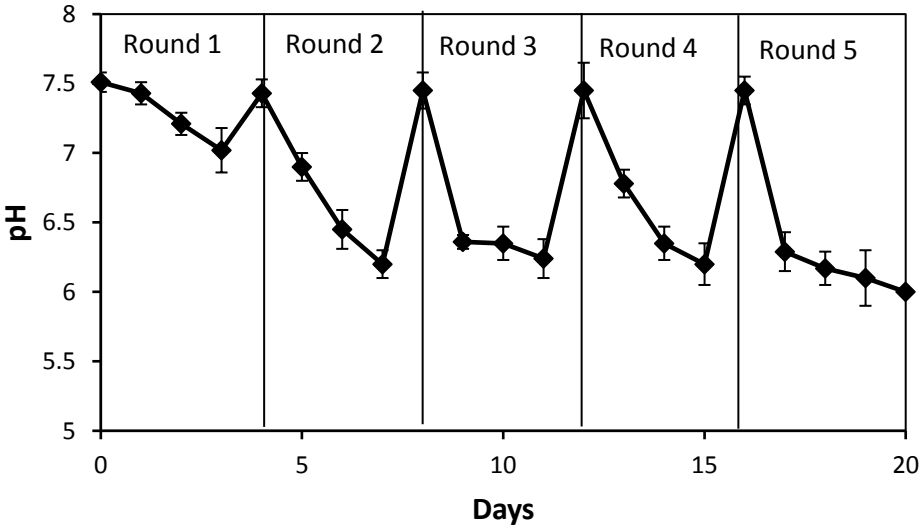

Figure 4.20 pH change vs time on molasses with 5 mM initial sucrose by immobilized *R. capsulatus* YO3 in indoor conditions. The values represent mean±STD.

The maximum hydrogen productivity (0.57 mmol H_2 L^{-1} h^{-1}) and yield (12.2 mol H_2/mol sucrose) were achieved in the 5th round (Table 4.10). The mean productivity and conversion efficiency were 0.47 mmol H_2 L^{-1} h^{-1} and 41%

throughout the experiment. Table 4.11 represents the final organic acids produced in each round.

Table 4.10 Summary of the results of indoor hydrogen production on molasses containing 5 mM sucrose.

Rounds	**Productivity** (mmol H_2 L-1 h-1)	**Molar Yield** (mol H_2/mol sucrose)	**Sub. Conv. Efficiency** (%)	**Total H2** (L)	**Light conversion efficiency (%)**	**Sucrose Consumption** (%)
Round 1	0.26	6.8	28.3	0.5	0.25	30
Round 2	0.41	7	29.2	0.8	0.41	32
Round 3	0.57	12.2	50.8	1.1	0.56	51
Round 4	0.54	10.8	45.0	1.05	0.55	53
Round 5	0.57	12.2	50.8	1.1	0.56	55
Mean	0.47	9.8	41.0	0.91	0.46	44

Table 4.11 Final organic acids produced during the indoor photofermentation on molasses containing 5 mM sucrose.

Rounds	**Acetic acid (mM)**	**Formic acid (mM)**	**Lactic acid (mM)**
Round 1	2.5	0.7	0.1
Round 2	2.8	1.2	0.2
Round 3	3.2	1.4	0.4
Round 4	4.1	1.2	0.4
Round 5	4.2	1.2	0.4

The maximum hydrogen production was 1.25 L in the 4th round (Figure 4.21). Also, the cumulative hydrogen production was higher (5.4 L) than in 5 mM (4.6 L) sucrose (Figure 4.22).

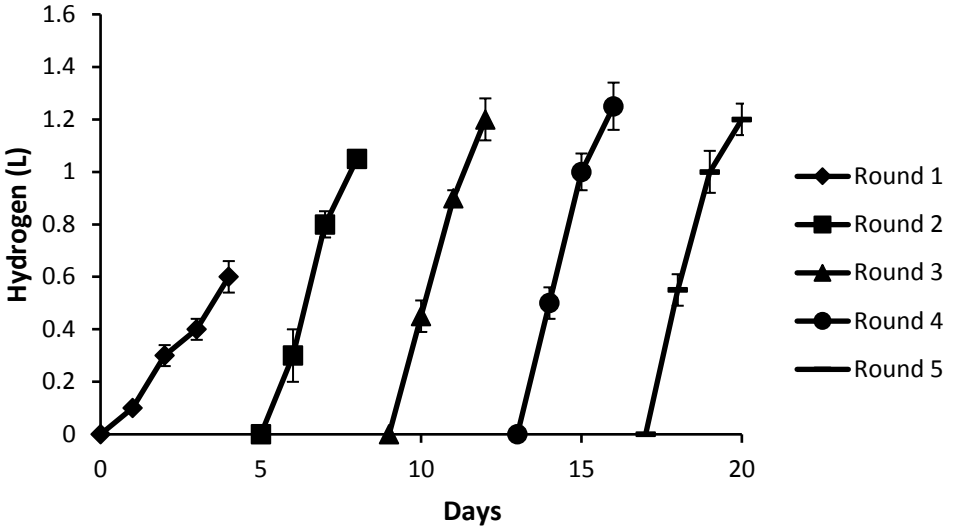

Figure 4.21 Sequential hydrogen production on molasses with 10 mM initial sucrose in indoor conditions. The values represent mean±STD

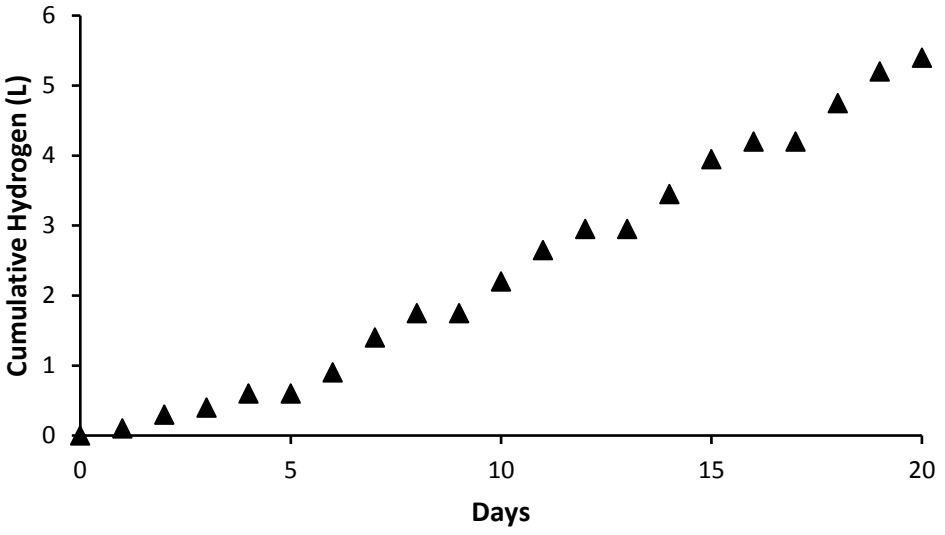

Figure 4.22 Cumulative hydrogen production on molasses with 10 mM initial sucrose in indoor conditions. The values represent mean±STD

pH change was similar to the pH change in 5 mM sucrose. The change in pH is shown in Figure 4.23. The initial pH was 7.5 while final pH in each round was around 6.0 except the first round, which had a final pH of 6.94. It can be asserted that the slow decrease of pH is a result of the diffusive transport of the organic acids from agar matrix into the liquid part. Therefore, steep pH drops in the bulk liquid were alleviated by the presence of agar matrix.

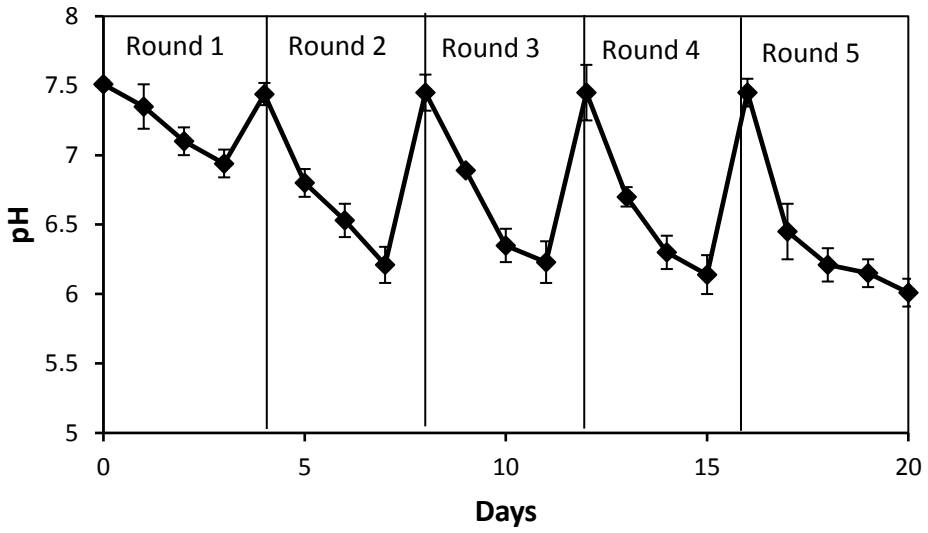

Figure 4.23 pH change vs time on molasses with 10 mM initial sucrose in indoor conditions. The values represent mean±STD.

The mean sucrose conversion efficiency decreased from 41% to 33% as the initial sucrose concentration increased from 5 mM to 10 mM (Table 4.12). However, sucrose consumption was close and 44%-46% in each concentration. This suggests sucrose conversion in favor of organic acid production rather than into hydrogen since the concentration of organic acids were higher in 10 mM than in 5 mM sucrose (Table 4.13). Besides, mean hydrogen productivity (0.55 mmol H_2 L^{-1} h^{-1}) was also high in 10 mM sucrose than in 5 mM (0.47 mmol H_2 L^{-1} h^{-1}). On the other hand, mean hydrogen yield decreased from 9.8 mol H_2/mol sucrose

to 7.9 mol H_2/mol sucrose when the initial sucrose concentration increased from 5 mM to 10 mM. The highest light conversion efficiency was 0.63, which was obtained on 10 mM initial sucrose.

Table 4.12 Summary of the results of indoor hydrogen production on molasses containing 10 mM sucrose.

Rounds	**Productivity** (mmol H_2 L^{-1} h^{-1})	**Molar Yield** (mol H_2/mol sucrose)	**Sub. Conv. Efficiency** (%)	**Total H2** (L)	**Light conversion efficiency** (%)	**Sucrose Consumption** (%)
Round 1	0.31	3.4	14.3	0.6	0.30	34
Round 2	0.54	7.8	32.5	1.05	0.53	45
Round 3	0.62	11	45.8	1.2	0.62	48
Round 4	0.64	9.1	37.9	1.25	0.63	52
Round 5	0.62	8.1	33.8	1.2	0.62	53
Mean	0.55	7.9	33.0	1.06	0.53	46

Table 4.13 Final organic acids produced during the indoor photofermentation on molasses containing 10 mM sucrose.

Rounds	**Acetate (mM)**	**Formate (mM)**	**Lactate (mM)**
Round 1	3.2	1.4	0.4
Round 2	3.5	1.6	0.6
Round 3	4.3	1.8	0.5
Round 4	3.8	1.9	0.8
Round 5	4.5	2.2	0.9

When the initial sucrose concentration in molasses was increased to 20 mM, lower hydrogen production was obtained compared to the lower sucrose concentrations (Figure 4.24). The mean hydrogen production was 0.54 L (Table 4.14). Also, the cumulative hydrogen was below 3 L (Figure 4.25). Mean hydrogen productivity of the process was 0.28, which is the lowest among various molasses concentrations. The H_2 productivity and yields were the lowest with 20 mM sucrose containing molasses considering all the initial sucrose concentrations. This indicates that the initial sucrose concentration must be kept below 20 mM for H_2 production.

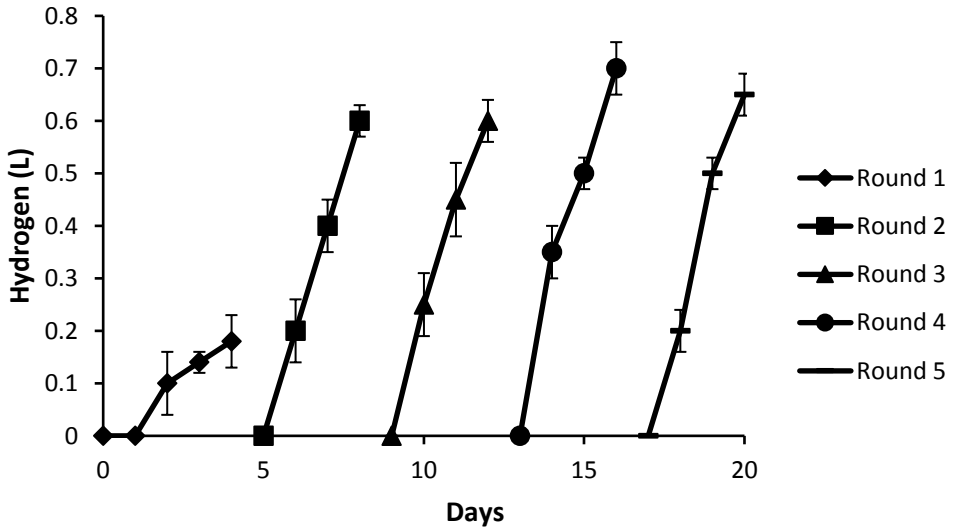

Figure 4.24 Cumulative hydrogen production of immobilized *R. capsulatus* YO3 on molasses with 20 mM initial sucrose in indoor conditions. The values represent mean±STD.

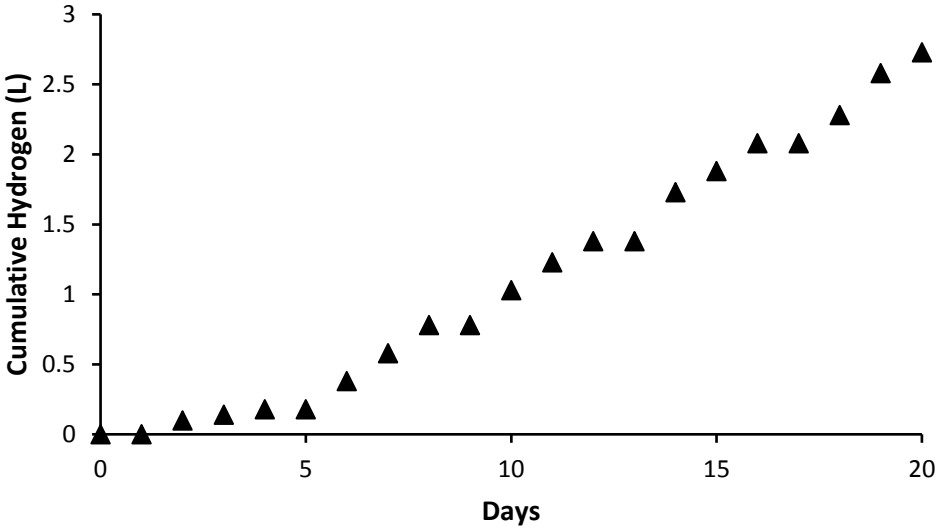

Figure 4.25 Cumulative hydrogen production on molasses with 20 mM initial sucrose in indoor conditions. The values represent mean±STD.

The final pH obtained from Round 2 to Round 5 was around 5.8-5.9. These values were the lowest among all the initial sucrose concentrations. (Figure 4.26). Higher organic acid concentrations probably caused lower pH values throughout the hydrogen production (Table 4.15). It was noticed that organic acid accumulation increased significantly as initial sucrose concentration increased from 5 mM to 20 mM. These results were also in agreement in a recent study where they reported higher organic acid accumulation when feeding of molasses increased from 5 mM to 100 mM (Kayahan et al., 2016).

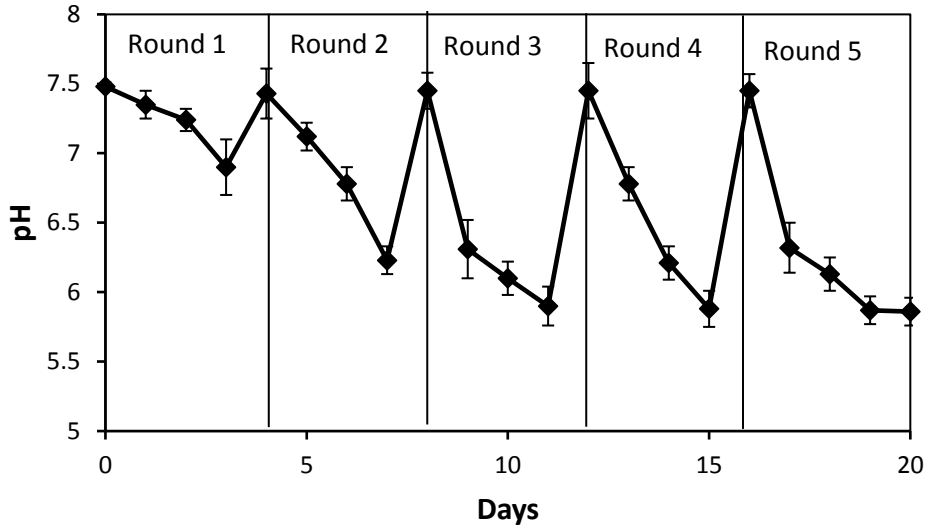

Figure 4.26 pH change vs time on molasses with 20 mM initial sucrose in indoor conditions. The values represent mean±STD.

Table 4.14 Summary of the results of indoor hydrogen production on molasses with 20 mM sucrose.

Rounds	**Productivity** (mmol H_2 L-1 h-1)	**Molar Yield** (mol H_2/mol sucrose)	**Sub. Conv. Efficiency** (%)	**Total H_2** (L)	**Light conversion efficiency (%)**	**Sucrose Consumption** (%)
Round 1	0.09	1.2	5.0	0.18	0.1	25
Round 2	0.31	3.2	13.2	0.6	0.3	48
Round 3	0.30	3.2	13.3	0.59	0.3	52
Round 4	0.35	3.4	14.1	0.68	0.35	54
Round 5	0.32	3.1	12.9	0.63	0.32	40
Mean	0.28	2.8	12.0	0.54	0.28	44

Table 4.15 Final organic acids produced during the indoor photofermentation on molasses with 20 mM sucrose.

Rounds	**Acetic acid (mM)**	**Formic acid (mM)**	**Lactic acid (mM)**
Round 1	6.7	1.8	0.5
Round 2	6.5	1.5	0.3
Round 3	5.8	1.6	0.7
Round 4	6.4	1.7	0.6
Round 5	6.8	2.4	0.8

4.2.2 Outdoor hydrogen production by immobilized *R. capsulatus* YO3 on molasses

Based on indoor studies the optimal sucrose concentration in molasses was 10 mM. Hydrogen production on molasses was realized in outdoor natural conditions on May and June 2016 in METU, Turkey. The sequential hydrogen production prolonged for 40 days including consecutive 10 rounds (Figure 4.27).

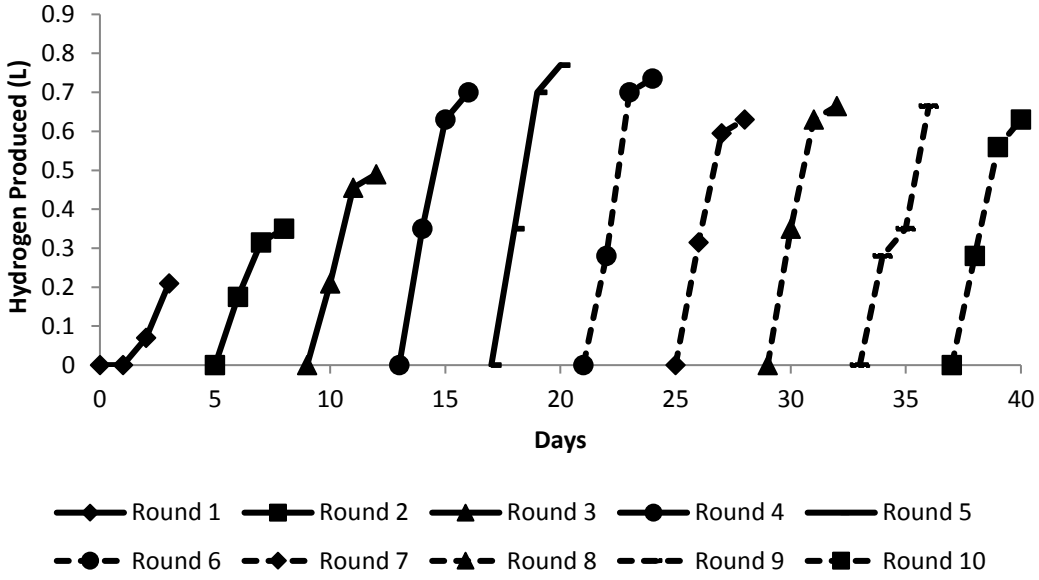

Figure 4.27 Sequential hydrogen production on molasses with 10 mM initial sucrose in outdoor conditions

Hydrogen production increased in steeply from the first round to the fifth round. The produced hydrogen started to decrease after the fifth round. The first round seemed to be an adaptation round for the long-term production. A more stable hydrogen production was observed between the 20th day and 40th day. Throughout 40 days of operation, a total hydrogen of 5.84 L was obtained including 10 rounds (Figure 4.28).

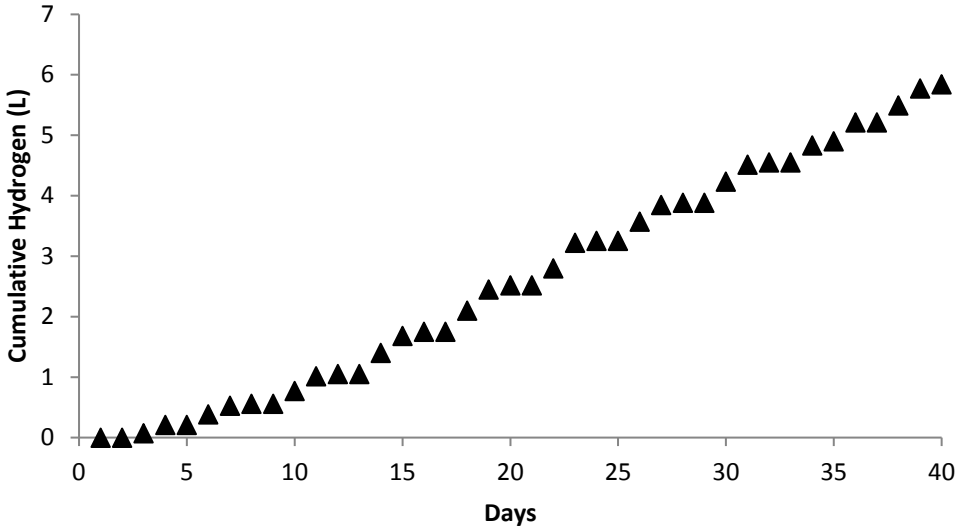

Figure 4.28 Cumulative hydrogen production on molasses with 10 mM initial sucrose in outdoor conditions.

The change in pH on molasses with 10 mM initial sucrose in outdoor conditions is given in Figure 4.29. It can easily be seen that pH decreased from 7.5 to around 6.0 in each round except the first one, which had a slightly higher final pH (6.3). This final pH was quite tolerable for growth and hydrogen production. Thus, it can be suggested that the immobilized bacteria were less affected by the pH changes and other produced metabolites by the protection of entrapment in agar compared to suspended culture systems. Besides, carbon dioxide production and its solubility during the process might also lead to the formation of carbonic acid, thereby lowering the pH (Montiel-Corona et al., 2015; Kayahan et al., 2016).

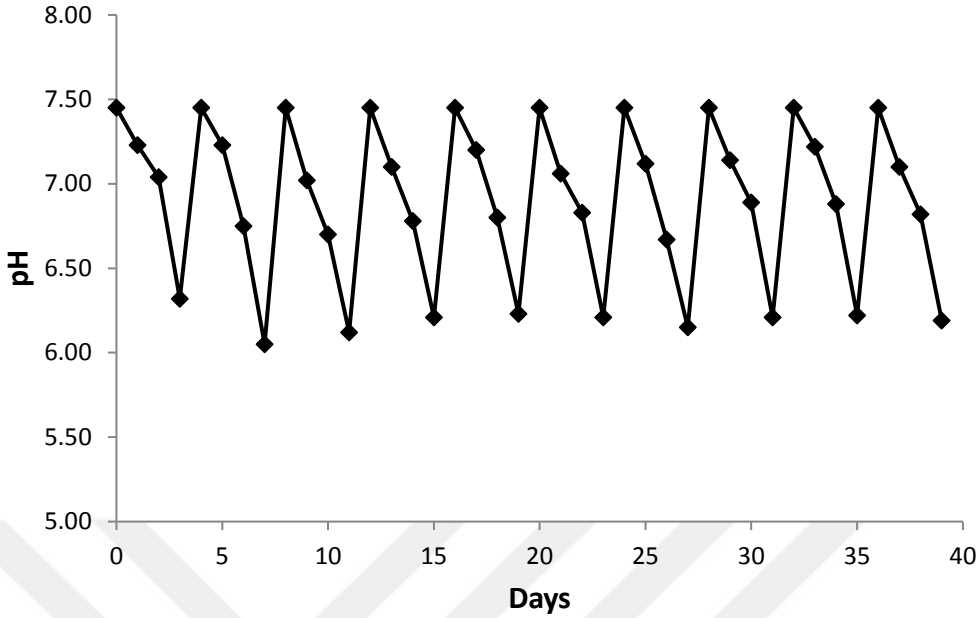

Figure 4.29 pH change vs time on molasses with 10 mM initial sucrose in outdoor conditions.

The temperature was measured by using thermocouples that were inserted to the mid-top of the reactor. The inner and outer temperature did not change too much (Figure 4.30). Therefore, it can be stated that the cooling system worked efficiently to keep the inner temperature at optimal values. Solar radiation also showed variations throughout the overall process. The solar radiation ranged between 0 and 1400 W/m^2. Optimal hydrogen production values were also obtained between days 28 and 35, where more optimal and higher solar radiation and temperature values were present.

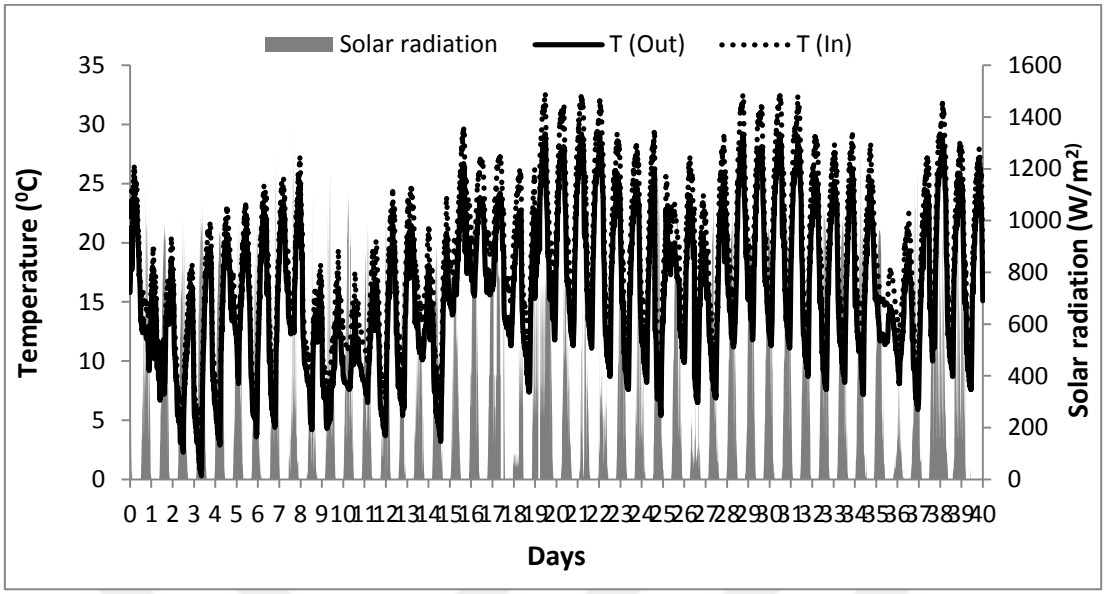

Figure 4.30 Temperature (In and out) and solar radiation vs time on molasses with 10 mM initial sucrose in outdoor conditions.

The maximum hydrogen productivity was 0.79 mmol H_2 L^{-1} h^{-1} and achieved in the 5th round (Table 4.16). Mean productivity of the 10 rounds were 0.6 mmol H_2 L^{-1} h^{-1}. The highest hydrogen yield was also obtained in the 5th round as 5.2 mol H_2/mol sucrose. The consumption of sucrose ranged between 28% and 57% and mean sucrose consumption was 50%. Acetic acid, formic acid and lactic acid were side products of photofermentation on molasses (Table 4.17). Notably, acetic acid was the dominant organic acid species among the others.

Table 4.16 Summary of the results of outdoor hydrogen production on molasses containing 10 mM sucrose.

Rounds	**Productivity** (mmol H_2 L^{-1} h^{-1})	**Yield** (mol/mol)	**Sub. conversion efficiency (%)**	**Total H_2** (L)	**Suc. Cons.(%)**
Round 1	0.22	2.8	11.7	0.21	28
Round 2	0.36	3.7	15.4	0.35	35
Round 3	0.50	3.9	16.3	0.49	48
Round 4	0.72	4.9	20.4	0.70	53
Round 5	0.79	5.2	21.7	0.77	57
Round 6	0.75	5.0	20.8	0.74	55
Round 7	0.65	4.1	17.1	0.63	57
Round 8	0.69	4.5	18.8	0.67	55
Round 9	0.69	4.5	18.8	0.67	53
Round 10	0.65	4.3	17.9	0.63	52
Mean	0.60	4.3	18.0	0.60	50

Table 4.17 Final organic acids produced during the outdoor photofermentation on molasses containing 10 mM sucrose.

Rounds	Acetate (mM)	Formate (mM)	Lactate (mM)
Round 1	2.7	1.1	0.2
Round 2	2.6	1.6	0.2
Round 3	3.1	1.5	0.4
Round 4	3.4	2.1	0.5
Round 5	3.8	2.4	0.4
Round 6	3.8	3.6	0.3
Round 7	4	3.2	0.5
Round 8	4.2	2.5	0.6
Round 9	4.3	3.2	0.5
Round 10	4.2	3.2	0.5

4.2.3 Comparison of indoor and outdoor hydrogen production by immobilized *R. capsulatus* YO3 on molasses

The results of hydrogen production experiments on sugar beet molasses indicated that the cumulative hydrogen production was lower in outdoors than in indoors (Figure 4.31). Hydrogen productivities (0.55-0.60 mmol H_2 L^{-1} h^{-1}) were similar in both indoor and outdoor conditions with 10 mM sucrose containing molasses. However, hydrogen yields in outdoor conditions were almost half of the yields in indoors. This is due to day/night cycle and illumination time for the photobioreactor. In outdoor, 10 mM sucrose containing molasses was supplied to the immobilized bioreactor for 40 days. The consumption of sucrose was also 50% in both conditions. However, mean conversion efficiency in outdoor (18 %) was lower than the indoors (33 %). In all experiments, it was apparently observed that hydrogen productivity decreased when the initial molasses concentration (sucrose, in particular) rised from 5 mM to 20 mM. For this reason, the initial

sucrose concentration should be kept below 20 mM sucrose containing molasses for a long-term hydrogen producing system.

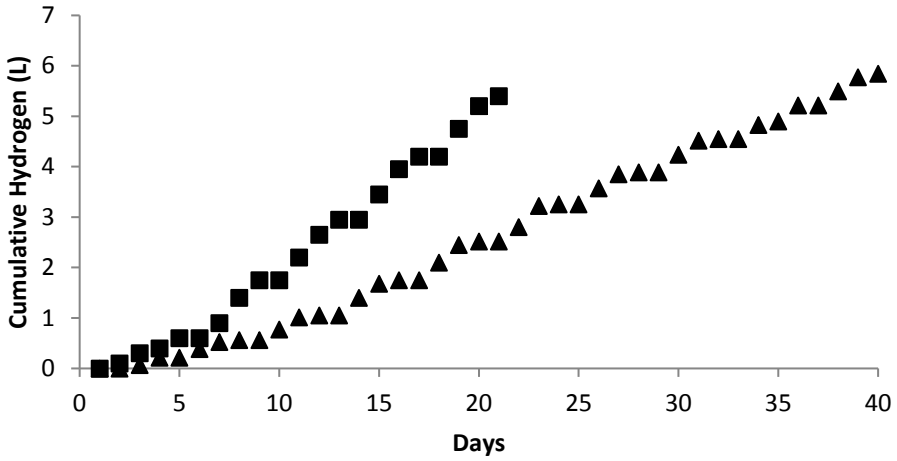

Figure 4.31 Cumulative hydrogen production in indoor (■) and outdoor (▲) conditions on 10 mM molasses.

4.2.4 Comparison of immobilized and suspended culture of *R. capsulatus* YO3

Hydrogen production capacity of immobilized culture was also compared with suspended cultures of *Rhodobacter capsulatus* YO3 with a volume of 50 mL. Mean productivity of 0.72±0.05 mmol H_2 L^{-1} h^{-1} was achieved with the immobilized culture on 10 mM sucrose while a mean productivity of 0.4±0.3 mmol H_2 L^{-1} h^{-1} was obtained with the suspended culture (Table 4.18). In this work, it was also demonstrated that hydrogen yields of the immobilized system were also higher than the yields obtained in the suspended culture. H_2 production decreased as the initial sucrose concentration increased from 5 mM to 20 mM in both suspended and immobilized cultures. The mean productivity (0.62±0.03 mmol H_2 L^{-1} h^{-1}) obtained in outdoor conditions was higher than the productivity (0.31 mmol H_2 L^{-1} h^{-1}) reported by operation of a tubular bioreactor on sucrose containing molasses in outdoor conditions (Kayahan et al., 2016). Hydrogen

productivity in outdoor conditions was also higher than a previous study in which a productivity of 0.51 mmol H_2 L^{-1} h^{-1} was obtained by a suspended culture of *Rhodobacter capsulatus* YO3 operated in an outdoor panel photobioreactor on acetate (Androga et al., 2011). Therefore, it can be concluded that sucrose can be a promising candidate for outdoor hydrogen production to replace with organic acids.

Table 4.18 Summary of the results with suspended and immobilized culture of *R. capsulatus* YO3 on different sucrose concentrations in indoor conditions.

Initial sucrose concentration (mM)	**Hydrogen productivity** (mmol/L.h)		**Hydrogen yield** (mol H_2/mol sucrose)		**Sucrose consumption** (%)	
	suspended	immobilized	suspended	immobilized	suspended	immo.
5	0.31±0.1	0.57	13.2±0.5	13.5	75±0.5	60
10	0.40±0.3	0.72±0.05	9.1±0.4	9.6±0.1	70±0.6	53±2.1
20	0.24±0.3	0.32±0.02	3.8±0.6	3.3±0.2	48±0.6	36±3.5

4.3 Microaerobic dark fermentative hydrogen production by *R. palustris* CGA009 and *R.capsulatus* JP91 on glucose

In this section, biohydrogen production was aimed to be demonstrated by several photosynthetic bacteria via microaerbic dark fermentation process. Biological hydrogen production was carried out under microaerobic dark fermentative conditions by using two different purple non-sulfur bacteria; *R. palustris* CGA009 and *R.capsulatus* JP91. The suspended cultures of *R. palustris* CGA009 were also compared with its agar immobilized cultures. The aim of this

part was to realize and demonstrate hydrogen production in microaerobic dark fermentation and then to improve hydrogen yield from glucose in sequential microaerobic dark and photofermentation. Response Surface Methodology (RSM) was used for optimization of some important parameters such as inoculum, oxygen and glucose concentrations.

4.3.1 Microaerobic dark fermentative hydrogen production by suspended culture of *Rp. palustris* CGA009 using RSM

In the first part of the studies, microaerobic dark fermentative hydrogen production by suspended culture of *Rp. palustris* CGA009 was carried out. Design of experiment with Response Surface Methodology (RSM) was used to optimize important parameters including inoculum, oxygen and glucose concentrations.
The purple non-sulfur bacterium *Rp. palustris* CGA009 was grown on RCV lactate medium and incubated at 30 ^{0}C in an Biotronette Mark III environmental chamber (Lab-line Instruments) with 150 W incandescent bulbs. The recipes of the media are given in Appendix A. The culture was used for hydrogen production experiments after the culture has grown and reached an OD of 1.5-2.0 at 660 nm.
The experiments were carried out with 160 mL glass bottles. These bioreactors were filled with 40 mL RCV glucose medium with a head space of 120 mL. Then, different volume of bacteria inocula (25-50-75 v/v %) were added over the medium. The initial pH of the medium was set to 7.0 with potassium buffer. The reactors were argon flushed for 10 min in order to have the anaerobic environment. Then, various oxygen concentrations were given to the reactors by using an injector. Same volume of argon was drawn before injecting the oxygen to provide the internal pressure constant. The experiment was continued for 9 days. Daily samples from the reactors were taken for the analysis of glucose concentration, pH, and OD.

Firstly, biohydrogen production by *Rp. palustris* CGA009 in microaerobic dark fermentative process was investigated. In this study, independent variables

were inoculum volume, initial substrate, and oxygen concentration. In addition, oxygen was supplied to the reactors when it has been completely consumed. Hydrogen yield was the response of the optimization process. Total 17 different runs were carried out according to RSM Box-Behnken design method by using Design Expert 10 (Table 4.19). Limit values of 2 mM and 10 mM for glucose concentration, 1% and 5% for oxygen concentration, and 25% and 75% for inoculum volume were used. The runs were repeated at least two times for each type of experiment.

Table 4.19 Box-Behnken experimental design table for hydrogen yield by *Rp. palustris* CGA009

Run	Glucose concentration (mM)		Oxygen concentration (%)		Inoculum conc. (v/v %)		H_2 Yield[c] (mol/mol) (Y)
	Coded[a]	Actual[b]	Coded[a]	Actual[b]	Coded[a]	Actual[b]	
1	-1	2	1	5	0	50	0.46
2	0	6	0	3	0	50	0.29
3	0	6	0	3	0	50	0.20
4	0	6	0	3	0	50	0.28
5	1	10	-1	1	0	50	0.17
6	0	6	0	3	0	50	0.37
7	0	6	1	5	-1	25	0.16
8	-1	2	0	3	-1	25	0.48
9	0	6	1	5	1	75	0.38
10	0	6	-1	1	-1	25	0.18
11	-1	2	0	3	1	75	0.70
12	0	6	-1	1	1	75	0.22
13	0	6	0	3	0	50	0.29
14	1	10	1	5	0	50	0.07
15	1	10	0	3	-1	25	0.10
16	1	10	0	3	1	75	0.23
17	-1	2	-1	1	0	50	0.71

[a]Coded factor values

[b]Actual factor values

[c]The hydrogen yields are the average of the two runs

ANOVA was used to test the significance of the quadratic polynomial model fitting. Three independent variables in this experiment were glucose concentration (X_1), oxygen concentration (X_2), and inoculum concentration (X_3).

The Model F-value of 8.64 implied the model was significant. Values of "Prob > F" less than 0.05 indicate model terms are significant. In this case X_1, X_3, X_1^2 are significant model terms. The measure of the goodness of fit (R^2, 0.92) shows a strong agreement between predicted and observed values.

$\mathbf{Y_{Coded}} = 0.29 - 0.22X_1 - 0.026X_2 + 0.076X_3 + 0.038X_1X_2 - 0.023X_1X_3 + 0.045X_2X_3 + 0.10X_1^2 - 0.038X_2^2 - 0.013X_3^2$

$\mathbf{Y_{Uncoded}} = 0.756 - 0.136X_1 - 0.029X_2 + 3.78 \times 10^{-3}X_3 + 4.68 \times 10^{-3}X_1X_2 - 2.25 \times 10^{-4}X_1X_3 + 9 \times 10^{-4}X_2X_3 + 6.53 \times 10^{-3}X_1^2 - 9.5 \times 10^{-3}X_2^2 - 2.08 \times 10^{-5}X_3^2$

The actual maximum hydrogen yield was 0.7 mol H_2/mol glucose and obtained on 2 mM glucose, 1% oxygen and 50 v/v %. The RSM plots indicated that H_2 yield increased at decreasing glucose concentration and increasing inoculum concentrations (Figure 4.32).

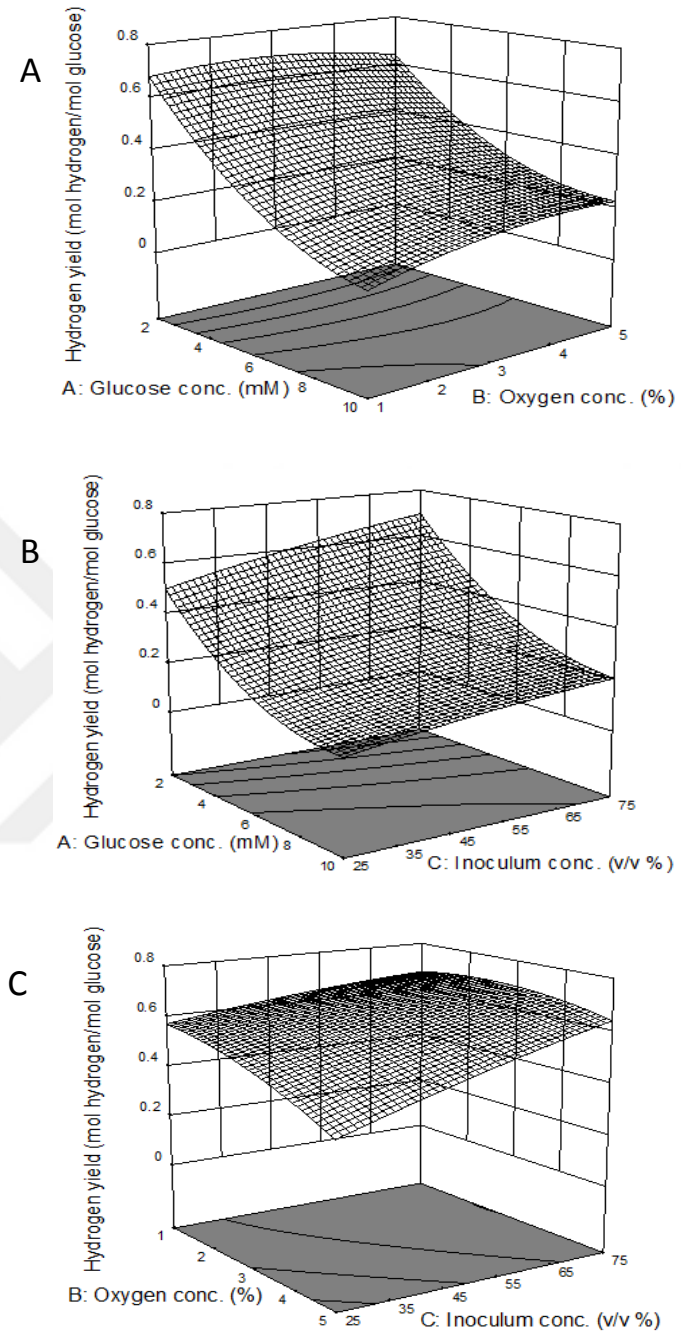

Figure 4.32 RSM contour plots for the hydrogen yields of *Rp. palustris* CGA009. (A) Hydrogen yield as a function of glucose and oxygen concentration at 50 v/v % inoculum concentration. (B) Hydrogen yield as a function of glucose and

inoculum concentration at 1 % oxygen concentration. (C) Hydrogen yield as a function of inoculum and oxygen concentration at 2 mM glucose.

4.3.2 Microaerobic dark fermentative hydrogen production by immobilized *Rp. palustris* CGA009 using RSM

In this part of the studies cell immobilization technology and design of experiments were used to improve hydrogen production. All the experiments are given in the following sections.

A purple non-sulfur bacterium, *Rp. palustris* CGA009 was immobilized on 4% agar matrix and used in different experiments. The cultures were firstly grown on RCV lactate medium and incubated at 30 ^{0}C in an Biotronette Mark III environmental chamber (Lab-line Instruments) with 150 W incandescent bulbs. The suspension cultures were centrifuged at 10,000 rpm for 20 min when the OD of the grown culture was 1.5-2.0 at 660 nm. Bacterial pellets were re-suspended and adjusted to various concentrations. Different concentration of bacterial inoculum (25-50-75 v/v %) was mixed with 10 mL molten agar in a falcon tube. Then, the mixture was transferred to the 160 mL glass bottles. Agar-bacteria complex solidified completely after 10 min. Then bioreactors were filled with 30 mL RCV glucose medium. The recipes of the hydrogen production media were given in Appendix A. The initial pH of medium was adjusted to 7.0 by using potassium 64 mM phosphate buffer. The reactors were argon flushed for 10 min in order to maintain the anaerobic environment. Afterwards, the bioreactors were placed to an incubator at 30 ^{0}C for microaerobic dark fermentative process (New Brunswick Scientific Co. Inc) with an agitation of 120 rpm. In the sequential process, the bioreactors were transferred to the environmental chamber with a continuous illumination of 120 W/m^2. Hydrogen gas production was analyzed with a gas chromatograph (Shimadzu GC-8A) equipped with a thermal conductivity detector and a 1 m column packed with molecular sieve 5A with argon as carrier gas. The oven temperature was maintained at 60 ^{0}C and the flow rate was 25 mL/min. Glucose concentration was determined by 3,5-Dinitrosalicylic Acid (DNS) Method (Miller, 1959).

Agar immobilized *Rp. palustris* CGA009 was used for microaerobic dark fermentative hydrogen production. RSM with Box-Behnken experimental design was employed to optimize hydrogen production and yield (Table 4.20). The effects of three independent variables on the certain responses have been evaluated. These variables were inoculum concentration, oxygen concentration and initial substrate concentration.

The model was significant and the highest hydrogen production and yield were obtained at 5.2% oxygen, 7.8 mM glucose and 73.4 v/v % inoculum concentration. The actual maximum hydrogen production and yield were 98.6 umol and 0.9 mol H_2/mol glucose, respectively (Figure 4.33 and 4.34). These values were higher than a previous study where they obtained 0.16 mol H_2/mol glucose on glucose by *R. capsulatus* JP91 (Abo-Hashesh and Hallenbeck, 2012).

Table 4.20 Box-Behnken experimental design table for hydrogen yield by immobilized *Rp. palustris* CGA009

Run	Glucose concentration (mM)		Oxygen concentration (%)		Inoculum conc. (v/v %)		H_2 Yield[c] (mol/mol) (Y)
	Coded[a]	Actual[b]	Coded[a]	Actual[b]	Coded[a]	Actual[b]	
1	-1	1	-1	1	0	62.5	0.35
2	0	6	0	4.5	0	62.5	0.82
3	0	6	-1	1	-1	25	0.26
4	-1	1	0	4.5	-1	25	0.43
5	0	6	0	4.5	0	62.5	0.87
6	0	6	0	4.5	0	62.5	0.84
7	0	6	1	8	-1	25	0.17
8	0	6	0	4.5	0	62.5	0.87
9	-1	1	0	4.5	1	100	0.53
10	0	6	1	8	1	100	0.56
11	1	11	0	4.5	-1	25	0.19
12	1	11	-1	1	0	62.5	0.07
13	0	6	0	4.5	0	62.5	0.90
14	1	11	1	4.5	1	100	0.42
15	0	6	-1	1	1	100	0.39
16	1	11	1	8	0	62.5	0.37
17	-1	1	1	8	0	62.5	0.32

ANOVA analysis showed that the model (F-value 59.68) was significant (Table 4.21). The results indicated that hydrogen yields were improved by the immobilized *Rp. palustris* CGA009 from 0.7 to 0.9 mol H_2/mol glucose. Therefore, most of the interest and research was devoted to immobilization in the following sections.

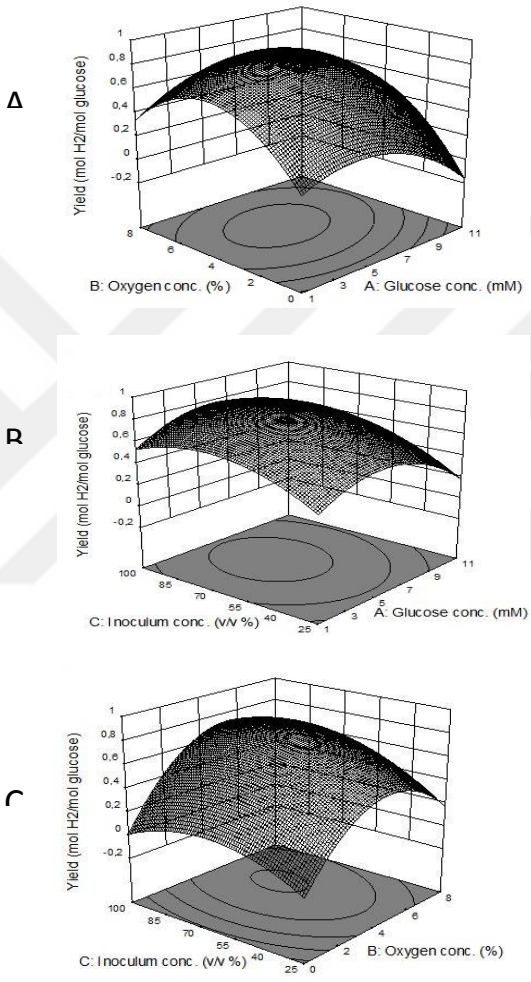

Figure 4.33 RSM contour plots for the hydrogen yields of immobilized *Rp. palustris* CGA009. (A) Hydrogen yield as a function of glucose and oxygen concentration at 73.4 v/v % inoculum concentration. (B) Hydrogen yield as a function of glucose and inoculum concentration at 5.2 % oxygen concentration. (C) Hydrogen yield as a function of inoculum and oxygen concentration at 7.8 mM glucose.

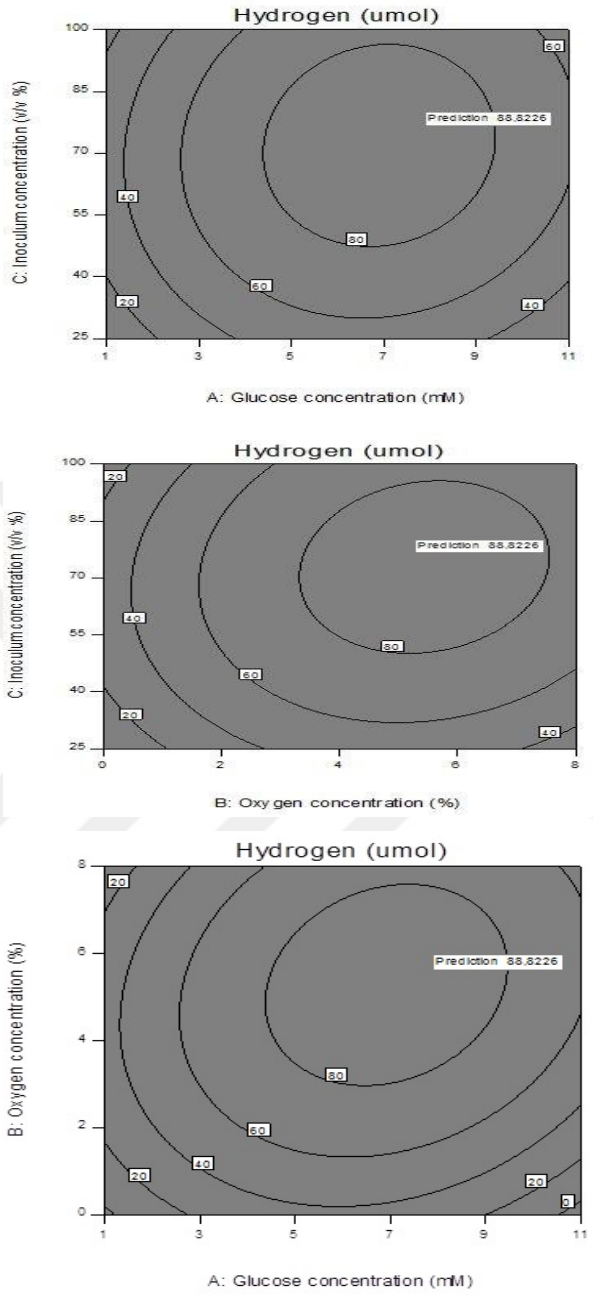

Figure 4.34 RSM contour plots for the hydrogen production of immobilized *Rp. palustris* CGA009. (A) Hydrogen production as a function of glucose and inoculum concentration at 73.4 v/v % inoculum concentration. (B) Hydrogen production as a function of oxygen and inoculum concentration at 5.2 % oxygen concentration. (C) Hydrogen production as a function of glucose and oxygen concentration at 7.8 mM glucose.

Table 4.21 ANOVA analysis for hydrogen yield by immobilized *Rp. palustris* CGA009

ANOVA for Response Surface Quadratic model

Analysis of variance table [Partial sum of squares - Type III]

Source	Sum of Squares	df	Mean Square	F Value	p-value Prob > F	
Model	1.19	9	0.13	59.68	< 0.0001	significant
A-Glucose concentration	0.055	1	0.055	24.68	0.0016	
B-Oxygen concentration	0.13	1	0.13	57.7	0.0001	
C-Inoculum concentration	0.074	1	0.074	33.63	0.0007	
AB	0.027	1	0.027	12.17	0.0101	
AC	4.49E-03	1	4.49E-03	2.03	0.1971	
BC	0.016	1	0.016	7.24	0.031	
A^2	0.3	1	0.3	135.98	< 0.0001	
B^2	0.42	1	0.42	190.15	< 0.0001	
C^2	0.17	1	0.17	76.13	< 0.0001	
Residual	0.015	7	2.21E-03			
Lack of Fit	0.011	3	3.77E-03	3.63	0.1223	not significant
Pure Error	4.15E-03	4	1.04E-03			
Cor Total	1.2	16				

4.3.3 Long-term hydrogen production via cyclic microaerobic dark fermentation by immobilized *Rp. palustris* CGA009

Hydrogen production was carried out via long-term cyclic microaerobic dark fermentation by immobilized *Rp. palustris* CGA009. The effects of inoculum volume, oxygen concentration and initial glucose concentration were investigated through five cycles for 25 days of batch operation. Fresh medium was given to the reactors at the end of each cycle and remaining effluent was removed simultaneously. Oxygen was supplied daily to keep the oxygen content constant.

It was observed that inoculum concentration significantly affected the hydrogen production. Hydrogen production was proportional to increasing inoculum volume (Figure 4.35). The maximum hydrogen (596 umol) and yield (1.25 mol H_2/mol glucose) were obtained with 100 % v/v inoculum at fixed 4.5% oxygen and 2 mM glucose concentrations (Table 4.22). Lag time for H_2 production also decreased as the inoculum volume increased from 25 to 100% v/v. Therefore, inoculum volume of 100% v/v was used for the subsequent experiments.

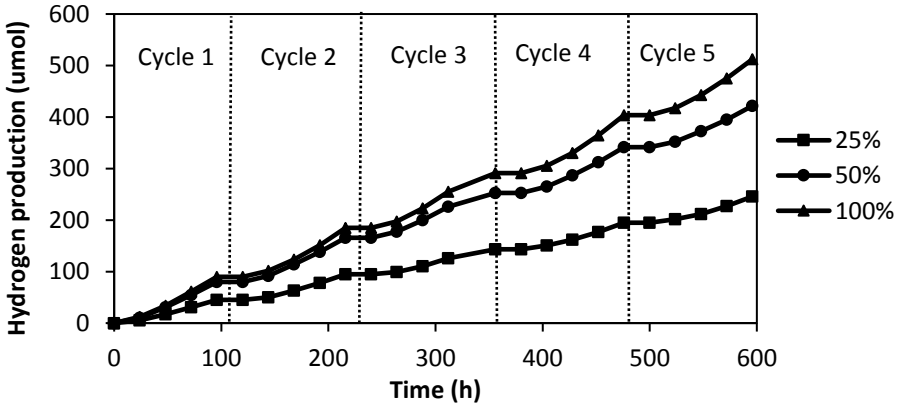

Figure 4.35 Hydrogen production by cyclic microaerobic dark fermentation by immobilized *Rp. palustris* CGA009 at different inoculum volume (25%, 50% and 100%)

Table 4.22 Hydrogen yields of cyclic microaerobic dark fermentation by immobilized *Rp. palustris* CGA009

Cycles	Hydrogen yields (mol H_2/mol glucose)		
	25%	**50%**	**100%**
1	0.55	0.76	0.96
2	0.60	0.81	1.06
3	0.67	0.92	1.17
4	0.67	0.97	1.25
5	0.72	0.91	1.23
Mean	0.64	0.87	1.14

The effect of oxygen concentration was also investigated at fixed cell inoculum volume (100%) and glucose concentration (2 mM). Different oxygen concentrations (1%, 4.5%, 8%) were supplied to the reactors under dark fermentative conditions (Figure 4.36). The oxygen was daily measured and was supplied to the reactors to keep it constant. The results showed that the optimum oxygen concentration was 4.5% for hydrogen production (Table 4.23).

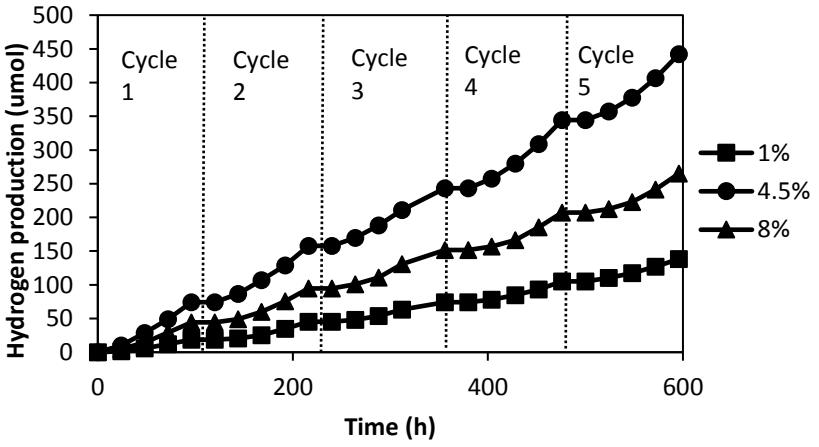

Figure 4.36 Hydrogen production by cyclic microaerobic dark fermentation by immobilized *Rp. palustris* CGA009 on different oxygen concentrations (1%, 4.5%, 8%).

Table 4.23 Hydrogen yields of cyclic microaerobic dark fermentation by immobilized *Rp. palustris* CGA009 on different oxygen concentrations (1%, 4.5%, 8%).

Cycles	Hydrogen yields (mol H_2/mol glucose)		
	1%	**4.5%**	**8%**
1	0.27	0.90	0.66
2	0.38	0.98	0.76
3	0.43	1.08	0.83
4	0.45	1.18	0.87
5	0.42	1.28	0.92
Mean	0.39	1.08	0.80

The effects of different initial glucose concentrations (2 mM, 6 mM and 10 mM) on hydrogen production and yield were examined throughout 600 h including consecutive five cycles (Figure 4.37). Cell inoculum volume and supplied oxygen concentration were 100% v/v and 4.5%, respectively. Initial glucose concentration was observed to have a significant effect on hydrogen production. It could be concluded that higher hydrogen production was obtained on 6 mM (750 umol) and 10 mM (840 umol) glucose concentrations, but hydrogen yields were lower than those on 2 mM glucose concentration. Hydrogen yields decreased at increasing initial glucose concentrations from 2 mM to 10 mM. The highest yield, (1.41 mol H_2/mol glucose), was obtained in the 5th cycle on 2 mM glucose (Table 4.24). Glucose consumption decreased at increasing initial glucose concentrations (Table 4.25).

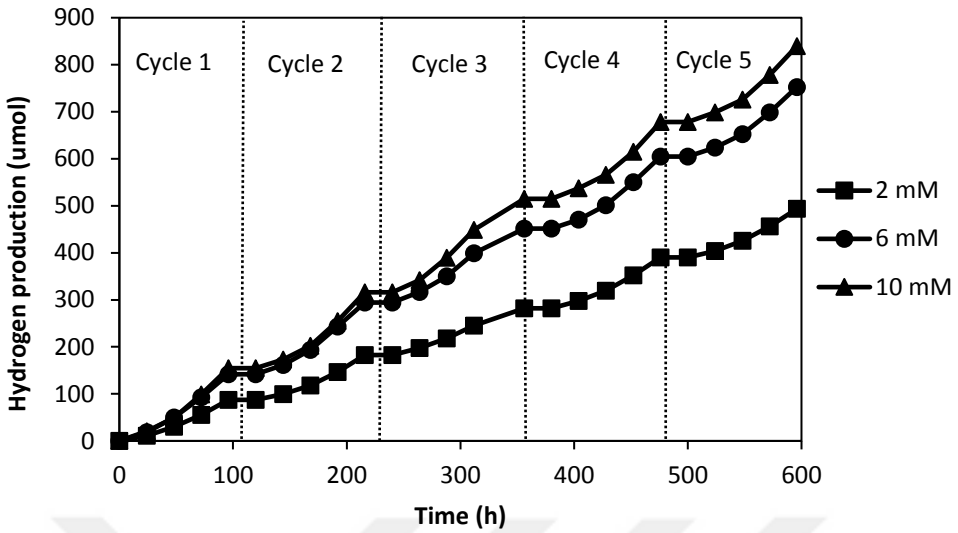

Figure 4.37 Hydrogen production via cyclic microaerobic dark fermentation by immobilized *Rp. palustris* CGA009 on different initial glucose concentrations (2 mM, 6 mM, 10 mM).

Table 4.24 Hydrogen yields of cyclic microaerobic dark fermentation by immobilized *Rp. palustris* CGA009 on different initial glucose concentrations (2 mM, 6 mM, 10 mM).

Cycles	**Hydrogen yields (mol H_2/mol glucose)**		
	2 mM	**6 mM**	**10 mM**
1	1.21	0.58	0.37
2	1.27	0.60	0.40
3	1.29	0.61	0.43
4	1.40	0.62	0.41
5	1.41	0.62	0.40
Mean	1.32	0.61	0.40

Table 4.25 Glucose consumption of cyclic microaerobic dark fermentation by immobilized *Rp. palustris* CGA009 on different initial glucose concentrations (2 mM, 6 mM, 10 mM).

Cycles	Glucose consumption (%)		
	2 mM	**6 mM**	**10 mM**
1	90	55	60
2	95	56	65
3	95	58	70
4	90	60	70
5	95	60	65
Mean	93	58	66

4.3.4 Hydrogen production by immobilized *Rp. palustris* CGA009 via sequential microaerobic dark and photofermentation

In this section, biohydrogen has been produced via sequential microaerobic dark and photofermentation. The aim of this part of the experiment is to enhance hydrogen production from glucose. Recently, a hydrogen yield of 9.0 mol H_2/mol glucose was obtained by using *Rhodobacter capsulatus* JP91 with a photobioreactor operated in continuous mode (Abo-Hashesh et al., 2013).

Immobilized *Rp. palustris* CGA009 was used through the 192 h operation. The effects of inoculum volume, oxygen concentration and initial substrate concentration have been examined. The first stage was continued for 96 hours with micaerobic dark fermentation and then the process continued with photofermentation. The results showed that inoculum concentration has significantly affects hydrogen yield. The maximum yield obtained (8.6±0.8) with 100 v/v % inoculum concentration (Table 4.26). Total hydrogen production was also higher at higher concentrations above 25 v/v % (Figure 4.38).

Table 4.26 Effects of different inoculum volume on hydrogen production and yield in sequential microaerobic dark fermentation and photofermentation. The values represent mean±STD.

Inoculum con. (% vol)	**Cumulative Hydrogen (umol)**		**Glucose consumption (%)**		**Hydrogen Yield (mol H_2/mol glucose)**	
	Microaerobic Dark F.	Sequential Mic. D. F. and Photoferm.	Microaerobic Dark F.	Sequential Mic. D. F. and Photoferm.	Microaerobic Dark F.	Sequential Mic. D. F. and Photoferm.
25	9.5±1.5	75±7.0	30±4.5	55±3.0	1.2±0.1	4.6±0.2
50	27±1.8	204±2.1	60±3.5	95±3.0	1.5±0.2	6.8±0.2
100	23±2.5	168±3.5	35±4.0	65±3.5	2.1±0.2	8.6±0.8

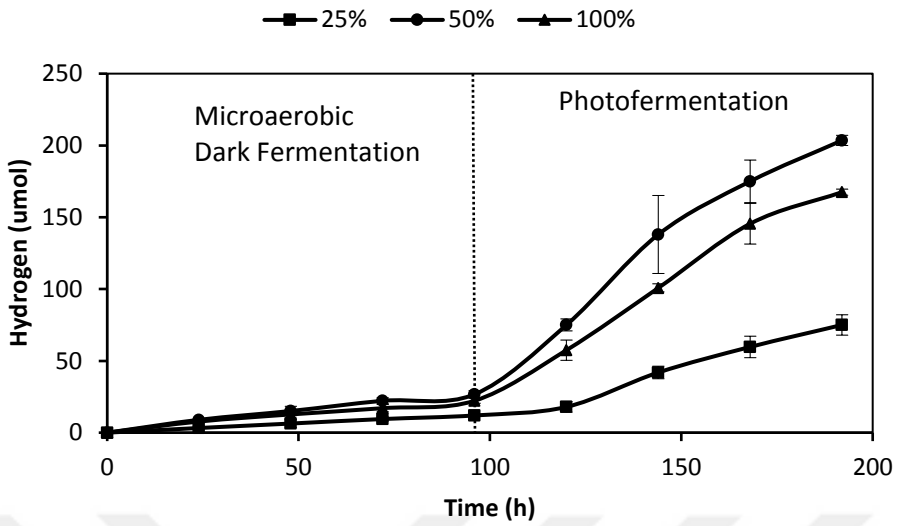

Figure 4.38 Cumulative hydrogen production throughout the sequential microaerobic dark fermentation and photofermentation on different inoculum concentration (25-50-100 v/v %). The values represent mean±STD.

Hydrogen production was the highest with 4.5% oxygen (Figure 4.39). However, the highest yield was obtained with 1% oxygen. Glucose consumption was also the highest (85%) with 4.5% oxygen concentration. Therefore, O_2 concentration of 4.5% was used in the other steps of the experiments. Hydrogen production and yield were the lowest with 8% oxygen concentration. The hydrogen yields decreased at increasing oxygen concentrations (Table 4.27).

Table 4.27 Effects of oxygen concentration on hydrogen production and yield in sequential microaerobic dark fermentation and photofermentation. The values represent mean±STD.

Oxygen con. (% vol)	**Cumulative Hydrogen (umol)**		**Glucose consumption (%)**		**Hydrogen Yield (mol H_2/mol glucose)**	
	Microaerobic Dark F.	Sequential Mic. D. F. and Photoferm.	Microaerobic Dark F.	Sequential Mic. D. F. and Photoferm.	Microaerobic Dark F.	Sequential Mic. D. F. and Photoferm.
1	15±3.5	163±3.5	35±3.5	65±3.5	1.4±0.1	8.3±0.5
4.5	38±2.7	198±2.5	45±2.5	85±3.5	2.7±0.3	7.9±0.8
8	22±1.7	58±2.5	30±3.0	45±3.0	2.4±0.5	4.1±0.4

Table 4.28 Effects of different initial glucose concentration hydrogen production and yield in sequential microaerobic dark fermentation and photofermentation.

Initial Glucose con.	**Cumulative Hydrogen (umol)**		**Glucose consumption (%)**		**Hydrogen Yield (mol H_2/mol glucose)**	
	Microaerobic Dark F.	Sequential Mic. D. F. and Photoferm.	Microaerobic Dark F.	Sequential Mic. D. F. and Photoferm.	Microaerobic Dark F.	Sequential Mic. D. F. and Photoferm.
2 mM	18±2.8	210±14	62.5±3.5	98.0±2.0	0.9±0.1	7.0±0.4
6 mM	35±6.7	723±50	36.5±2.0	62.5±3.5	0.71±0.1	7.2±0.7
10 mM	42±12	262±24	32.5±3.5	47.5±3.5	0.19±0.1	1.6±0.2

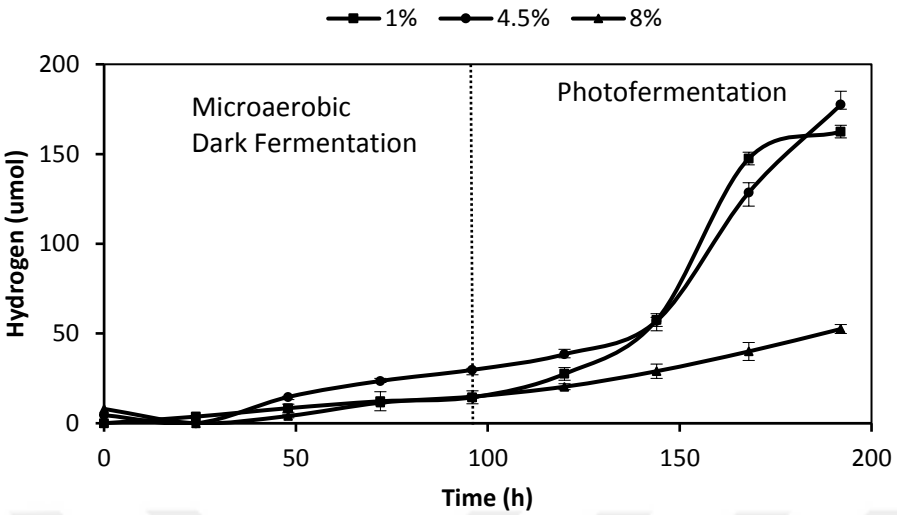

Figure 4.39 Cumulative hydrogen production throughout the sequential microaerobic dark fermentation and photofermentation on different oxygen concentration (1%, 4.5% and 8 %). The values represent mean±STD.

Figure 4.40 represents the cumulative hydrogen production throughout the sequential microaerobic dark fermentation and photofermentation on different initial glucose concentration (2-6-10 mM). The highest hydrogen was obtained on 6 mM initial glucose. The highest yield of 7.2 mol hydrogen/mol glucose was also achieved on 6 mM initial glucose (Table 4.28).

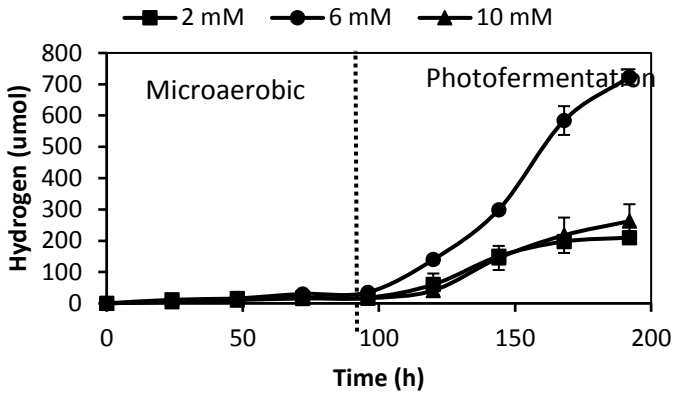

Figure 4.40 Cumulative hydrogen production throughout the sequential microaerobic dark fermentation and photofermentation on different initial glucose concentration (2-6-10 mM). The values represent mean±STD.

Figure 4.41 illustrates the change of pH during the sequential microaerobic dark fermentation and photofermentation on different initial glucose concentration (2-6-10 mM). The pH started to decrease through the first stage and then slightly increased and stabilized above pH 6.4.

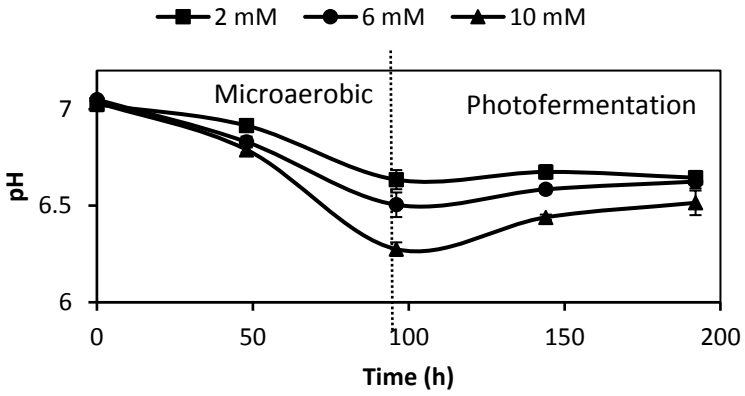

Figure 4.41 pH change of the sequential microaerobic dark fermentation and photofermentation on different initial glucose concentration (2-6-10 mM). The values represent mean±STD.

4.3.5 Hydrogen production by immobilized *Rp. palustris* CGA009 via sequential microaerobic dark and photo fermentation using RSM

In this part, biohydrogen has been produced via sequential microaerobic dark and photofermentation using RSM with Box-Behnken experimental design (Table 4.29). Immobilized *Rp. palustris* CGA009 was used through the 192 h operation. The effects of different variables including inoculum, oxygen, and initial substrate concentration have been examined. The sequential hydrogen production started with microaerobic dark fermentation and then the process continued with photofermentation.

Table 4.29 Actual design and results of the experiments by *Rp. palustris* CGA009

Run	Glucose concentration (mM)		Oxygen concentration (%)		Inoculum conc. (v/v %)		H_2 Prod. (umol)	H_2 Yield[c] (Y)	Glucose Cons. (%)
	Coded[a]	Actual[b]	Coded[a]	Actual[b]	Coded[a]	Actual[b]	Actual	Actual	
1	-1	2	-1	1	0	62.5	205	6.83	100
2	0	6	-1	1	-1	25	65	0.65	63
3	-1	2	0	4.5	1	100	155	5.17	100
4	0	6	0	4.5	0	62.5	650	6.63	62
5	0	6	-1	4.5	0	62.5	660	6.80	62
6	1	10	1	8	0	62.5	200	1.28	74
7	-1	2	0	4.5	-1	25	50.5	1.68	100
8	1	10	0	4.5	1	100	435	2.81	74
9	0	6	1	8	-1	25	60	0.59	64
10	0	6	-1	1	1	100	356	3.52	64
11	-1	2	1	8	0	62.5	50	1.67	100
12	1	10	0	4.5	-1	25	100	0.65	73
13	1	10	-1	1	0	62.5	300	1.86	77
14	0	6	0	4.5	0	62.5	642	6.36	63
15	0	6	1	8	1	100	60	0.58	65
16	0	6	0	4.5	0	62.5	641	6.68	62
17	0	6	0	4.5	0	62.5	564	5.70	63

The results indicated that the model and the variables were found significant. The maximum hydrogen yield (6.8 mol hydrogen/mol glucose)

obtained on 2 mM glucose, 1% oxygen and 62.5% inoculum concentration (Figure 4.42-4.43). ANOVA was used to test the significance of the quadratic polynomial model fitting (Table 4.30). Three independent variables in this experiment are inoculum concentration (X_1), glucose concentration (X_2), and oxygen concentration (X_3). The Model F-value of 25.18 implies the model is significant. In this case X_1, X_2, X_3, X_2X_3, X_1^2, X_2^2, X_3^2 are significant model terms. Perturbation analysis for hydrogen yield is given in Figure 4.44.

Table 4.30 ANOVA analysis of the quadratic model by *Rp. palustris* CGA009

ANOVA for Response Surface Quadratic model

Analysis of variance table [Partial sum of squares - Type III]

Source	Sum of Squares	df	Mean Square	F Value	p-value Prob > F
Model	102.54	9	11.39	25.18	0.0002
A-Inoculum conc.	9.03	1	9.03	19.96	0.0029
B-Glucose conc.	9.57	1	9.57	21.15	0.0025
C-Oxygen conc.	9.58	1	9.58	21.18	0.0025
AB	0.44	1	0.44	0.98	0.3556
AC	2.08	1	2.08	4.6	0.0691
BC	5.26	1	5.26	11.62	0.0113
A^2	31.05	1	31.05	68.62	< 0.0001
B^2	5.48	1	5.48	12.1	0.0103
C^2	23.91	1	23.91	52.84	0.0002
Residual	3.17	7	0.45		ns
Lack of Fit	2.38	3	0.79	4.05	0.1051
Pure Error	0.78	4	0.2		
Cor Total	105.71	16			

A

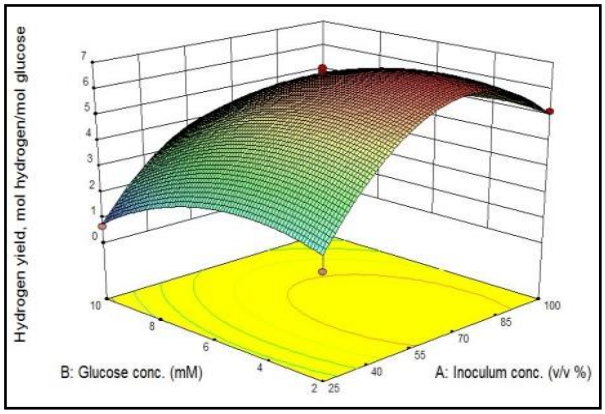

B

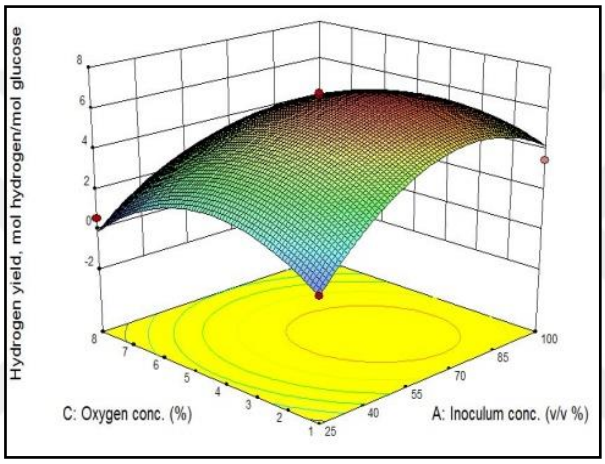

C

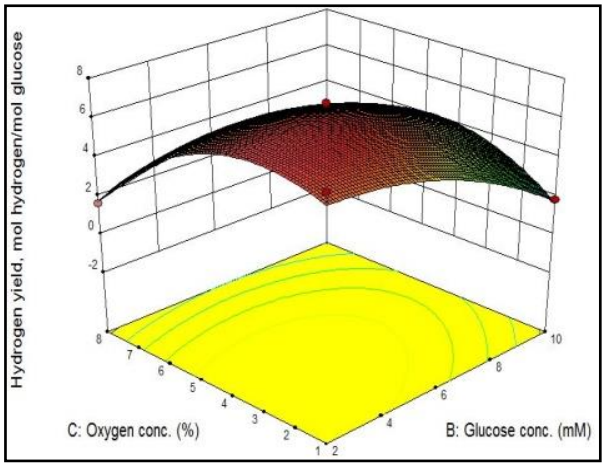

Figure 4.42 RSM plots for hydrogen yields (A, B, C) of immobilized *Rp. palustris* CGA009. The responses are given as functions of glucose, oxygen and inoculum concentrations. The fixed values are 4.5% oxygen, 6 mM glucose and 62.5 % v/v inoculum concentration for hydrogen production and yields.

A

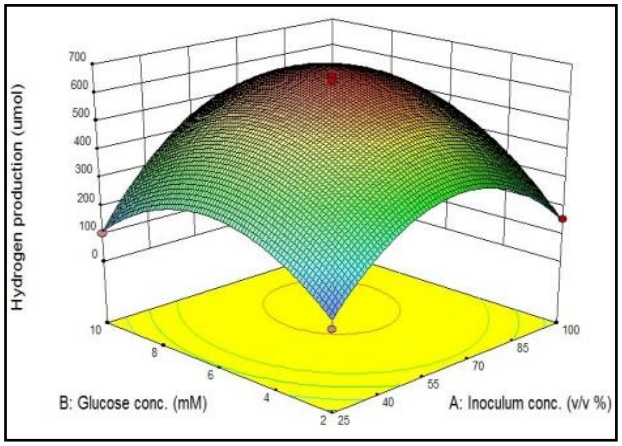

B

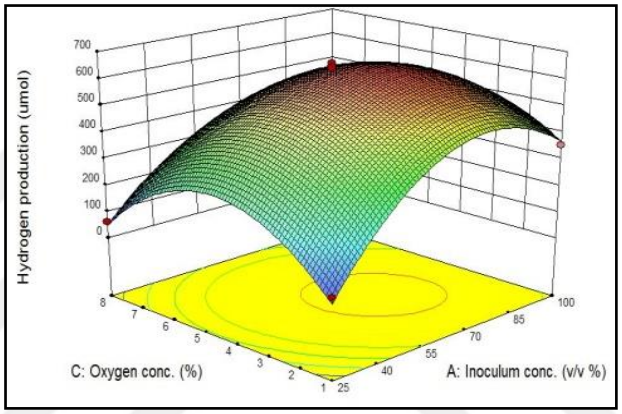

C

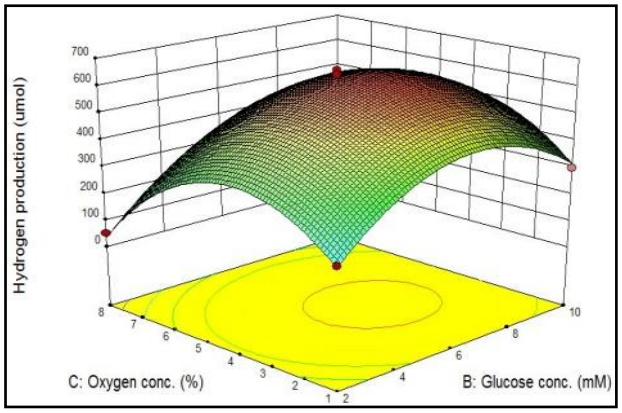

Figure 4.43 RSM plots for hydrogen production (A, B, C) of immobilized *Rp. palustris* CGA009. The responses are given as functions of glucose, oxygen and inoculum concentrations. The fixed values are 4.5% oxygen, 6 mM glucose and 62.5 % v/v inoculum concentration for hydrogen production and yields.

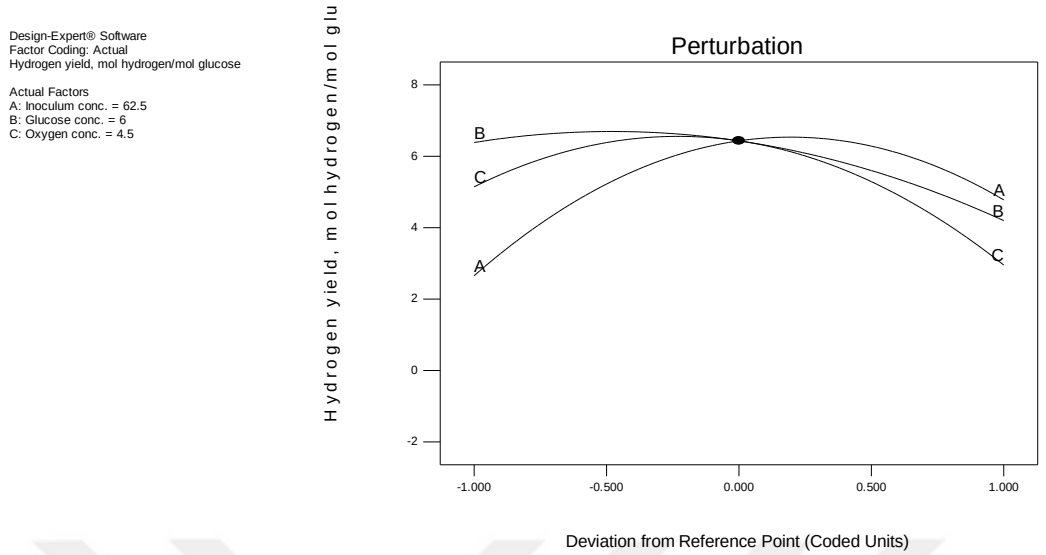

Figure 4.44 Perturbation analysis for hydrogen yield as functions of changes in inoculum conc; (A), glucose conc; (B) and oxygen conc; (C).

4.3.6 Hydrogen production by immobilized *R. capsulatus* JP91 via sequential microaerobic dark and photofermentation using RSM

Biological hydrogen was produced via sequential microaerobic dark and photofermentation using RSM with Box-Behnken experimental design (Table 4.31). Immobilized *R. capsulatus* JP91 was used in this part. The effects of different variables including inoculum, oxygen, and initial substrate concentration have been examined. The sequential hydrogen production started with microaerobic dark fermentation and then the process continued with photofermentation. ANOVA was used to test the significance of the quadratic polynomial model fitting (Table 4.32).

Table 4.31 Actual design and results of the experiments by *R. capsulatus* JP91.

Run	Inoculum concentration (%v/v)		Oxygen concentration (%)		Glucose conc. (mM)		H_2 Yield[c] (Y) (mol/mol)	Hydrogen Production[c] (umol)	Glucose consumption[c] (%)
	Coded[a]	Actual[b]	Coded[a]	Actual[b]	Coded[a]	Actual[b]			
1	0	62.5	-1	1	-1	2	6.50	195	100
2	-1	25	-1	1	0	6	1.25	135	68
3	+1	100	0	4.5	-1	2	5.50	165	100
4	0	62.5	0	4.5	0	6	6.72	720	67
5[d]	0	62.5	0	4.5	0	6	7.45	745	64
6	0	62.5	+1	8	+1	10	1.37	220	80
7	-1	25	0	4.5	-1	2	2.66	80	100
8	+1	100	0	4.5	+1	10	3.99	615	77
9	-1	25	+1	8	0	6	0.88	90	65
10	+1	100	-1	1	0	6	5.71	600	66
11	0	62.5	+1	8	-1	2	3.50	105	100
12	-1	25	0	4.5	+1	10	1.96	300	76
13	0	62.5	-1	1	+1	10	2.94	500	85
14[d]	0	62.5	0	4.5	0	6	6.98	705	64
15	+1	100	+1	8	0	6	2.30	240	65
16[d]	0	62.5	0	4.5	0	6	7.63	840	69
17[d]	0	62.5	0	4.5	0	6	7.80	820	65

[a]Coded factor values

[b]Actual factor values

[c]The hydrogen yields are the average of the three runs

[d]Center points

Table 4.32 ANOVA analysis of the quadratic model by *R. capsulatus* JP91.

Source	Sum of Squares	df	Mean Square	F Value	p-value Prob > F	
Model	106.41	9	11.82	35.42	< 0.0001	significant
A-Inoculum	9.03	1	9.03	27.06	0.0013	
B-Glucose	10.02	1	10.02	30.02	0.0009	
C-Oxygen	4.48	1	4.48	13.41	0.008	
AB	0.44	1	0.44	1.33	0.2873	
AC	2.08	1	2.08	6.24	0.0411	
BC	13.54	1	13.54	40.55	0.0004	
A^2	30.47	1	30.47	91.29	< 0.0001	
B^2	5.72	1	5.72	17.15	0.0043	
C^2	24.42	1	24.42	73.17	< 0.0001	
Residual	2.34	7	0.33			
Lack of Fit	1.55	3	0.52	2.64	0.1861	not significant
Pure Error	0.78	4	0.2			
Cor Total	108.74	16				

Three independent variables in this experiment are inoculum concentration (X_1), glucose concentration (X_2), and oxygen concentration (X_3). The Model F-value of 29.48 implies the model is significant. In this case X_1, X_2, X_3, X_1X_3, X_1^2, X_2^2, X_3^2 are significant model terms. The maximum hydrogen yield (7.8 mol hydrogen/mol glucose) obtained on 6 mM glucose, 4.5% oxygen and 62.5% inoculum concentration (Figure 4.45). The maximum hydrogen productivity was 0.15 mmol H_2 L^{-1} h^{-1}. Figure 4.46 illustrates RSM plots for hydrogen production. Perturbation analysis for hydrogen yield is given in Figure 4.47.

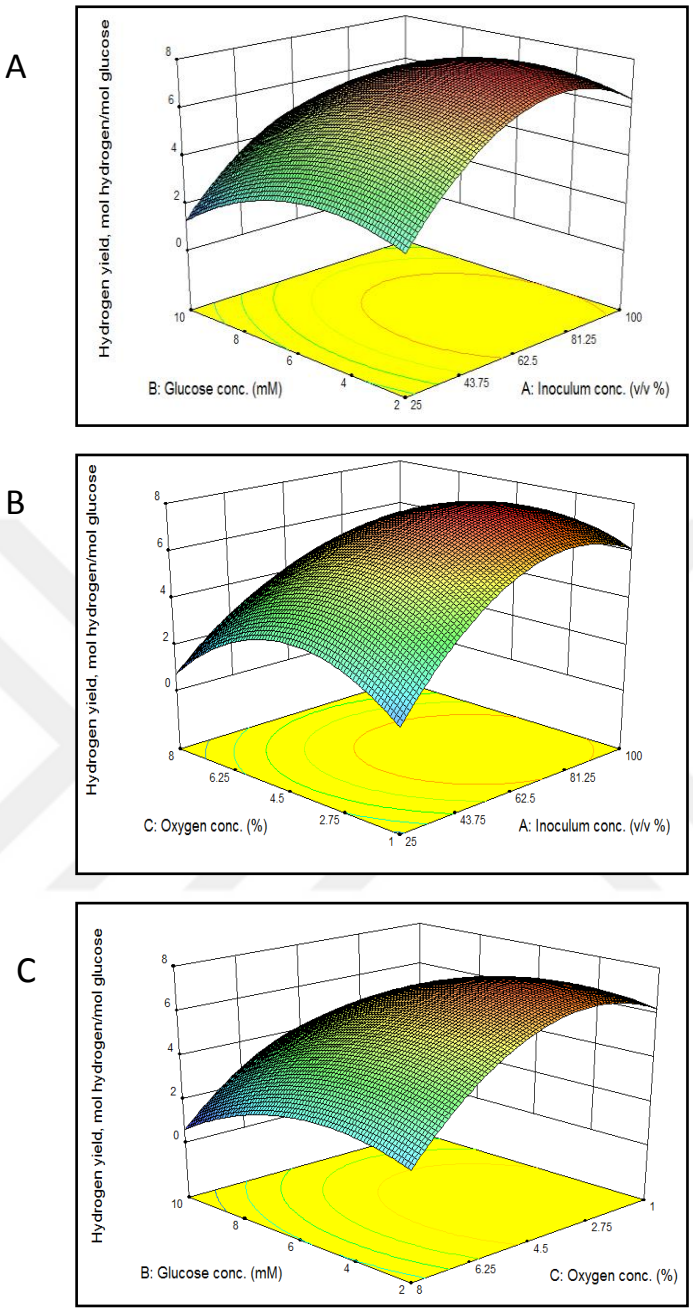

Figure 4.45 RSM plots for hydrogen yields (A, B, C) of immobilized *R. capsulatus* JP91. The responses are given as functions of glucose, oxygen and inoculum concentrations. The fixed values are 4.5% oxygen, 6 mM glucose and 62.5 % v/v inoculum concentration for both maximized hydrogen production and yields.

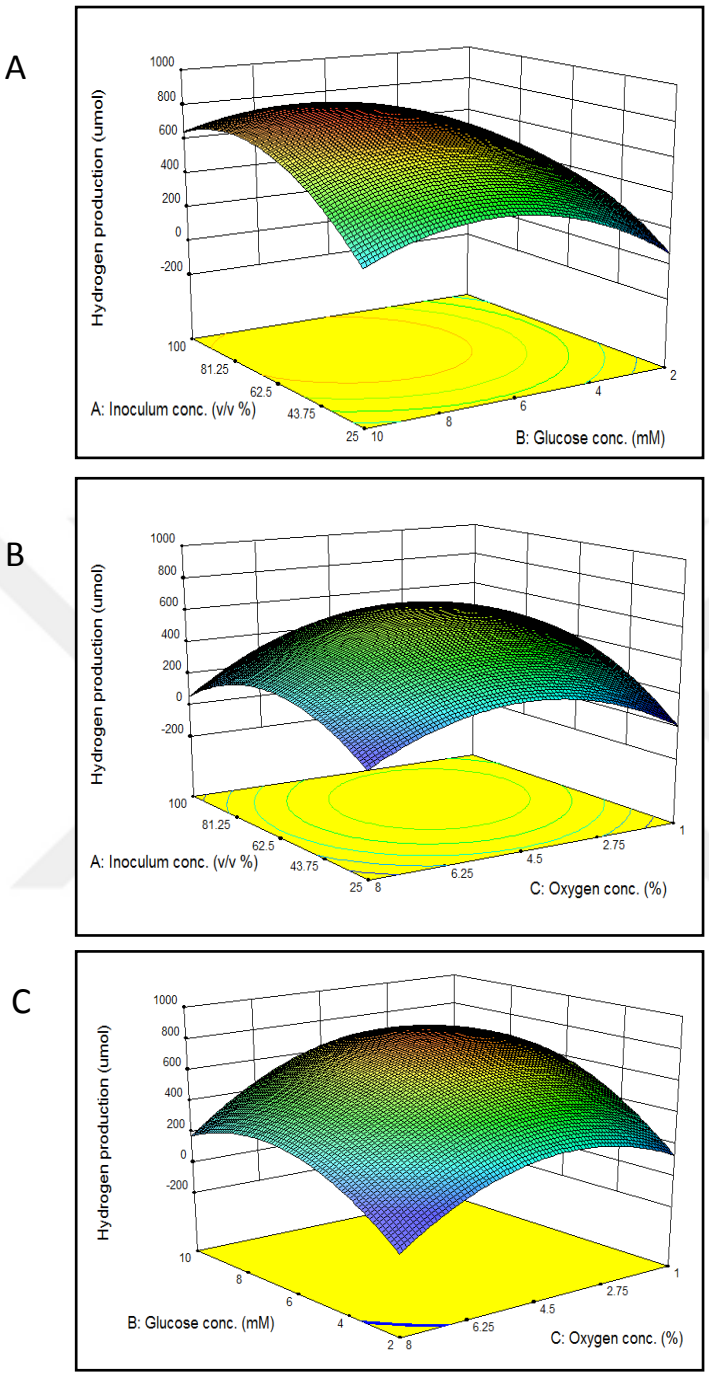

Figure 4.46 RSM plots for hydrogen production (A, B, C) of immobilized *R. capsulatus* JP91. The responses are given as functions of glucose, oxygen and inoculum concentrations. The fixed values are 4.5% oxygen, 6 mM glucose and

62.5 % v/v inoculum concentration for both maximized hydrogen production and yields.

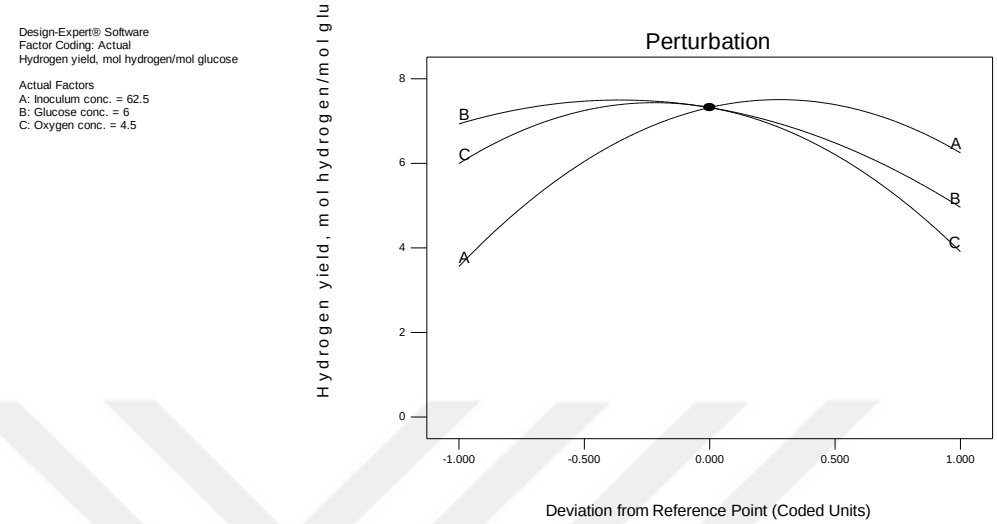

Figure 4.47 Perturbation analysis for hydrogen yield as functions of changes in inoculum conc; (A), glucose conc; (B) and oxygen conc; (C).

The sequential microaerobic dark- and photofermentative process was demonstrated to improve hydrogen production and yield. The values obtained in the present study were higher than previously obtained (0.16 mol H_2/mol glucose) by a single microaerobic dark fermentation process (Abo-Hashesh and Hallenbeck, 2012). In this work, the highest hydrogen yield was higher than the yield obtained on glucose by an immobilized system (Asada et al., 2006).

CHAPTER 5

CONCLUSIONS

Indoor and outdoor biohydrogen production was carried out by using agar-immobilized *Rhodobacter capsulatus* YO3 on sucrose and sugar beet molasses. To our knowledge, this is the first report that demonstrates operation of an immobilized photobioreactor in outdoor conditions for photofermentative hydrogen production. In outdoor runs, the highest H_2 productivity and yield were 0.87±0.06 mmol H_2 L^{-1} h^{-1} and 6.1±0.2 mol H_2/mol sucrose, respectively. The highest H_2 yield, 11.4±0.2 mol H_2/mol sucrose, was obtained in the indoor experiments with a H_2 productivity of 0.91±0.02 mmol H_2 L^{-1} h^{-1} on 10 mM sucrose. The raw sugar beet molasses were diluted to several different sucrose concentrations and used as carbon source for the immobilized bacteria. The effects of sucrose concentration in molasses were also examined. It was found that sucrose concentration in molasses should be kept below 20 mM for higher hydrogen production and yields. The highest hydrogen productivity and yield were 0.64±0.06 mmol H_2 L^{-1} h^{-1} and12.2±1.5 mol H_2/mol sucrose, respectively in indoor conditions. For outdoors, the highest productivity of 0.79±0.04 mmol H_2 L^{-1} h^{-1} and yield of 5.2±0.4 mol H_2/mol sucrose were achieved throughout 40 days of the sequential operation. The cumulative hydrogen production was lower in outdoor than in indoors. Hydrogen yields of outdoor photofermentation were almost half that obtained in indoors. This was due to illumination time of the photobioreactor causing from day and night cycle. These findings demonstrated that hydrogen production from sugar beet molasses in photofermentation is feasible by using agar immobilized bacteria in this system. The results showed

that the initial sucrose concentration of 10 mM was favorable for hydrogen production by the immobilized *R. capsulatus* YO3 in terms of the productivity and total amount of H_2 production. The present study also confirmed that sequential-batch immobilized process is promising as it offers the advantages of short time between batches, ease in bioreactor operation, and hydrogen production for extended periods, with the potential to use sucrose-containing feedstocks as feedstock. Metabolic activities such as sucrose utilization and production of acetate, lactate and formate were quite similar in indoor and outdoor conditions. However, outdoor hydrogen production and yields were lower than the indoor as hydrogen production highly is dependent on light. The light conversion efficiency also decreased on sucrose media (0.9%) compared to molasses (0.72%). This is probably due to relative dark color of the molasses which inhibits light penetration. Further studies are required to improve hydrogen production in outdoor natural conditions.

In the last part of the study, the effects of various key parameters on hydrogen production and yield were investigated in microaerobic dark fermentation and photofermentation of PNSB. Design of experiments and Response Surface Methodology (RSM) were also used to optimize factors such as inoculum volume, glucose and oxygen concentrations. The immobilized system has been shown to improve hydrogen production. Microaerobic dark fermentation was employed either in single stage or sequential with photofermentation. Cell entrapment technique was used to immobilize *Rp. palustris* CGA009 and *R. capsulatus* JP91 on agar matrix. It can be concluded that the immobilized system slightly improved hydrogen yield (from 0.7 to 0.9 mol H_2/mol glucose) in a single microaerobic dark fermentative process. Long-term microaerobic dark fermentative hydrogen production was also conducted by using *Rp. palustris* CGA009 for 600 h including five cycles. The results demonstrated that immobilized system worked properly for the long-term without any disintegration on the agar-bacteria complex. Hydrogen yields and glucose consumption also increased through the consecutive cycles. The highest hydrogen yield obtained

was 1.41 mol H_2/mol glucose on 2 mM glucose, 4.5% oxygen, 100 v/v % inoculum concentrations.

The sequential microaerobic dark and photo fermentation were shown to improve hydrogen production and yield. The highest hydrogen yields obtained with RSM by *Rp. palustris* CGA009 and *R. capsulatus* JP91 were 6.8 and 7.8 mol H_2/mol glucose, respectively. Also, the maximum hydrogen productivity was 0.15 mmol H_2 L^{-1} h^{-1}. Further research on *R. capsulatus* JP91 is required to improve hydrogen production. Large-scale operations can be suggested for the further research. Moreover, glucose containing wastes or biomass can also be used in these systems for waste treatment and hydrogen production.

Different support materials can be combined with agar to improve the stability of the agar-bacteria complex for the future work. The glass frame can be modified or improved to prevent agar cracks.

REFERENCES

Abo-Hashesh, M., Wang, R., Hallenbeck, P.C. (2011). Metabolic engineering in dark fermentative hydrogen production; theory and practice. *Bioresource Technology*, *102*, 8414–8422.

Abo-Hashesh, M., & Hallenbeck, P.C. (2012). Microaerobic dark fermentative hydrogen production by the photosynthetic bacterium, *Rhodobacter capsulatus* JP91. *International Journal of Low-Carbon Technologies, 7*(2), 97–103.

Abo-Hashesh, M., Desaunay, N., Hallenbeck, P.C. (2013). High yield single stage conversion of glucose to hydrogen by photofermentation with continuous cultures of *Rhodobacter capsulatus* JP91. *Bioresource Technol*ogy, *128*, 513–517.

Adessi, A., & De Philippis, R. (2014). Photobioreactor design and illumination systems for H_2 production with anoxygenic photosynthetic bacteria: a review. *International Journal of Hydrogen Energy, 39*, 3127-3141.

Asada, Y., Tokumoto, M., Aihara, Y., Oku, M., Ishimi, K., Wakayama, T., Miyake, J., Tomiyama, M., Kohno, H. (2006). Hydrogen production by co-cultures of Lactobacillus and a photosynthetic bacterium, *Rhodobacter sphaeroides* RV. *International Journal of Hydrogen Energy, 31*(11), 1509–1513.

Androga, D. D. (2009). Biological hydrogen production on acetate in continuous panel photobioreactors using *Rhodobacter capsulatus*. M. Sc. Thesis in Chemical Engineering Department of Middle East Technical University.

Androga, D.D., Ozgur, E., Gunduz, U., Yucel, M., Eroglu, I. (2011). Factors affecting the longterm stability of biomass and hydrogen productivity in outdoor photofermentation. *International Journal of Hydrogen Energy, 36*(17), 11369–11378.

Androga, D.D., Ozgur, E., Eroglu, I., Gunduz, U., Yucel, M. (2011). Significance of carbon to nitrogen ratio on the long-term stability of continuous photofermentative hydrogen production. *International Journal of Hydrogen Energy, 36,* 15583–15594.

Androga, D.D., Sevinc, P., Koku, H., Yucel, M., Gunduz, U., Eroglu, I. (2014). Optimization of temperature and light intensity for improved photofermentative hydrogen production using *Rhodobacter capsulatus* DSM 1710. *International Journal of Hydrogen Energy,* 39, 2472–2480.

Avcioglu, S.G., Ozgur, E., Eroglu, I., Yucel, M., Gunduz, U. (2011). Biohydrogen production in an outdoor panel photobioreactor on dark fermentation effluent of molasses. *International Journal of Hydrogen Energy, 36*(17), 11360–11368.

Asada Y., Ohsawa M., Nagai Y., Ishimi K., Fukatsu M., Hideno A., Wakayama T., Miake J., 2008 "Re-evaluation of hydrogen productivity fromacetate by some photosynthetic bacteria", *International Journal of Hydrogen Energy, 33,* 5147-5150.

Bai, X., Ye, Z., Li, Y., Ma, Y. (2010) Macroporous Poly(vinyl alcohol) Foam Crosslinked with Epichlorohydrin for microorganism immobilization. *Journal of Applied Polymer Sciences. 117,* 2732-2739.

Basak, N., Jana, A.K, Das, D., Saikia, D. (2014). Photofermentative molecular biohydrogen production by purple-non-sulfur (PNS) bacteria in various modes: The present progress and future perspective. *International Journal of Hydrogen Energy, 39,* 6853-6871.

Biebl, H., & Pfennig, N. (1981). Isolation of members of the family Rhodospirillaceae. In: Starr MP, Stolp H, Truper HG, Balows A, Schlegel HG, editors. The prokaryotes. Springer- Verlag; p. 267-273.

Boran, E., Ozgur, E., Yucel, M., Gunduz, U., & Eroglu, I. (2012). Biohydrogen production by Rhodobacter capsulatus Hup- mutant in pilot solar tubular

photobioreactor. *International Journal of Hydrogen Energy*, 37(21), 16437–16445.

Chen, C.Y., Yang, M.H., Yeh, K.L., Liu, C.H., Chang, J.S. (2008). Biohydrogen production using sequential two-stage dark and photo fermentation processes. *International Journal of Hydrogen Energy 33*, 4755-4762.

Chen, C.Y., Yeh, K.L., Lo, Y.C., Wang, H.M., Chang, J.S. (2010). Engineering strategies for the enhanced photo-H_2 production using effluents of dark fermentation processes as substrate. *International Journal of Hydrogen Energy 35*(24), 13356-13364.

Chittibabu, G., Nath, K., & Das, D. (2006). Feasibility studies on the fermentative hydrogen production by recombinant *Escherichia coli* BL-21. *Process Biochemistry*,*41*, 682-688.

Das, D., & Veziroglu, T.N. (2001). Hydrogen production by biological processes: a survey of literature. *International Journal of Hydrogen Energy*, *26*(1), 13–28.

Das, D. & Veziroglu, N. (2008). Advances in biological hydrogen production. *International Journal of Hydrogen Energy*, 33, 6046-6057.

De Vrije, T., Bakker, R.R., Budde, M.A.W., Lai, M.H., Mars, A.E., Claassen, P.A.M. (2009). Efficient hydrogen production from the lignocellulosic energy crop Miscanthus by the extreme thermophilic bacteria *Caldicellulosiruptor saccharolyticus* and *Thermotoga neapolitana*. *Biotechnology and Biofuels, 2*:12.

Dickson, J.D., Page, J.C., & Ely, I. R. (2009). Photobiological hydrogen production from *Synechocystis* sp. PCC 6803 encapsulated in silica sol-gel. *International Journal of Hydrogen Energy*, *34*, 204-215.

Ding, J., Liu, B. F., Ren, N. Q., Xing, D. F., Guo, W. Q., Xu, J. F., & Xie, G. J. (2009). Hydrogen production from glucose by co-culture of Clostridium

Butyricum and immobilized *Rhodopseudomonas faecalis* RLD-53. *International Journal of Hydrogen Energy*, *34*(9), 3647–3652.

Dincer, I., & Acar, C. (2015). Review and evaluation of hydrogen production methods for better sustainability. *International Journal of Hydrogen Energy*, *40*, 11094–11111.

Eroglu, E., & Melis, A. (2011). Photobiological hydrogen production: Recent advances and state of the art. *Bioresource Technology*, *102*, 8403-8413.

Eroglu, I., Aslan, K., Gunduz, U., Yucel, M., Turker, L. (1999). Substrate consumption rates for hydrogen production by *Rhodobacter sphaeroides* in a column photobioreactor. *Journal of Biotechnology*, 70, 103–113.

Fabiano, B., & Perego, P. (2002). Thermodynamic study and optimization of hydrogen production by *Enterobacter aerogenes*. *International Journal of Hydrogen Energy*, *27*: 149-156.

Felton, P.V., Zurrrer, H., & Bachofen, R. (1985). Production of molecular hydrogen with immobilized cells of *Rhodospirllum rubrum*. *Applied Microbiology and Biotechnology*, *23*, 15–20.

Fißler, J., Kohring, G.W., & Giffhorn, F. (1995). Enhanced hydrogen production from aromatic acids by immobilized cells of *Rhodospseudomonas palustris*. *Applied Microbiology and Biotechnology*, *44*, 43-46.

Ghosh, D., & Hallenbeck, P.C. (2009). Fermentative hydrogen yields from different sugars by batch cultures of metabolically engineered *Escherichia coli* DJT135. *International Journal of Hydrogen Energy*, *34*, 7979-7982.

Gosse, J.L., Engel, B.J., Rey, F.E., Harwood, C.S., Scriven, L.E., Flickinger, M.C. (2007). Hydrogen production by photoreactive nanoporous latex coatings of nongrowing *Rhodopseudomonas palustris* CGA009. *Biotechnology Progress*, *23*, 124–130.

Guevara-Lopez, E., & Buitron G. (2015). Evaluation of different support materials used with a photo-fermentative consortium for hydrogen production. *International Journal of Hydrogen Energy*, *40*:17231–17238.

Guo, C.L., Zhu, X., Liao, Q., Wang, Y.Z., Chen, R., Lee, D.J. (2011). Enhancement of photo-hydrogen production in a biofilm photobioreactor using optical fiber with additional rough surface. *Bioresource Technology*, *102*, 8507-8513.

Hallenbeck, P.C. (2014). Bioenergy from Microorganisms: An Overview. In D. Zannoni & R. De Philips (Eds.), *Microbial Bioenergy*: Hydrogen Production (pp. 3–21).

Hallenbeck, P.C., & Benemann, J.R. (2002). Biological hydrogen production; fundamentals and limiting proceses. *International Journal of Hydrogen Energy*, *27*, 1185-1193.

Hallenbeck, P. C., & Liu, Y. (2015). Recent advances in hydrogen production by photosynthetic bacteria. *International Journal of Hydrogen Energy*, 1–9.

Holladay, J.D., Hu, J., King, D.L., Wang, Y. (2009). An overview of hydrogen production technologies. *Catalysis Today*, 139, (244-260).

Ivanova, G., Rakhely, G., Kovacs, K.L. (2009). Thermophilic biohydrogen production from energy plants by *Caldicellulosiruptor saccharolyticus* and comparison with related studies. *International Journal of Hydrogen Energy*, *34*, 3659-3670.

Imhoff, J.F. (2006). The Phototrophic Alpha-Proteobacteria. Prokaryotes, 5: 41-64. New York, NY: Springer New York.

International Energy Agency, Technology Roadmap, Hydrogen and Fuel Cells, 2015. https://www.iea.org/publications/freepublications/publication/technology-roadmap-hydrogen-and-fuel-cells.html

International Energy Agency, Key World Energy Statistics, 2016. Website: https://www.iea.org/publications/freepublications/publication/KeyWorld2016.pdf

International Energy Agency, Key World Energy Trends, 2016. https://www.iea.org/publications/freepublications/publication/KeyWorldEnergyTrends.pdf

Intergovernmental Panel on Climate Change (IPCC), 2014. https://www.ipcc.ch/pdf/assessmentreport/ar5/syr/SYR_AR5_FINAL_full_wcover.pdf

Kayahan, E., Eroglu, I., Koku, H. (2016). Design of an outdoor stacked-tubular reactor for biological hydrogen production. *International Journal of Hydrogen Energy*, *41*:19357–66.

Kayahan, E., Eroglu, I., Koku, H. (2017). A compact tubular photobioreactor for outdoor hydrogen production from molasses. *International Journal of Hydrogen Energy*, *42*:2575–82.

Keskin T, Hallenbeck PC. (2012). Hydrogen production from sugar industry wastes using single-stage photofermentation. Bioresource Technology, *112*:131–6.

Kosourov, S.N., Seibert, M. (2009). Hydrogen photoproduction by nutrient-deprived *Chlamydomonas reinhardtii* cells immobilized within thin alginate films under aerobic and anaerobic conditions. *Biotechnology and Bioengineering*, *102*: 50–58.

Kothari, R., Buddhi, D., & Sawhney, R. L. (2008). Comparison of environmental and economic aspects of various hydrogen production methods. *Renewable and Sustainable Energy Reviews*, *12*(2), 553–563.

Kothari, R., Singh, D.G., Tyagi, V.V., Tyagi, S.K. (2012). Fermentative hydrogen production – An alternative clean energy source. *Renewable and Sustainable Energy Reviews*, *16*, 2337-2346.

Kourkoutas, Y., Bekatorou, A., Banat, I.M., Marchant, R., Koutinas, A.A. (2004) Immobilization technologies and support materials suitable in alcohol beverages production: a review. *Food Microbiology*, *21*: 377–397.

Lazaro, C.Z., Hitit, Z.Y., Hallenbeck, P.C. (2017). Optimization of the yield of dark microaerobic production of hydrogen from lactate by *Rhodospeudomonas palustris*, *Bioresource Technology*, 245, 123-131.

Levin, D. B., & Chahine, R. (2010). Challenges for renewable hydrogen production from biomass. *International Journal of Hydrogen Energy*, *35*(10), 4962–4969.

Liu, F.B., Ren, Q.N., Xing, F.D., Ding, J., Zheng X.G., Guo, Q.W., Xu, F.J., Xie, J. G. (2009). Hydrogen production by immobilized *R. faecalis* RLD-53 using soluble metabolites from ethanol fermentation bacteria *E. harbinense* B49. *Bioresource Technology*, *100*, 2719-2723.

Madigan, M.T., Martinko, J.M., Parker, J. (2000). Brock Biology of Microorganisms, ninth ed. Prentice Hall Inc., New Jersey.

McKinlay, J. B., & Harwood, C. S. (2010). Photobiological production of hydrogen gas as a biofuel. *Current Opinion in Biotechnology*, *21*(3), 244–51.

Merugu, R., Rudra, M. P. P., Nageshwari, B., Rao, A. S., & Ramesh, D. (2012). Photoproduction of Hydrogen under Different Cultural Conditions by Alginate Immobilized *Rhodopsedomonas palustris* KU003, 2012(1989). https://doi.org/10.5402/2012/757503

Miller, G.L. (1959). Use of dinitrosalicylic acid reagent for determination of reducing sugar. *Analytical Chemistry*, *31*, 426-428.

Montiel-Corona, V., Revah, S., & Morales, M. (2015). Hydrogen production by an enriched photoheterotrophic culture using dark fermentation effluent as substrate: Effect of flushing method, bicarbonate addition, and outdoor-indoor conditions. *International Journal of Hydrogen Energy*, 40: 9096–105.

Noparat, P., Prasertsan, P., O-Thong, S. (2011). Isolation and characterization of high hydrogen-producing strain *Clostridium beijerinckii* PS-3 from fermented oil palm sap. *Int J Hydrogen Energy, 36,* 14086-14092.

Ozgur, E., Uyar, B., Ozturk, Y., Yucel, M., Gunduz, U., Eroglu, I. (2010). Biohydrogen production by *Rhodobacter capsulatus* on acetate at fluctuating temperatures. *Resources, Conservation and Recycling, 54,* 310-314.

Ozgur, E., Uyar, B., Öztürk, Y., Yucel, M., Gunduz, U., & Eroğlu, I. (2010). Biohydrogen production by *Rhodobacter capsulatus* on acetate at fluctuating temperatures. *Resources, Conservation and Recycling*, *54*(5), 310–314.

Ozgur, E., & Peksel, B. (2013). Biohydrogen production from barley straw hydrolysate through sequential dark and photofermentation. *Journal of Cleaner Production*, *52*, 14–20.

Ozgur, E., Mars, A.E., Peksel, B., Louwerse, A., Yucel, M.., Gunduz, U. (2010). Biohydrogen production from beet molasses by sequential dark and photo-fermentation. *International Journal of Hydrogen Energy 35*, 511-517.

Pandey A., Pandey A., 2008 "Reverse micelles as suitable microreactor for increased biohydrogen production" *International Journal of Hydrogen Energy* 33 (1), 273 – 278.

Patel, S.K.S., Kumar, P., Kalia,V.P. (2012). Enhancing biological hydrogen production through complementary microbial metabolisms. *International Journal of Hydrogen Energy*, 37, 10590-10603.

Pattra, S., Sangyoka, S., Boonmee, M., Reungsang, A. (2008). Biohydrogen production from the fermentation of sugarcane bagasse hydrolysate by *Clostridium butyricum*. *International Journal of Hydrogen Energy*, *33*, 5256-5265.

Planchard, A., Mignot, L., Jouenne, T., Junter, G.A. (1984). Photoproduction of molecular hydrogen by *Rhodospirillum rubrum* immobilized in composite agar

layer/microporous membrane structures. *Applied Microbiology and Biotechnology 31*, 49–54.

Redwood, M.D., Paterson-Beedle, M., & Macaskie, L.E. (2009). Integrating dark and light bio-hydrogen production strategies: towards the hydrogen economy. *Reviews in Environmental Science and Biotechnology*, *8*, 149–185.

Rey, F. E., & Harwood, C. S. (2010). FixK , a global regulator of microaerobic growth , controls photosynthesis in *Rhodopseudomonas palustris*, *Molecular Microbiology*, *75*(4), 1007–1020.

Sagir, E., Alipour, S., Elkahlout, K., Koku, H., Gunduz, U., Eroglu, I., & Yucel, M. (2017b). Scale-up studies for stable, long-term indoor and outdoor production of hydrogen by immobilized *Rhodobacter capsulatus*. *International Journal of Hydrogen Energy*, 42(36): 22743-22755.

Sagir, E., Yucel, M., & Hallenbeck, P. C. (2017c). Demonstration and optimization of sequential microaerobic dark- and photo-fermentation biohydrogen production by immobilized *Rhodobacter capsulatus* JP91. *Bioresource Technology*,250:43-52.

Sagir, E., Ozgur, E., Gunduz, U., Eroglu, I., Yucel, M. (2017a). Single-stage photofermentative biohydrogen production from sugar beet molasses by different purple non-sulfur bacteria. *Bioprocess and Biosystems Engineering*. *40*(11): 1589-1601.

Sasikala, K., Ramama, C. V., & Raghuveer Rao, P. (1991). Environmental regulation for optimal biomass yield and photoproduction of hydrogen by *Rhodobacter sphaeroides* O.U.001. *Biotechnology*, *16*(9), 597–601.

Show, K.Y., Lee, D. J., Tay, J. H., Lin, C. Y., & Chang, J. S. (2012). Biohydrogen production: Current perspectives and the way forward. *International Journal of Hydrogen Energy*, *37*(20), 15616–15631.

Singh, L., Wahid, Z.A. (2015). Methods for enhancing bio-hydrogen production from biological process: A review. *Journal of Industrial and Engineering Chemistry*, *21*, 70-80.

Singh, L., & Wahid, Z.A. (2015). Enhancement of hydrogen production from palm oil mill effluent via cell immobilisation technique. *International Journal of Energy Research*, *39*, 215-222.

Sun, Q., Xiao, W., Xi, D., Shi, J., Yan, X., Zhou, Z. (2010). Statistical optimization of biohydrogen production from sucrose by a co-culture of *Clostridium acidisoli* and *Rhodobacter sphaeroides*. *International Journal of Hydrogen Energy, 35*, 4076-4084.

Smirnova, T.A., Didenko, L.V., Azizbekyan, R.R., Romanova, Y.M. (2010). Structural and functional characteristics of bacterial biofilms. *Microbiology, 79*:413–423.

Song, W., Rashid, N., Choi, W., Lee, K. (2011). Biohydrogen production by immobilized *Chlorella* sp. Using cycles of oxygenic photosynthesis and anaerobiosis. *Bioresource Technology*, *102*: 8676–81.

Tao, Y., Chen, Y., Wu, Y., He, Y., Zhou, Z. (2007). High hydrogen yield from a two-step process of dark- and photo-fermentation of sucrose. *International Journal of Hydrogen Energy, 32*(2), 200-206.

Tian X, Liao Q, Liu W, Wang YZ, Zhu X, Li J, Wang H (2009) Photo-hydrogen production rate of a PVA-boric acid gel granule containing immobilized photosynthetic bacteria cells. *International Journal of Hydrogen Energy* 34:4708–4717.

Tian, X., Liao, Q., Zhu, X., Wang, Y., Zhang, P., Li, J. (2010). Characteristics of a biofilm photobioreactor as applied to photo-hydrogen production. Bioresource Technology, *101*, 977-983.

Tsygankov, A.A., Hirata, Y., Miyake, M., Asada, Y., Miyake, J. (1994). Photobioreactor with photosynthetic bacteria immobilized on porous glass for

hydrogen photoproduction. *Journal of Fermentation and Bioengineering, 77*, 575-578.

Tsygankov, A.A. (2001). Hydrogen production by purple bacteria: immobilized vs. suspension cultures. In: Miyake J, Matsunaga T, San Pietro A (eds) Biohydrogen 2. An approach to environmentally acceptable technology. Pergamon Press, Amsterdam, pp 229–244.

Tsygankov, A. & Kosourov, S. (2014). Bioenergy from Microorganisms: An Overview. In D. Zannoni & R. De Philips (Eds.), *Microbial Bioenergy: Hydrogen Production* (pp. 321–342). Springer.

Urbaniec, K., & Grabarczyk, R. (2009). Raw materials for fermentative hydrogen production. *Journal of Cleaner Production*, *17*(10), 959–962.

Urbaniec, K., & Grabarczyk, R. (2014). Hydrogen production from sugar beet molasses – a techno-economic study. *Journal of Cleaner Production, 65*, 324–329.

Wang, Y.Z., Liao, Q., Zhu, X., Chen, R., Guo, C.L., Zhou, J. (2013). Bioconversion characteristics of *Rhodopseudomonas palustris* CQK 01 entrapped in a photobioreactor for hydrogen production. *Bioresource Technology, 135*: 331-338.

Xie G-J, Liu B-F, Ding J, Xing D-F, Ren H-Y, Guo W-Q, et al. Enhanced photo-H2 production by *Rhodopseudomonas faecalis* RLD-53 immobilization on activated carbon fibers. Biomass Bioenergy 2012b;44:122e9.

Xie, G.J., Liu, B.F., Xing, D.F., Nan, J., Ding, J., Ren, H.Y. (2012a). Photo-hydrogen production by *Rhodopseudomonas faecalis* RLD-53 immobilized on the surface of modified activated carbon fibers. *RSC Advances, 2*(6), 2225-2228.

Zagrodnik, R., Thiel, M., Seifert, K., Włodarczak, M., Łaniecki, M. (2013). Application of immobilized *Rhodobacter sphaeroides* bacteria in hydrogen generation process under semi-continuous conditions. *International Journal of Hydrogen Energy*, 38, 7632-639.

Zhang, C., Zhu, X., Liao, Q., Wang, Y.Z., Li, J., Ding, Y.D., Wang, H. (2010). Performance of a groove-type photobioreactor for hydrogen production by immobilized photosynthetic bacteria. *International Journal of Hydrogen Energy*, *35* (11), 5284–5292.

Zhu, H., Wakayama, T., Suzuki, T., Asada, Y., Miyake, J. (1999a). Entrapment of *Rhodobacter sphaeroides* RV ic cationic polymer/agar gels for hydrogen production in the presence of NH_4^+. *Journal of Bioscience and Bioengineering*, *88*(5), 507-512.

Zhu, H., Suzuki, T., Tsygankov, A.A., Asada, Y., Miyake, J. (1999b). Hydrogen production from tofu wastewater by *Rhodobacter sphaeroides* immobilized in agar gels. *International Journal of Hydrogen Energy*, *24*(4), 305-310.

A. COMPOSITION OF THE GROWTH AND HYDROGEN PRODUCTION MEDIA AND SOLUTIONS

Table A.1 Composition of the growth medium (Acetate/Glutamate, 20 mM /10 mM, MERCK CHEMICALS)

Components	Amount	Unit
KH_2PO_4	3.0	g/L
$MgSO_4.7H_2O$	0.5	g/L
$CaCl_2.2H_2O$	0.05	g/L
Vitamin Solution (1X)	1	mL/L
Fe-Citrate Solution (50X)	0.5	mL/L
Trace Element Solution (10X)	0.1	mL/L
Monosodium Glutamate (10 mM)	1.8	g/L
Acetic acid (20 mM)	1.15	mL/L

Table A.2 Composition of sucrose/acetate growth medium (Sucrose/Acetate/Glutamate, 10 mM/20 mM/2 mM).

Components	Amount	Unit
KH_2PO_4 (30 mM)	4.1	g/L
$MgSO_4.7H_2O$	0.5	g/L
$CaCl_2.2H_2O$	0.05	g/L
Vitamin Solution (1X)	1.0	mL/L
Fe-Citrate Solution (50X)	0.5	mL/L
Trace Element Solution (10X)	0.1	mL/L
Monosodium Glutamate (2 mM)	0.36	g/L
Acetic acid (20 mM)	1.15	mL/L
Sucrose (10 mM)	3.42	g/L

Table A.3 Composition of sucrose growth medium (Sucrose/Glutamate, 10 mM/2 mM)

Components	Amount	Unit
KH_2PO_4 (20 mM)	2.73	g/L
$MgSO_4.7H_2O$	0.5	g/L
$CaCl_2.2H_2O$	0.05	g/L
Vitamin Solution (1X)	1.0	mL/L
Fe-Citrate Solution (50X)	0.5	mL/L
Trace Element Solution (10X)	0.1	mL/L
Monosodium Glutamate (2 mM)	0.36	g/L
Sucrose (20 mM)	3.42	g/L

Table A.4 Hydrogen production media with different sucrose concentrations. [a]: 5 mM, [b]: 10 mM, [c]: 20 mM.

Components	Amount	Unit
KH_2PO_4 (30 mM)	4.09	g/L
$MgSO_4.7H_2O$	0.5	g/L
$CaCl_2.2H_2O$	0.05	g/L
Vitamin Solution (1X)	1.0	mL/L
Fe-Citrate Solution (50X)	0.5	mL/L
Trace Element Solution (10X)	0.1	mL/L
Monosodium Glutamate (4 mM)	0.72	g/L
[a]Sucrose (5 mM)	1.71	g/L
[b]Sucrose (10 mM)	3.42	g/L
[c]Sucrose (20 mM)	6.84	g/L

Table A5. Composition of trace elements solution (1X) components.

Component	Amount/Unit
HCl (25% v/v)	1 mL/L
$ZnCl_2$	70 mg/L
$MnCl_2.4H_2O$	100 mg/L
H_3BO_3	60 mg/L
$CoCl_2.6H_2O$	200 mg/L
$CuCl_2.2H_2O$	20 mg/L
$NiCl_2.6H_2O$	20 mg/L
$NaMoO_4.2H_2O$	40 mg/L

Table A6. Composition of RCV-lactate medium.

Components	Amount	Unit
Na-lactate (10%)	40	mL/L
Super-salts	50	mL/L
K-phosphate buffer (0.64 M)	15	mL/L

Table A7. Composition of RCV-glucose medium.

Components	Amount	Unit
Glucose	2-6-10	mM
Super-salts	50	mL/L
K-phosphate buffer (0.64 M)	15	mL/L

Table A8. Composition of the supersalts of RCV medium.

Components	Amount/Unit
1% EDTA	40 mL/L
20% $MgSO_4 \cdot 7H_2O$	20 mL/L
7.5% $CaCL_2 \cdot 2H_2O$	20 mL/L
1% $FeSO_4 \cdot 7H_2O$	20 mL/L
0.1% Thiamine·HCl	20 mL/L
Trace elements	20 mL/L

Table A9. Composition of the trace elements of RCV medium.

Components	Amount/Unit
$MnSO_4 \cdot H_2O$	398 mg/250 mL
H_3BO_3	700 mg/250 mL
$Cu(NO_3)_2 \cdot H_2O$	10 mg/250 mL
$ZnSO_4 \cdot 7H_2O$	60 mg/250 mL
$Na_2MoO_4 \cdot 2H_2O$	188 mg/250 mL

B. ORGANIC ACID ANALYSIS

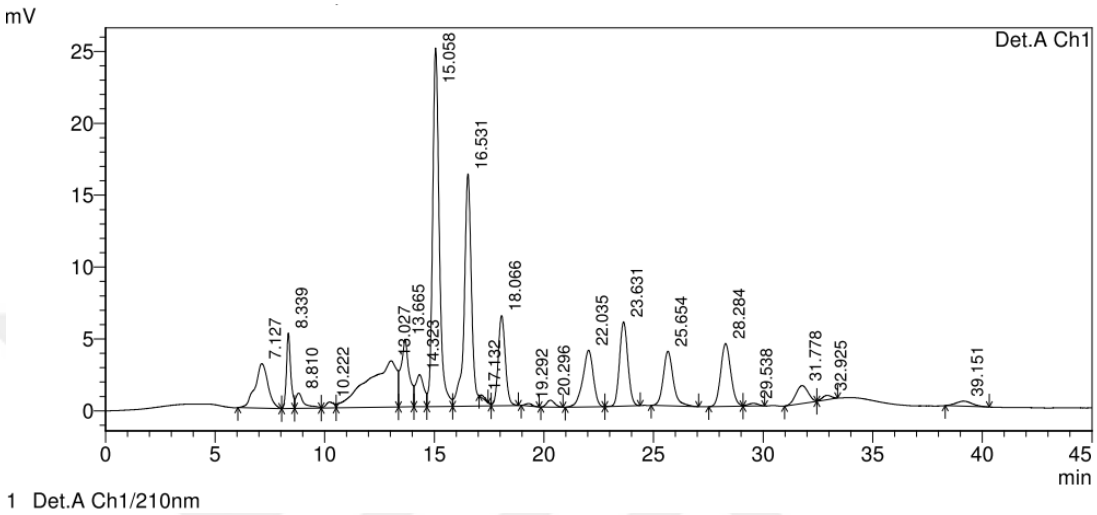

Figure B1. Sample HPLC organic acid chromatogram

(Retention times for Lactic acid peak in 22.035, Acetic acid peak in 25.654 min and Formic acid peak is in 23.631 min, Shimadzu Agilent 10A series HPLC, UV 210 nm detector).

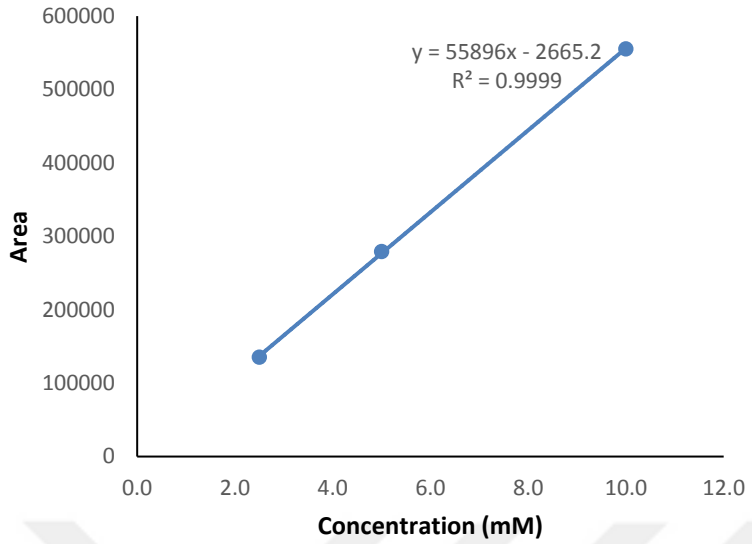

Figure B2. HPLC calibration for acetic acid.

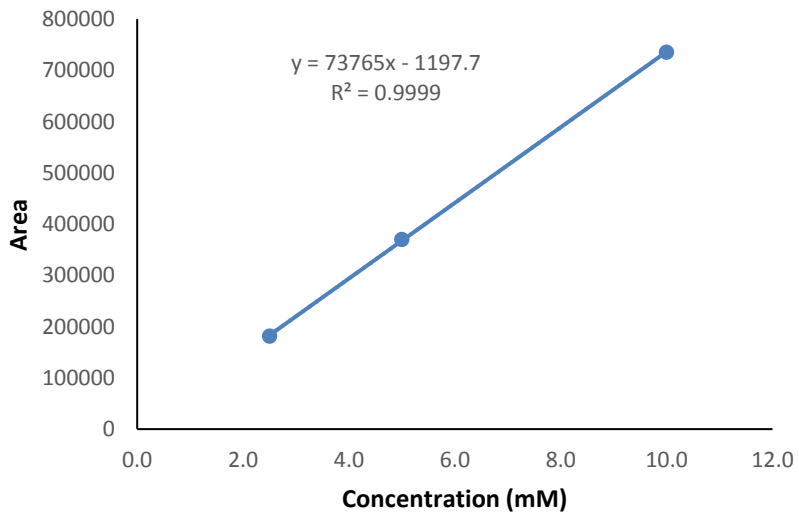

Figure B3. HPLC calibration for formic acid

C. SAMPLE SUGAR ANALYSIS

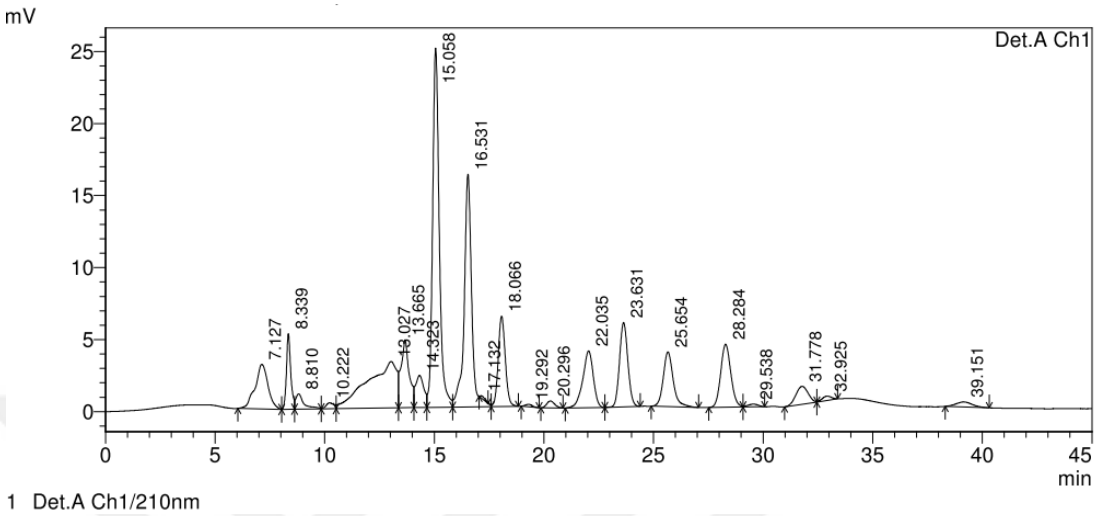

Figure C1. Sample HPLC sucrose chromatogram

(Retention times for sucrose peak is in 15.058 min, for glucose 16.531 min, Shimadzu Agilent 10A series HPLC, UV 210 nm detector).

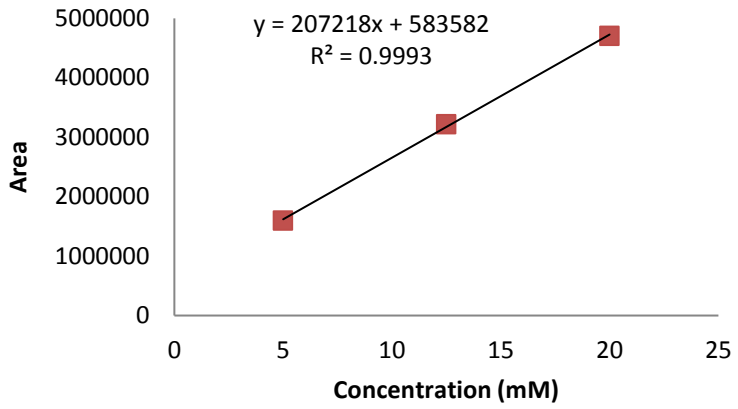

Figure C.2 Sample standard sucrose calibration curve (HPLC, Agilent 10A series).

D. SAMPLE GAS CHROMATOGRAM

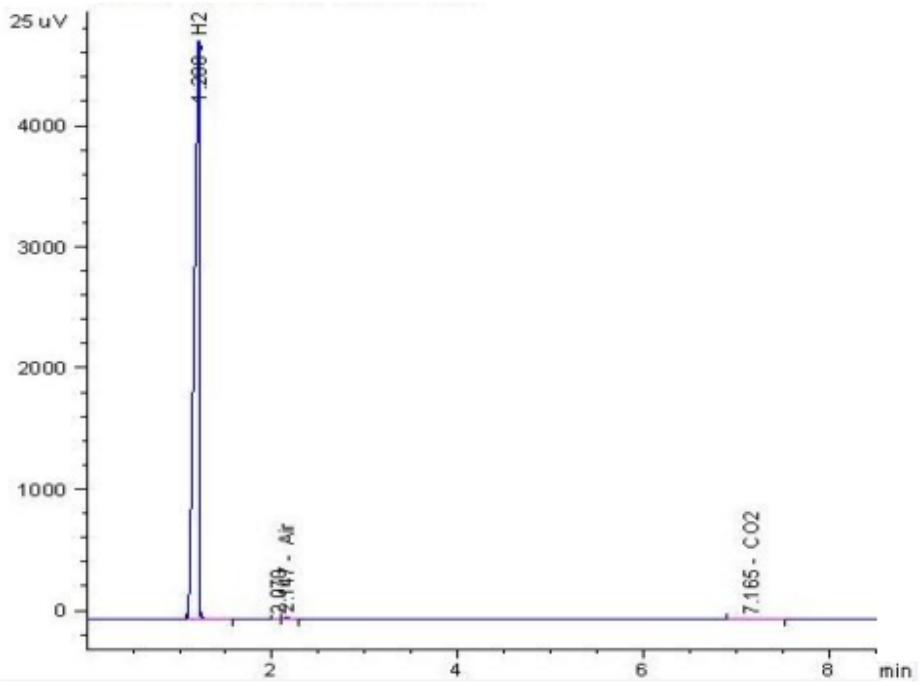

RetTime [min]	Type	Area [25 uV*s]	Amt/Area	Norm %	Grp	Name
1.208	BB	1.78157e4	5.36760e-3	92.790983		H2
2.147	VB	104.16668	4.30476e-2	4.351104		Air
7.165	BB	52.88443	5.56929e-2	2.857913		CO2

Figure D1. Sample gas chromatogram

(Agilent Technologies 6890 N gas chromatography) (Androga, 2009)

E. COMPOSITION OF SUGAR BEET MOLASSES

Table E1. Composition of raw sugar beet molasses. The analysis was carried out by Düzen Norwest Laboratory in Ankara.

Parameters	**Units**	**Results of Chemical Analysis**
Sucrose	(% w/w)	51.85
Iron (Fe)	mg/kg	14.1
Molybdenum (Mo)	mg/kg	0.22
Sulphur (S)	g/kg	1.03
Potassium (K)	g/kg	35.6
Total amino acids	g/100g	4.7
Aspartic acid	g/100g	0.358
Glutamic acid	g/100g	2.541
Asparagine	g/100g	<0.10(1)
Serine	g/100g	0.229
Histidine	g/100g	<0.25(1)
Glycine	g/100g	0.192
Threonine	g/100g	0.066
Citrulline	g/100g	<0.07(1)

Arginine	g/100g	0.08
Alanine	g/100g	0.252
Tyrosine	g/100g	0.191
Cystine	g/100g	<0.30(1)
Valine	g/100g	0.139
Methionine	g/100g	<0.12(1)
Tryptophan	g/100g	<0.28(1)
Phenylalanine	g/100g	<0.23(1)
Isoleucine	g/100g	0.202
Ornithine	g/100g	<0.29(1)
Lysine	g/100g	0.172
Hydroxyproline	g/100g	<0.27(1)
Sarcosine	g/100g	<0.09(1)
Proline	g/100g	0.234
(1) MDL, Method detection limit		

Table E2. Composition of raw sugar beet molasses. The analysis was carried out by Ankara Sugar Factory.

Parameters	**Method**	**Results**
Refractometric dry matter	ICUMSA Method GC 4-13	82.36
Polar sugar (%)	British Sugar Method	51.52
Invert sugar [(2)] (%)	Berlin Institude Method	8.62
Sucrose (w/w %)	ICUMSA method GS 4/3-7	51.85
Total nitrogen (%)	British sugar method	1.7
Density (g/cm^3)	Density without air	1.27

(2) Invert sugar is the mixture of glucose and fructose.

F. INDOOR EXPERIMENTAL DATA

Table F.1 pH change and hydrogen production of long-term process on 5 mM sucrose medium by *R. capsulatus* YO3

Days	pH	H_2 (L)	Days	pH	H_2 (L)
0	7.46	0	20	7	5.47
1	7.28	0.04	21	6.87	5.97
2	6.8	0.28	22	6.54	6.53
3	6.34	0.36	23	6.45	6.83
4	7.44	0.36	24	7	6.83
5	7.21	0.68	25	6.8	7.33
6	6.85	1.24	26	6.74	7.93
7	6.35	1.27	27	6.6	8.08
8	7.45	1.27	28	7	8.08
9	6.57	1.72	29	6.82	8.48
10	6.45	2.52	30	6.76	9.18
11	6.25	2.62	31	6.6	9.38
12	7.45	2.62	32	7	9.38
13	6.65	3.12	33	6.8	9.88
14	6.6	3.77	34	6.6	10.46
15	6.53	4.02	35	6.58	10.67
16	7.45	4.02	36	7	10.67
17	6.54	4.57	37	6.8	11.12
18	6.5	5.27	38	6.6	11.72
19	6.45	5.47	39	6.58	11.82

Days	pH	H_2 (L)
40	7	11.82
41	6.82	12.34
42	6.74	12.8
43	6.62	13
44	7	13
45	6.86	13.4
46	6.72	13.85
47	6.6	14.05
48	7	14.05
49	6.85	14.47
50	6.75	14.82
51	6.61	15.12
52	7	15.12
53	6.87	15.52
54	6.76	15.97
55	6.64	16.17
56	7	16.17
57	6.78	16.57
58	6.68	16.87
59	6.58	17.07
60	7	17.07
61	6.78	17.47
62	6.65	17.82
63	6.58	17.97
64	6.54	17.97

Table F.2 pH change and hydrogen production on 10 mM sucrose medium by *R. capsulatus* YO3

Days	**pH**	**H_2 (L)**
0	7.51	0
1	7.43	0.01
2	7.39	0.12
3	7.02	0.4
4	6.2	0.18
5	7.43	0
6	6.89	0.445
7	6.45	0.63
8	6.23	0.29
9	7.45	0
10	6.36	0.69
11	6.35	0.775
12	6.27	0.295
13	7.45	0
14	6.78	0.74
15	6.34	0.67
16	6.2	0.245
17	7.44	0
18	6.29	0.68
19	6.14	0.75
20	6.1	0.235

Table F.3 pH change and hydrogen production on 20 mM sucrose medium by *R. capsulatus* YO3

Days	**pH**	**H_2 (L)**
0	7.51	0
1	7.43	0.01
2	7.39	0.12
3	7.02	0.4
4	6.2	0.18
5	7.43	0
6	6.89	0.445
7	6.45	0.63
8	6.23	0.29
9	7.45	0
10	6.36	0.69
11	6.35	0.775
12	6.27	0.295
13	7.45	0
14	6.78	0.74
15	6.34	0.67
16	6.2	0.245
17	7.44	0
18	6.29	0.68
19	6.14	0.75
20	6.1	0.235

Table F.4 pH change and hydrogen production on molasses with 5 mM sucrose by *R. capsulatus* YO3

Days	**pH**	**H_2 (L)**
0	7.51	0
1	7.43	0
2	7.21	0.04
3	7.02	0.03
4	7.43	0.02
5	6.9	0
6	6.45	0.07
7	6.2	0.05
8	7.45	0.03
9	6.36	0
10	6.35	0.07
11	6.24	0.03
12	7.45	0.04
13	6.78	0
14	6.35	0.06
15	6.2	0.07
16	7.45	0.05
17	6.29	0
18	6.17	0.06
19	6.1	0.05
20	6	0.04

Table F.5 pH change and hydrogen production on molasses with 10 mM sucrose by *R. capsulatus* YO3

Days	**pH**	**H_2 (L)**
0	7.51	0
1	7.35	0.1
2	7.1	0.3
3	6.94	0.4
4	7.44	0.6
5	6.8	0
6	6.53	0.3
7	6.21	0.8
8	7.45	1.05
9	6.89	0
10	6.35	0.45
11	6.23	0.9
12	7.45	1.2
13	6.7	0
14	6.3	0.5
15	6.14	1
16	7.45	1.25
17	6.45	0
18	6.21	0.55
19	6.15	1
20	6.01	1.2

Table F.6 pH change and hydrogen production on molasses with 20 mM sucrose by *R. capsulatus* YO3

Days	**pH**	**H_2 (L)**
0	7.48	0
1	7.35	0
2	7.24	0.06
3	6.9	0.02
4	7.43	0.05
5	7.12	0
6	6.78	0.06
7	6.23	0.05
8	7.45	0.03
9	6.31	0
10	6.1	0.06
11	5.9	0.07
12	7.45	0.04
13	6.78	0
14	6.21	0.05
15	5.88	0.03
16	7.45	0.05
17	6.32	0
18	6.13	0.04
19	5.87	0.03
20	5.86	0.04

G. OUTDOOR EXPERIMENTAL DATA

Table G.1 pH change and hydrogen production on 10 mM sucrose by *R. capsulatus* YO3

Days	pH	H_2 (L)
0	7.45	0
1	7.1	0.05
2	6.84	0.12
3	6.7	0.085
4	7.45	0
5	7.13	0.1875
6	6.65	0.22
7	6.26	0.0675
8	7.45	0
9	7.11	0.29
10	6.76	0.34
11	6.25	0.085
12	7.45	0
13	7.22	0.325
14	6.8	0.425
15	6.27	0.085
16	7.45	0
17	7.11	0.29
18	6.87	0.425
19	6.32	0.085
20	6.32	0

Table G.2 pH change and hydrogen production on molasses with 10 mM sucrose by *R. capsulatus* YO3

Days	pH	H_2 (L)	Days	pH	H_2 (L)
1	7.45	0	21	7.45	0
2	7.23	0	22	7.06	0.28
3	7.04	0.07	23	6.83	0.7
4	6.32	0.21	24	6.21	0.735
5	7.45	0	25	7.45	0
6	7.23	0.175	26	7.12	0.315
7	6.75	0.315	27	6.67	0.595
8	6.05	0.35	28	6.15	0.63
9	7.45	0	29	7.45	0
10	7.02	0.21	30	7.14	0.35
11	6.7	0.455	31	6.89	0.63
12	6.12	0.49	32	6.21	0.665
13	7.45	0	33	7.45	0
14	7.1	0.35	34	7.22	0.28
15	6.78	0.63	35	6.88	0.35
16	6.21	0.7	36	6.22	0.665
17	7.45	0	37	7.45	0
18	7.2	0.35	38	7.1	0.28
19	6.8	0.7	39	6.82	0.56
20	6.23	0.77	40	6.19	0.63

H. DATA IN MICROAEROBIC DARK FERMENTATION

Table H.1 Hydrogen production by cyclic microaerobic dark fermentation by immobilized *Rp. palustris* CGA009 on 2 mM glucose, 4% oxygen and different inoculum volume (Cycle 1)

Hydrogen (umol)			
Hours	**25 (v/v%)**	**50 (v/v%)**	**100 (v/v%)**
0	0	0	0
24	15	30	35
48	35	60	65
72	40	70	80
96	42	75	85

Table H.2 Hydrogen production by cyclic microaerobic dark fermentation by immobilized *Rp. palustris* CGA009 on 2 mM glucose, 4% oxygen and different inoculum volume (Cycle 2)

Hydrogen (umol)			
Hours	**25 (v/v%)**	**50 (v/v%)**	**100 (v/v%)**
120	0	0	0
144	15	35	34
168	38	65	64
192	45	72	82
216	48	80	98

Table H.3 Hydrogen production by cyclic microaerobic dark fermentation by immobilized *Rp. palustris* CGA009 on 2 mM glucose, 4% oxygen and different inoculum volume (Cycle 3).

Hydrogen (umol)			
Hours	**25 (v/v%)**	**50 (v/v%)**	**100 (v/v%)**
240	0	0	0
264	14	35	38
288	33	66	75
312	45	76	95
356	52	80	105

Table H.4 Hydrogen production by cyclic microaerobic dark fermentation by immobilized *Rp. palustris* CGA009 on 2 mM glucose, 4% oxygen and different inoculum volume (Cycle 4).

Hydrogen (umol)			
Hours	**25 (v/v%)**	**50 (v/v%)**	**100 (v/v%)**
380	0	0	0
404	22	35	42
428	32	65	74
452	45	75	100
476	52	85	115

Table H.5 Hydrogen production by cyclic microaerobic dark fermentation by immobilized *Rp. palustris* CGA009 on 2 mM glucose, 4% oxygen and different inoculum volume (Cycle 5).

Hydrogen (umol)			
Hours	**25 (v/v%)**	**50 (v/v%)**	**100 (v/v%)**
500	0	0	0
524	21	32	40
548	28	60	75
572	46	65	95
596	55	80	110

Table H.6 Hydrogen production by cyclic microaerobic dark fermentation by immobilized *Rp. palustris* CGA009 on 2 mM glucose, 100 (v/v%) inoculum and different oxygen concentrations (Cycle 1).

Hydrogen (umol)			
Hours	**1 (%)**	**4.5 (%)**	**8 (%)**
0	0	0	0
24	5	30	15
48	12	54	28
72	18	60	42
96	20	75	45

Table H.7 Hydrogen production by cyclic microaerobic dark fermentation by immobilized *Rp. palustris* CGA009 on 2 mM glucose, 100 (v/v%) inoculum and different oxygen concentrations (Cycle 2).

Hydrogen (umol)			
Hours	**1 (%)**	**4.5 (%)**	**8 (%)**
120	0	0	0
144	5	35	15
168	15	60	32
192	28	65	46
216	30	85	55

Table H.8 Hydrogen production by cyclic microaerobic dark fermentation by immobilized *Rp. palustris* CGA009 on 2 mM glucose, 100 (v/v%) inoculum and different oxygen concentrations (Cycle 3).

Hydrogen (umol)			
Hours	**1 (%)**	**4.5 (%)**	**8 (%)**
240	0	0	0
264	8	35	18
288	17	55	30
312	28	66	58
356	33	96	62

Table H.9 Hydrogen production by cyclic microaerobic dark fermentation by immobilized *Rp. palustris* CGA009 on 2 mM glucose, 100 (v/v%) inoculum and different oxygen concentrations (Cycle 4)

Hydrogen (umol)			
Hours	**1 (%)**	**4.5 (%)**	**8 (%)**
380	0	0	0
404	10	42	15
428	20	65	28
452	25	85	56
476	35	105	65

Table H.10 Hydrogen production by cyclic microaerobic dark fermentation by immobilized *Rp. palustris* CGA009 on 2 mM glucose, 100 (v/v%) inoculum and different oxygen concentrations (Cycle 5).

Hydrogen (umol)			
Hours	**1 (%)**	**4.5 (%)**	**8 (%)**
500	0	0	0
524	15	38	15
548	22	60	30
572	28	85	55
596	33	105	70

Table H.11 Hydrogen production via cyclic microaerobic dark fermentation by immobilized *Rp. palustris* CGA009 on 100 (%v/v) inoculum, 4% oxygen and different initial glucose concentrations (Cycle 1).

Hydrogen (umol)			
Hours	**2 mM**	**6 mM**	**10 mM**
0	0	0	0
24	32	55	60
48	56	92	85
72	75	125	145
96	94	145	165

Table H.12 Hydrogen production via cyclic microaerobic dark fermentation by immobilized *Rp. palustris* CGA009 on 100 (%v/v) inoculum, 4% oxygen and different initial glucose concentrations (Cycle 2).

Hydrogen (umol)			
Hours	**2 mM**	**6 mM**	**10 mM**
120	0	0	0
144	35	58	55
168	55	95	85
192	85	145	155
216	105	150	180

Table H.13 Hydrogen production via cyclic microaerobic dark fermentation by immobilized *Rp. palustris* CGA009 on 100 (%v/v) inoculum, 4% oxygen and different initial glucose concentrations (Cycle 3).

Hydrogen (umol)			
Hours	**2 mM**	**6 mM**	**10 mM**
240	0	0	0
264	45	66	75
288	60	98	140
312	80	145	175
356	108	155	195

Table H.14 Hydrogen production via cyclic microaerobic dark fermentation by immobilized *Rp. palustris* CGA009 on 100 (%v/v) inoculum, 4% oxygen and different initial glucose concentrations (Cycle 4)

Hydrogen (umol)			
Hours	**2 mM**	**6 mM**	**10 mM**
380	0	0	0
404	45	55	65
428	65	90	84
452	95	145	145
476	112	160	185

Table H.15 Hydrogen production via cyclic microaerobic dark fermentation by immobilized *Rp. palustris* CGA009 on 100 (%v/v) inoculum, 4% oxygen and different initial glucose concentrations (Cycle 5).

Hydrogen (umol)			
Hours	**2 mM**	**6 mM**	**10 mM**
500	0	0	0
524	40	55	60
548	65	85	82
572	90	135	154
596	110	160	180

Table H.16 Cumulative hydrogen production throughout the sequential microaerobic dark fermentation and photofermentation on different inoculum concentration.

Hydrogen (umol)			
Hours	**25 (v/v %)**	**50 (v/v %)**	**100(v/v %)**
0	0	0	0
24	3.25	7.75	8.95
48	6.35	12.7	15.1
72	9.5	17.05	22.2
96	12	22.25	26.75
120	17.95	57.45	75
144	41.9	100.8	138
168	59.7	145.5	175
192	75	167.5	203.5

Table H.17 Cumulative hydrogen production throughout the sequential microaerobic dark fermentation and photofermentation on different oxygen concentration.

Hydrogen (umol)			
Hours	**1 (%)**	**4.5 (%)**	**8 (%)**
0	0	0	0
24	3.7	14.64	4.05
48	8.4	23.55	11.44
72	12.25	29.75	14.82
96	14.45	38.45	20.35
120	27.5	57	29
144	57.5	128.5	40
168	147.5	177.5	52.5
192	162.5	197.5	57.5

Table H.18 Cumulative hydrogen production throughout the sequential microaerobic dark fermentation and photofermentation on different initial glucose concentration.

Hydrogen (umol)			
Hours	**2 mM**	**6 mM**	**10 mM**
0	0	0	0
24	11.25	6	5
48	15	16	12.5
72	18	35	15
96	18	40	15
120	60	149.5	32
144	150.5	326.5	140
168	197.5	544	185
192	210	761.6	245

I. SAMPLE CALCULATION

I1 Calculation of substrate conversion efficiency (%)

For calculation of substrate conversion efficiency of *R. capsulatus* YO3 on 5 mM initial sucrose medium.

Substrate conversion efficiency (%) = (Experimentally produced mole H_2) / (Theoretical mole of H_2 over consumed substrate) / x 100

Volume of reactor = 1.1 L

Theoretical mole of hydrogen on sucrose = 24

C_o = Initial concentration of sucrose (mM) = 5.0

C_f = Final concentration of sucrose (mM) = 2.2

Theoretical H_2 = (C_f - C_o) x Volume of reactor (L)

= (5.0-2.2) x (1.1) = 2.53 x 24 =0.06 moles H_2

Experimental Produced H_2 = 1.2 L / 24.5 = 0.049 mol

Substrate conversion efficiency (%) = (0.049)/(0.06) x 100 = 81.2 %

I2 Calculation of hydrogen productivity

Hydrogen Productivity = Cumulative millimoles of hydrogen produced / volume of culture (L) x t (hour)

The formula for calculation of hydrogen productivity is given as an example for calculation of *R. capsulatus* YO3

t = Duration of hydrogen production (hour) =72

V = Volume of culture = 1.1 L

V_{H2} = Produced hydrogen = 1.2 L

Hydrogen productivity (mmol $H_2/L_c.h$) = [1.2/ 24.5 L] / [1.1 x 72] = 0.62

I3 Calculation of hydrogen yield

Hyrogen yield is measured by the ratio of the actual mole of produced H_2 to the mole of H_2 that could be produced by the complete utilization of the consumed sucrose. The evolved hydrogen was calculated using ideal gas equation (P V= n R T).

Assume that hydrogen produced in the process is 1.2 L and consumed sucrose is 5 mM.

Using the ideal gas equation, produced hydrogen is converted into moles (0.049 mol). Consumed sucrose is calculated using HPLC (0.0055 mol). Hydrogen yield is 0.049/0.0055 = 8.9 mol H_2/mol sucrose.

Light conversion efficiency (%) = $(33.6 \times d_{H2} \times V_{H2}) / (I \times A \times t) \times 100$

Example: Vol. H_2: 1.4 L; A: 0.04 m^2; I: 200 W/m^2 ; t: 72 h

Light conversion efficiency (%) = 0.72

CURRICULUM VITAE

Surname, Name : Sağır Emrah

Date and Place of Birth : 5 August 1984, İstanbul

Marital Status : Married

Phone : +903122106462

E-mail : esagir@metu.edu.tr

Education:

Degree	Institution	Year of Graduation
Ph.D	Middle East Technical University, Biochemistry	2018
M.Sc	Middle East Technical University, Biochemistry	2012
BS	Abant İzzet Baysal University, Biology	2007

Work Experience:

Year	Place	Enrollment
2008-2017	Middle East Technical University, Department of Biological Sciences	R&T Assistant
2016-2017	University of Montreal, School of Medicine Microbiology, Infectious Diseases and Immunology Department (Patrick C. Hallenbeck Lab.)	Researcher

Publications:

Peer-reviewed Publications in International Journals

Sagir, E., Alipour, S., Elkahlout, K., Koku, H., Gunduz, U., Eroglu, I., & Yucel, M. (2017). Scale-up studies for stable, long-term indoor and outdoor production of hydrogen by immobilized *Rhodobacter capsulatus*. *International Journal of Hydrogen Energy*, 42, 22743-22755.

Sagir, E., Yucel, M., & Hallenbeck, P. C. (2017). Demonstration and optimization of sequential microaerobic dark- and photo-fermentation biohydrogen production by immobilized *Rhodobacter capsulatus* JP91. *Bioresource Technology*, 250, 43-50

Sagir, E., Ozgur, E., Gunduz, U., Eroglu, I., Yucel, M., (2017). Single-stage photofermentative biohydrogen production from sugar beet molasses by different purple non-sulfur bacteria. *Bioprocess and Biosystems Engineering*. 40(11): 1589-1601.

Publications in International Conference Proceedings

E. Sagir, E. Özgür, U. Gündüz, I. Eroglu, M. Yücel. Photobiological hydrogen production from sugar beet molasses. "ECB15 Biocrossroads, 15th European Biotechnology Congress, İstanbul/Turkey/New Biotechnology, issue S", 29, (2012), p.540.

Sagir E., Ozgur E., Gunduz U., Eroglu I.,Yucel M. Photobiological hydrogen production by co-cultivation of PNS bacteria on sugar beet molasses. "37th FEBS Congress Sevilla/Spain", 279, (2012), p.600-608.

E. Sagir, E. Özgür, U. Gündüz, I. Eroglu, M. Yücel. Biological hydrogen production from sugar beet molasses by a single-step photofermentation, "International Conference on Microalgae and Biofuel", 30-31 July 2015, Koç University, İstanbul.

Master thesis: Sağır, E. (2012). Photobiological hydrogen production from sugar beet molasses. M. Sc. thesis in Biochemistry, Middle East Technical University.

Foreign Language: English

Laboratory & Computer Skills:

Biochemistry, Cell Biology, General Biology, Microbiology, Chromatography (HPLC, GC), Microscopy, Eukaryotic cell culture, Enzymes, SDS-PAGE, Western Blot, Zymography, Immunohistochemistry, Microsoft Office Applications (Word, Excel, Powerpoint), Minitab, Matlab, Photoshop

Memberships : Turkish Biochemical Society

Hobbies : Photography